January 1970

Subcritical Flow at Open Channel Structures Open Channel Expansions

Lloyd H. Austin

Gaylord V. Skogerboe

Ray S. Bennett

Subcritical Flow at Open Channel Structures

OPEN CHANNEL EXPANSIONS

Prepared by

Lloyd H. Austin
Gaylord V. Skogerboe
Ray S. Bennett

OWRR Project No. B-018-UTAH
Matching Grant Agreement No. 14-01-0001-1952
Investigation Period–July 1, 1968 to June 30, 1970

Partial technical completion report prepared for

Office of Water Resources Research
United States Department of the Interior

and

Utah Center for Water Resources Research
Utah State University

Utah Water Research Laboratory
College of Engineering
Utah State University
Logan, Utah 84321

August 1970 PRWG71-1

ABSTRACT

Subcritical Flow at Open Channel Structures
OPEN CHANNEL EXPANSIONS

Analyzing the hydraulics of open channel constrictions has been modified to allow the analysis of energy loss in open channel expansions. The modified technique has been compared with previous methods of analysis using data collected in the laboratory on open channel expansions with vertical walls, and triangular-shaped baffles. Also, a design procedure for such baffled outlet structures has been developed.

Austin, Lloyd H., Gaylord V. Skogerboe, and Ray S. Bennett. SUBCRITICAL FLOW AT OPEN CHANNEL STRUCTURES: OPEN CHANNEL EXPANSIONS. Partial Technical Completion Report to Office of Water Resources Research, Department of the Interior, and Utah Center for Water Resources Research. PRWG71-1, Utah Water Research Laboratory, College of Engineering, Utah State University, Logan, Utah. August 1970.

KEYWORDS—*energy losses, head loss, hydraulic design, *hydraulic structures, non-uniform flow, *open channel flow, *subcritical flow.

ACKNOWLEDGMENTS

This publication reports the research findings of a project supported in part from funds provided by the United States Department of the Interior, Office of Water Resources Research, as authorized under the Water Resources Research Act of 1964, Public Law 88-379 and administered by the Utah Center for Water Resources Research, Utah State University, Logan, Utah. Without the financial assistance of the Office of Water Resources Research, this research project could never have been undertaken. The writers are indeed grateful for the support given this project and have actively pursued the proposed research effort in order to prove this gratitude.

The cooperation of Mr. Gilbert Peterson in providing the technical services during the fabrication and installation of the various open channel expansions is appreciated.

The services of the Utah Water Research Laboratory were invaluable in the publication of this report. Thanks are extended to Mrs. Donna Falkenborg for editing and supervising the publication of this manuscript.

Lloyd H. Austin
Gaylord V. Skogerboe
Ray S. Bennett

TABLE OF CONTENTS

Page

INTRODUCTION 1

Background 1
Purpose 2

LITERATURE REVIEW 3

Flow Characteristics 3
Warped Transitions 5
Simplified Inlet 6
Pipe to Canal Transitions 8
Broken Plane Transitions 8
Curved Expansions 10
Trapezoidal Baffled Outlet 13
Rectangular Baffled Outlets 14

EXPERIMENTAL DESIGN 17

Physical Layout 17
Instrumentation 18

ENERGY LOSS ANALYSIS 25

DEVELOPMENT OF BAFFLE DESIGN 35

HYDRAULIC CHARACTERISTICS OF FINAL BAFFLE DESIGN 43

HYDRAULIC DESIGN CRITERIA 49

SUMMARY 65

SELECTED REFERENCES 69

APPENDIX: HYDRAULIC DATA 71

LIST OF FIGURES

Figure		Page
1	Plan view of open channel expansion	4
2	Schematic sketch of plan view of warped wall inlet transition	6
3	Schematic sketch of simplified inlet transition structure	7
4	Head loss in simplified inlet transition structures	7
5	Broken-back transitions	9
6	Round-to-rectangular pipeline transitions	10
7	Typical trapezoidal broken plane transitions investigated by Haszpra (1961, 1962)	11
8	Curved expansions investigated by Chaturvedi (1963)	12
9	Typical velocity distributions for curved expansions. (Taken from Chaturvedi, 1963)	12
10	Model trapezoidal flume	13
11	Typical velocity distribution at exit of trapezoidal expansion	14
12	Definition sketch for the baffled outlet	15
13	Fluid Mechanics Laboratory	17
14	Experimental expansion design layout	19
15	View from upstream (looking downstream) of the experimental expansion design	20
16	View from downstream (looking upstream) of the experimental expansion design	20

17 View of downstream section with expansion ratio of 1.3 and B/b ratio of 5 21

18 View of downstream section with expansion ratio of 1.3 and B/b ratio of 3 21

19 Layout of flumes showing range of expansion and channel widths 22

20 Reference to points of measurement through expansion 22

21 Measurement carriage 23

22 Measurement carriage showing Ott current meter and point gage 23

23 Typical submerged flow calibration curves for an open channel constriction 26

24 Head loss for subcritical flow in abrupt outlets 28

25 Head loss for subcritical flow in baffled outlets 30

26 Relationship between the head loss coefficient and specific energy ratio for the baffled outlet 32

27 Relationship between the head loss coefficient and inlet Froude number for the baffled outlet 33

28 Arrangement of baffles used in developing final baffle designs 36

29 Experimental flume with 2-3 expansion ratio and a B/b ratio of 3, operating with final baffle design 39

30 Experimental flume with 2-3 expansion ratio and a B/b ratio of 5, operating with final baffle design 39

31 Illustration of the range of divergences (abrupt to 1:6) and expansion ratios of B/b = 5 and 3 respectively 40

32 A definition sketch detailing the location of the baffles for the final design of triangular-shaped baffles for open channel expansions 41

33 Velocity distributions in downstream channel for Q = 1 cfs, B/b = 3, and $E_r > 0.9$ 43

34 Velocity distributions in downstream channel for Q = 3.5 cfs, B/b = 3, and $0.8 < E_r < 0.9$ 44

35 Velocity distributions in downstream channel for Q = 1 cfs, B/b = 5, and $E_r > 0.9$ 45

36 Velocity distributions in downstream channel for Q = 3.5 cfs, B/b = 5, and $0.8 < E_r < 0.9$ 46

37 Flow conditions in 2:3 expansion with B/b = 5 47

38 Flow conditions in 1:6 expansion with B/b = 3 47

39 Discharge-energy loss curves for abrupt expansion with B/b = 5 51

40 Discharge-energy loss curves for 1:6 expansion with B/b = 5 52

41 Distribution of specific energy ratio for various expansions with B/b = 5 53

42 Theoretical relationship between constriction ratio, b/B, and subcritical flow exponent, n_2, for open channel constrictions 54

43 Relationships between expansion ratio, B/b, and subcritical flow exponent, n_2, for open channel expansions with vertical side walls 55

44 Relationship between inlet Froude number and specific energy ratio for open channel expansions with triangular-shaped baffles 57

45 Typical relationship between head loss and the change in velocity head at the inlet and outlet of an open channel expansion structure 58

46 Relationships between head loss and inlet velocity head for expansions having triangular-shaped baffles and vertical walls with B/b = 5 60

47 Relationships between head loss and inlet velocity head for expansions having triangular-shaped baffles and vertical walls with B/b = 3 61

48 Relationships between the inlet Froude number and head loss coefficient for expansions having triangular-shaped baffles and vertical walls with B/b = 5 62

49 Relationships between the inlet Froude number and head loss coefficient for expansions having triangular-shaped baffles and vertical walls with B/b = 3 63

50 Design procedure for open channel expansions with vertical walls and triangular-shaped baffles 66

51 Reference to location of point measurements 71

LIST OF TABLES

Table **Page**

1 Hydraulic data for abrupt outlets 27

2 Hydraulic data for baffled outlets 29

3 Hydraulic data for abrupt expansion for B/b = 5 (Runs 1-16) and B/b = 3 (Runs 17-32) 74

4 Hydraulic data for 1:1 expansion for B/b = 5 (Runs 1-16) and B/b = 3 (Runs 17-32) 75

5 Hydraulic data for 2:3 expansion for B/b = 5 (Runs 1-16) and B/b = 3 (Runs 17-32) 76

6 Hydraulic data for 1:3 expansion for B/b = 5 (Runs 1-16) and B/b = 3 (Runs 17-32) 77

7 Hydraulic data for 1:6 expansion for B/b = 5 (Runs 1-16) and B/b = 3 (Runs 17-32) 78

NOMENCLATURE

Symbol	Definition
A	cross-sectional area of flow
A_1	cross-sectional area of flow at section 1 in inlet channel
A_2	cross-sectional area of flow at section 2 in outlet channel or at 3/4 L of expansion
A_3	cross-sectional area of flow two feet downstream from end of expansion
A_r	ratio of A_1/A_2 or A_1/A_3
B	width of downstream channel
b	width of upstream channel
C_L	head loss coefficient
C_1	coefficient in the numerator of the submerged flow equation
C_2	coefficient in the denominator of the submerged flow equation
E_u	specific energy at a section upstream from a constriction or expansion
E_d	specific energy at a section downstream from a constriction or expansion
E_1	specific energy at section 1 in inlet channel
E_2	specific energy at section 2 in downstream channel or at 3/4 L in expansion
E_3	specific energy at section 3 in downstream outlet channel
E_r	ratio of E_d/E_u, E_2/E_1, or E_3/E_1
F	Froude number
F_1	Froude number at section 1 in inlet channel
g	acceleration due to gravity

h_L head loss E_u-E_d, E_1-E_2, or E_1-E_3

L length of open channel expansion

n_1 power of y_1 in the free flow equation

n_2 power of the submergence term in the denominator of the subcritical flow equation

Q flow rate, or discharge

$Q_{h_L=1}$ value of Q when $h_L = 1$

Q_o total free flow discharge based on upstream depth of flow which has been increased due to submergence

V_u average velocity in channel upstream from constriction or expansion

V_d average velocity in channel downstream from constriction or expansion

V_1 average velocity at section 1 in inlet channel

V_2 average velocity at section 2 in downstream channel or at 3/4 L in expansion

V_3 average velocity at section 3 in downstream channel

W_b expansion width at b distance downstream from inlet to expansion

y_u flow depth at section upstream from constriction or expansion

y_d flow depth at section downstream from constriction or expansion

y_1 flow depth at section 1 in inlet channel

y_2 flow depth at section 2 in downstream channel or at 3/4 L of expansion

y_3 flow depth at section 3 in downstream channel

θ angle of divergence of expansion wall

INTRODUCTION

An open channel transition may be defined as a change either in the direction, slope, or cross section of the channel, which produces a change in flow conditions (nonuniform flow). Most transitions of engineering interest are comparatively short structures, although they may affect the flow for a great distance upstream or downstream (Henderson, 1966).

Transition sections are needed where conduit or channel cross sections, and consequently velocities, are appreciably changed. Their purposes are to prevent disturbances in flow, minimize losses of head where velocities are increased, and recover as much velocity head as possible where velocities are decreased.

An open channel expansion may be defined as an increase in cross-sectional flow area of the channel in the direction of flow, thereby decreasing the mean velocity of the flow. The flow conditions in the outlet channel are complicated by the likelihood of flow separation along one expansion wall, or both, if the rate of change of cross-sectional flow area is too rapid. Usually, the engineer is interested in minimizing the length of the structure in order to minimize construction costs, which requires a rapid increase of cross-sectional flow area. Thus, a balance must be sought between economics and the importance of minimizing energy losses, as well as an accounting of downstream erosion if an earthen outlet channel is to be used.

Background

At Utah State University considerable effort has been devoted to the analysis of submerged (subcritical) flow at open channel constrictions. A method of analyzing submerged flow was first developed for a trapezoidal flume by Hyatt (1965). Later studies verified the method of analysis for a rectangular flume (Skogerboe, Walker, and Robinson, 1965), Parshall flumes (Skogerboe, Hyatt, Johnson, and England, 1965), and weirs (Skogerboe, Hyatt, and Austin, 1966). Because of these findings, along with limited analysis of data by other authors, the writers were encouraged to extend the method of analysis to expansions in open channels.

The original development of the parameters and relationships which describe the submerged flow condition came from a combination of dimensional analysis and empiricism. Further verification of the parameters developed in this manner is obtained by employing momentum relationships. The application of this method of analysis to open channel expansions requires that specific energy be employed rather than hydraulic depth in the analysis.

A number of efforts by previous investigators are reported regarding transitions and expansions in open channels. However, little of the work has been directed to the analysis of subcritical flow relationships for open channel expansions. For certain proposed open channel expansion structures, various equations for describing energy losses occurring in the expansion have been utilized. The validity of these various energy loss equations needs to be determined.

Purpose

The intent of the writers is to develop a basis for the design of open channel expansions utilizing the techniques previously developed for flow measuring flumes and weirs. This method of analysis would employ the use of specific energy rather than flow depth, as indicated before, but this substitution has been found valid through previous analysis of data from other research (Skogerboe and Hyatt, 1966). Through laboratory studies, the task of developing design criteria for open channel expansions operating under subcritical flow conditions has been undertaken. As part of this development, the applicability of the submerged flow techniques for analyzing the efficiency of various energy dissipation structures operating under subcritical flow conditions will be shown. At the same time, the validity of various energy loss equations used by previous investigators in reporting proposed designs for particular expansion structures will be demonstrated.

LITERATURE REVIEW

The literature review that follows describes many transition structures, but deals mainly with those transitions which are expansions. An attempt has been made to report that portion of the literature which would assist in developing an understanding of the flow conditions that might be expected in various geometrical forms of expansion structures. Also, literature citing various energy loss equations applicable to subcritical flow in open channel expansions are reported. An expansion may be defined as a change in either slope or cross section, or both, of the channel that will decrease the velocity of the flow.

Flow Characteristics

Although the design of inlet and outlet transitions is somewhat similar, the behavior of flow in inlet and outlet transitions is quite different. A. R. Thomas (1940), in his paper entitled "Flow in Expansion in Open Channels," has revealed some of the problems related to the flow of water in open channel expansions. These problems have to do with the separation of flow from the expansion wall, thereby causing either (a) flow on one side of the expansion and the forming of a large return eddy on the other side, or (b) separation on both sides causing a large central jet. Both of these flow patterns in an unlined channel have disastrous results in the form of scour of the downstream banks under condition (a), or scour of the downstream channel bed when condition (b) occurs.

Thomas' quantitative analysis of flow in expansions uses the aid of several basic principles of fluid mechanics which are quoted below.

These principles are:

(i) Newton's 2nd law, by which an acceleration takes place proportional to and in the direction of a positive pressure gradient. This may be applied by resolving forces acting on any "block" of water, i.e. water enclosed within an imaginary boundary; and equating the resultant to the net rate of increase of momentum in the block.

(ii) Bernoulli's Theorem–The energy of flowing water may be in the form of potential energy (pressure and gravity) or kinetic energy (velocity), so that with a given total energy the increase of one reduces the others (under ideal flow conditions).

(iii) Turbulence has the effect of spreading or equalizing velocity, due to interchange of momentum caused by the "mixing" of the fluid.

This report, without going into the reasons for the formation of a return eddy as shown in Fig. 1, examines geometric designs which tend to reduce or increase the size of the return eddy.

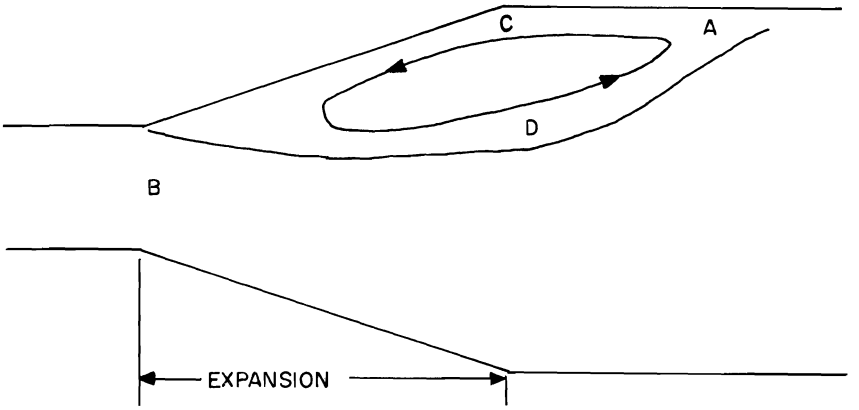

Fig. 1. Plan view of open channel expansion. (Taken from Thomas, 1940.)

Once an eddy has formed, the forces which tend to increase or reduce the eddy size are quoted below:

(a) The pressure gradient from A to B (Fig. 1);

(b) The shear force on the fluid at D (Fig. 1) adjacent to the high velocity jet, caused by turbulent intermixing and by viscous drag (mainly intermixing except when the Reynolds number is low); and

(c) The frictional drag of the bed and sides.

Expansions in open channels tend to favor the development of a return eddy. The conversion of velocity head to pressure head causes a decrease in momentum in the direction from B to A (Fig. 1) because of a greater depth and, therefore, a greater pressure at A (Thomas, 1940).

The degree of expansion, along with the quantity of flow, determines the shape of the return eddy and also the degree of intermixing of the fluid. The process is described below by Thomas (1940).

> The result depends on the degree of intermixing. If it [the return eddy] extends past D to the fluid against the boundary at C, as it may if the eddy is narrow, the addition of forward momentum there may overcome the adverse pressure gradient, so that the whole eddy fluid will move forward and the eddy will disappear.

If, on the other hand, the intermixing is sufficient to outbalance the adverse pressure gradient at D, but not at C, there will be forward motion at D and return flow at C, and the eddy will persist.

If the intermixing is not sufficient to outbalance the adverse pressure gradient even at D, the width of eddy will increase, contracting the main stream until the transmitted momentum is sufficient to outbalance the pressure gradient to the required degree.

The effect of frictional drag is likely to be relatively small. It tends to slow up the eddy, but also the more the main stream is contracted the greater the frictional loss therein, tending to reduce the pressure gradient.

In converging flow, the pressure gradient is unfavorable to the formation of a return eddy. So, while an expansion creates conditions favorable to creating a return eddy, a convergence is a stabilizing influence.

The effect of depth, width, quantity, and Froude number on the stability of open channel expansions are summarized below by Thomas (1940).

For a given [discharge] Q, increase in either depth or width of a channel stabilizes flow. For a given Froude number, increase in depth assists the formation of a return eddy, while increase in width stabilizes flow.

Increase in Q, Froude number, angle of divergence or expansion ratio, assist the formation of a return eddy, other dimensions remaining constant in each case. Reynolds number (VR/ν) [R is hydraulic radius, V is mean velocity, and ν is the kinematic viscosity] also has an effect on expanding flow in that it is a measure of turbulence–the greater the Reynolds number the more stable the flow–also greater the head loss.

The influence of upstream conditions may just be touched upon. If the expansion immediately follows a contraction, the flow will follow the expansion more easily than if the contracted channel is parallel for some length, as in the former case there is concentration of flow at the sides which easily expands, whereas in the latter, the flow adjusts itself to the contracted section, the concentration expanding inwards from the sides, thus equalizing the flow, upstream of the expansion.

Also, one-sided flow at the entrance to the expansion tends to make one-sided flow in the expansion.

Because of the tendency for a return eddy to form in an open channel expansion, several structural methods have been studied which induce the flow to follow the expansion. Methods used include increased bed roughness, a raised floor as the width increases, grids, baffles, blocks, and vanes.

Warped Transitions

From previous design work by the U.S. Bureau of Reclamation, Hinds (1928) formulated a new criterion for transition design. This design stipulated that the computed water surface profile through the transition shall be a smooth, continuous curve, approximately tangent to the water-surface curves in

the channels above and below. By properly curving the walls of the transition entrance (flume bottom not level) as shown in Fig. 2, the rate of change in acceleration will occur in such a manner that the water-surface profile becomes a smooth, continuous curve. Although the warped transition (Hinds, 1928) is costly to construct, it has usually been considered the lowest head (energy) loss transition. The outlet transition or open channel expansion from a flume is designed in the same way as an inlet. The only essential difference in the design is that the conversion loss is subtracted from the change in velocity head to obtain the change in water surface. The design procedure can be found in several references (e.g. Chow, 1959).

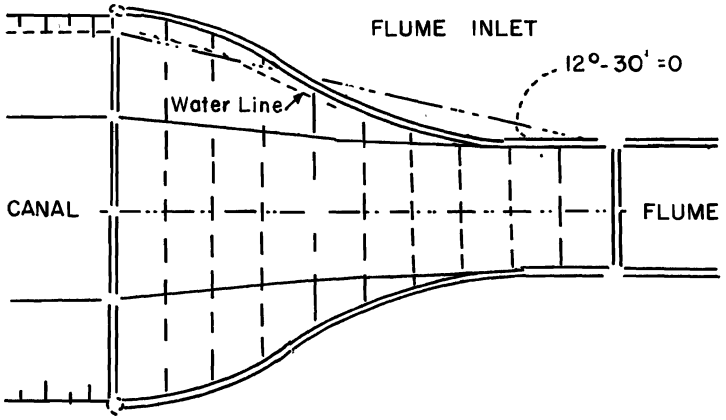

Fig. 2. Schematic sketch of plan view of warped wall inlet transition.

Simplified Inlet

The warped transition is not only tedious to design, but it is costly to construct and is a relatively large structure. Smith (1967) suggests a simplified flume inlet for subcritical velocities with almost the same efficiency as the more elaborate design. The simplified transition, along with important dimensions, is shown in Fig. 3. Four hydraulic requirements of a satisfactory flume inlet transition are: (1) smooth, predictable, and level water surface; (2) minimum transition head loss; (3) absence of scour in the vicinity of the contraction; and (4) simple and economical design and construction. A plot of the downstream velocity head against the head loss through the transition is shown in Fig. 4 for various ratios of the downstream channel width, b, to the average upstream channel width, B. The equation describing Fig. 4 is,

$$h_L = 0.06\ (1 - b/B)\ V_b^2/2g \quad \ldots\ldots\ldots \quad (1)$$

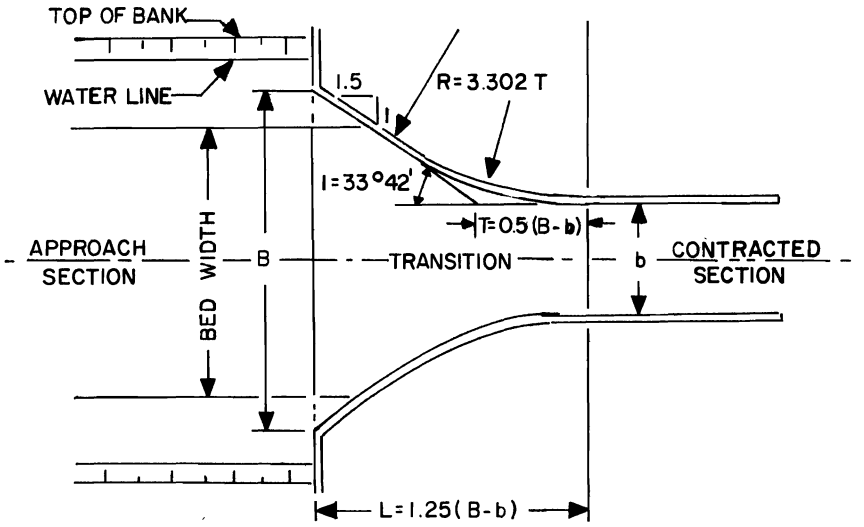

Fig. 3. Schematic sketch of simplified inlet transition structure. (Taken from Smith, 1967.)

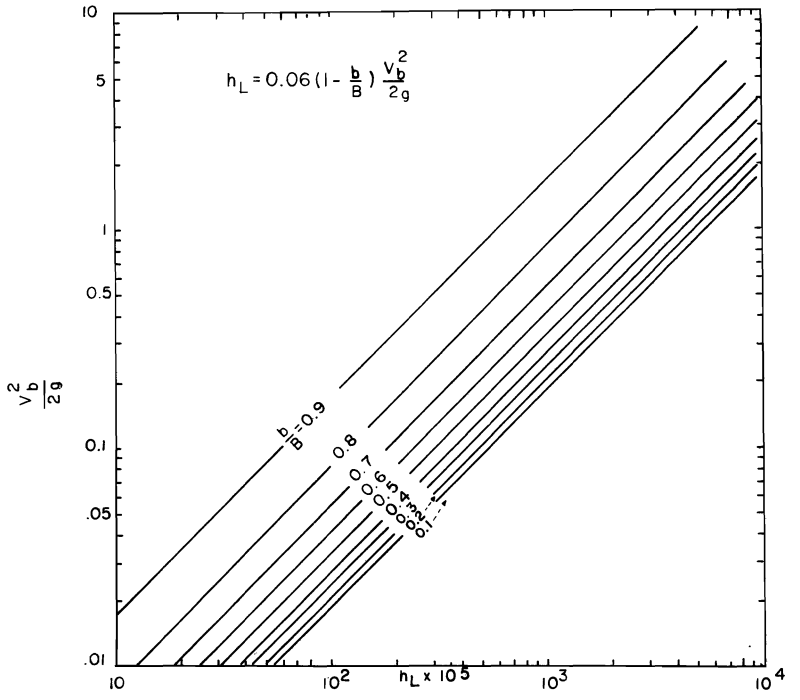

Fig. 4. Head loss in simplified inlet transition structures.

where h_L is the head loss in feet, V_b is the downstream velocity in ft./sec., and g is the acceleration of gravity.

Pipe to Canal Transitions

Studies made by the U.S. Bureau of Reclamation (Simmons, 1964) on erosion and energy losses produced by transitions from pipes to canals and from canals to pipes produced the following conclusions:

1. The energy losses for conventional broken-back transitions (Fig. 5) from pipes to canals are from 0.6 to 0.7 times the difference between the upstream and downstream velocity heads, h_v.
2. Reasonable changes in the angle of divergence of the sidewalls, slope of the invert of the open transitions, and the attitude of the inlet pipe line have little effect upon energy losses.
3. Outlet losses can be reduced to 0.4 h_v by using a short closed conduit expanding section and 0.1 h_v using a 6D-long closed conduit transition having circular inlets and rectangular outlets (Fig. 6).
4. The head loss for the broken-back type of inlet or outlet transition should be taken as 0.5 to 0.7 h_v for design purposes.

Broken Plane Transitions

Haszpra (1961, 1962) has studied the hydraulics of broken plane transitions for inlet transitions, outlet transitions, and Venturi flumes. Most of the broken plane transitions investigated by Haszpra had trapezoidal cross sections (Fig. 7). In addition, Haszpra compared the hydraulic efficiency of broken plane transitions with the warped transition developed by Hinds (1928).

A summary of the results reported by Haszpra (1961, 1962) is quoted below:

> The new broken transition is advantageous in every respect. It causes, in general, smaller head loss as compared to that caused by the warped surface, furthermore its construction is cheaper and can be performed with greater accuracy.
>
> The head loss attained by the broken plane transition amounted to 0-11 percent as compared to that occurring with a warped surface in [some] cases....
>
> Head losses in Venturi flumes having a broken plane transition decreased by 15-35 percent as compared to those occurring with warped surfaces, if losses are considered at the limit of submergence [transition submergence].
>
> On the strength of investigations performed hitherto, it can be stated that a broken plane transition is hydraulically superior to the warped surface in the case of expansions, Venturi flumes, and of contractions where at least 40 percent decrease in bottom width occurs. On account of constructional advantages, it is to be expected that the broken plane transition will take precedence over warped surface in every instance....

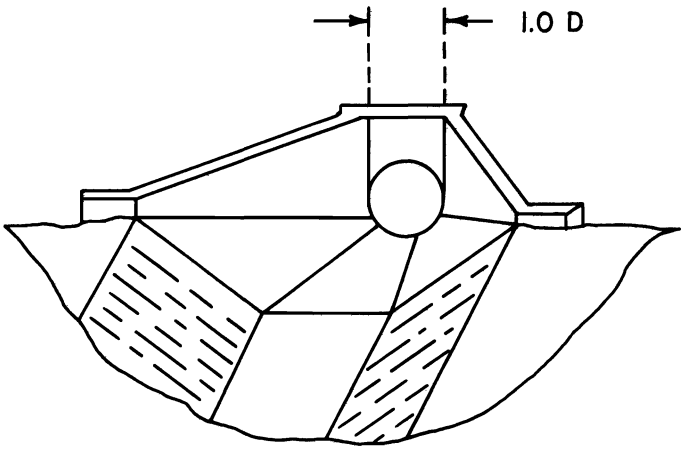

Barrel of pipeline attached to transition:
Loss as an inlet = $0.50\,\Delta h_v$
Loss as an outlet = $0.65\,\Delta h_v$
Scour–moderate to extensive

$$h_v = \frac{V_i^2 - V_o^2}{2g}$$

where
V_i = inlet velocity
V_o = outlet velocity

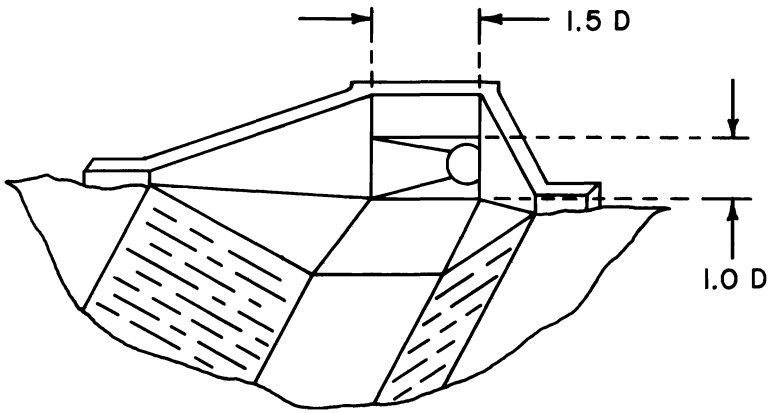

Pipeline barrel connects to transition with round-to-rectangular pipe transition:
Loss as an inlet = $0.40\,\Delta h_v$
Loss as an outlet = $0.40\,\Delta h_v$
Scour–moderate

Fig. 5. Broken-back transitions.

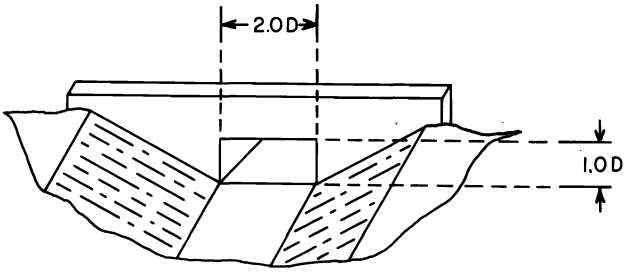

6D-long pipe transition connects pipeline to headwall across canal:
Loss as an inlet = 0.10 h_v
Loss as an outlet = 0.40 h_v
Scour–moderate

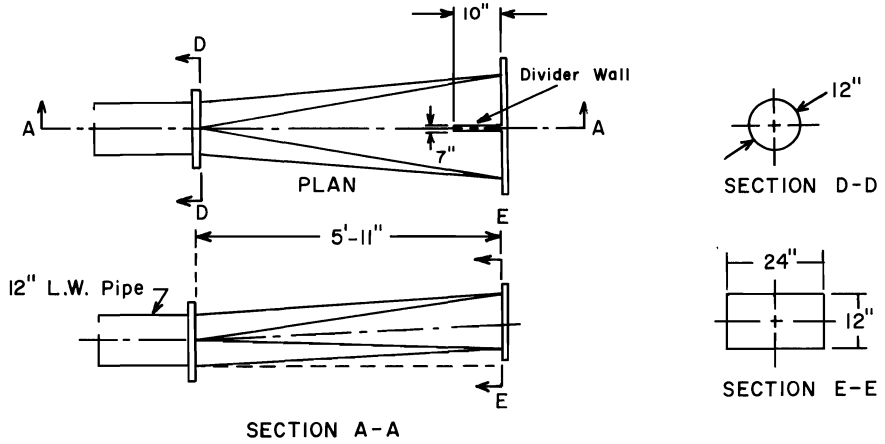

Fig. 6. Round-to-rectangular pipeline transitions.

Curved Expansions

Chaturvedi (1963) conducted experiments on open channel expansions having vertical curved walls (Fig. 8). The experiments were performed in a flume 3 feet wide and 80 feet long. Expansion ratios (B/b) of 2, 2.67, and 4 (Fig. 8) were used, while the divergence of the walls from the inlet to the outlet was 1:5 ($2\theta = 13^{\circ}$) in all cases. Curve No. 7 in Fig. 8 is a straight wall with 1:5 divergence, while the dashed line in Fig. 8 represents the warped transition proposed by Hinds (1928).

Some of the typical velocity distributions measured by Chaturvedi are shown in Fig. 9 for an expansion ratio of 4. These curves portray the wide

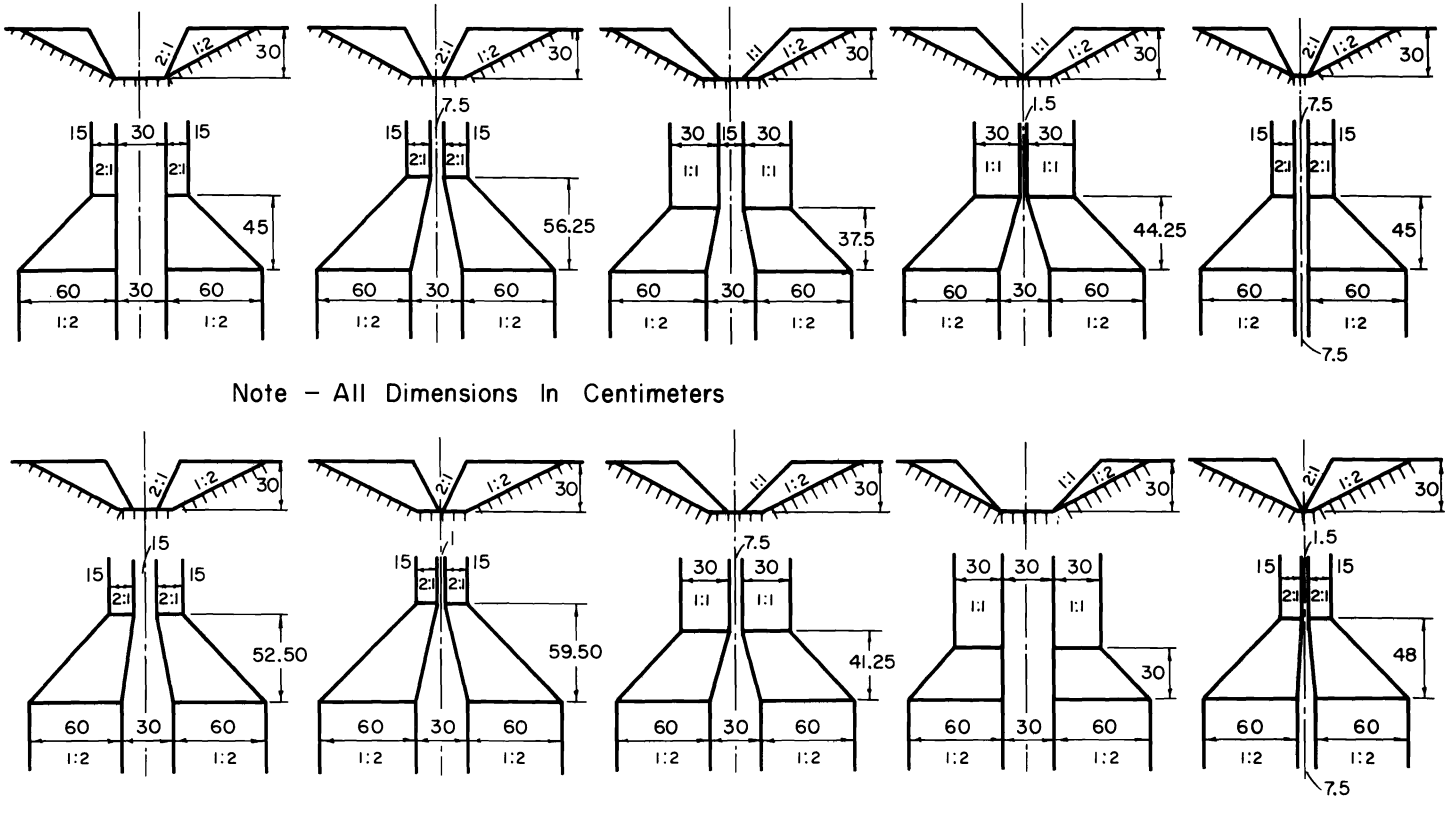

Fig. 7. Typical trapezoidal broken plane transitions investigated by Haszpra (1961, 1962).

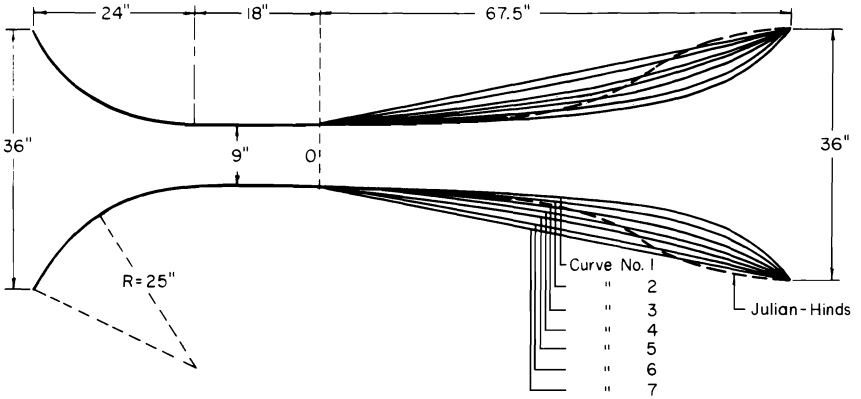

Fig. 8. Curved expansions investigated by Chaturvedi (1963).

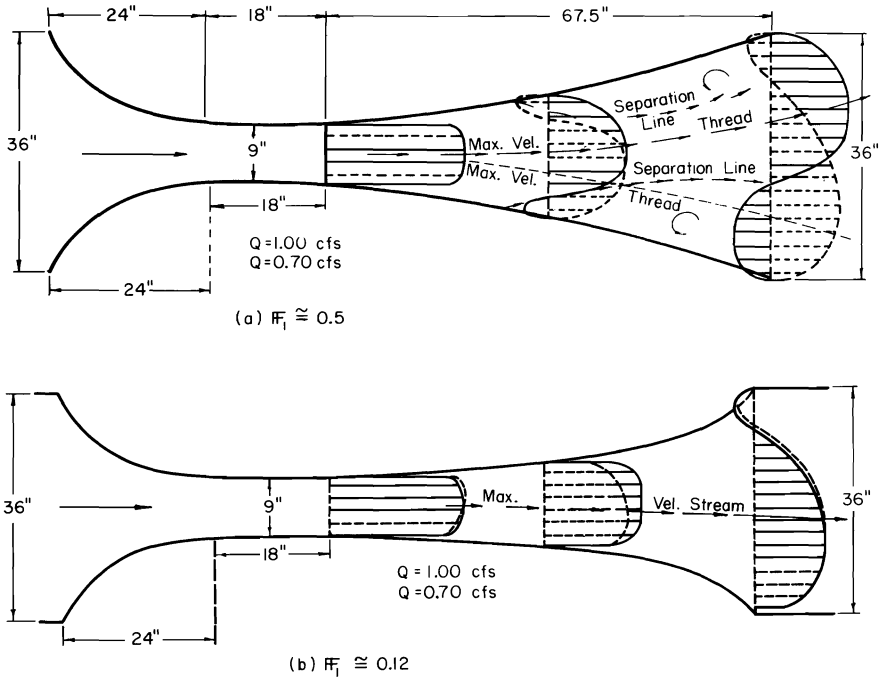

Fig. 9. Typical velocity distributions for curved expansions. (Taken from Chaturvedi, 1963.)

variation in velocity distribution that can be expected in open channel expansions. The average Froude number at the inlet and outlet was 0.5 and 0.12, respectively. The velocity distributions obtained for expansion ratios of 2 and 2.67 showed considerable improvement over those shown in Fig. 9.

In each case, the curved wall represented by curve No. 6 in Fig. 8 resulted in the best hydraulic performance. Chaturvedi (1963) also concluded that flow conditions in the approach channel have a significant effect upon flow conditions leaving the expansion. Any flow instability at the inlet will become more aggravated as the flow moves through the expansion. Thus, the flow at the outlet will be improved if uniform flow with uniform velocity distribution and hydrostatic pressure distribution occurs at the inlet.

Trapezoidal Baffled Outlet

Hyatt (1965) has studied the use of baffles in a trapezoidal open channel expansion. The trapezoidal expansion was required to operate under conditions of both subcritical and supercritical flow in the approach channel (flume throat). After considerable experimentation with various divergences and numerous combinations of vanes, blocks, and columns for spreading the flow to prevent separation, the design shown in Fig. 10 was found satisfactory. The use of a leading baffle (column) with a triangular cross section was found to be more successful in curbing separation than the square baffle. The velocity distribution at the exit of the trapezoidal expansion (Fig. 11) is fairly uniform. The head loss in the trapezoidal expansion was nearly the same with or without the columns, which can probably be attributed to the streamlining effect of the triangular baffles. In order to satisfactorily distribute the flow in the expansion, it was necessary to extend the height of the baffles through the entire depth of flow. Also, the studies pointed out the desirability of minimizing the cross-sectional area of the baffles, thereby minimizing the amount of constriction in the expansion with consequent improvements in flow conditions.

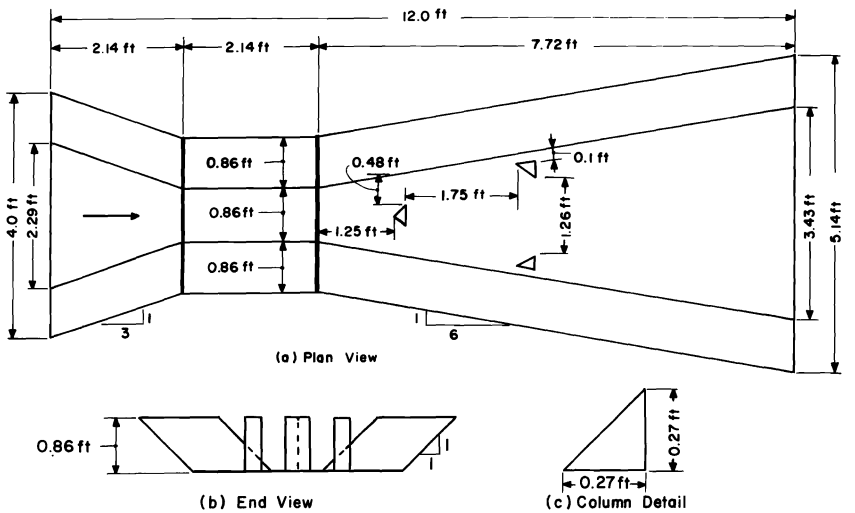

Fig. 10. Model trapezoidal flume.

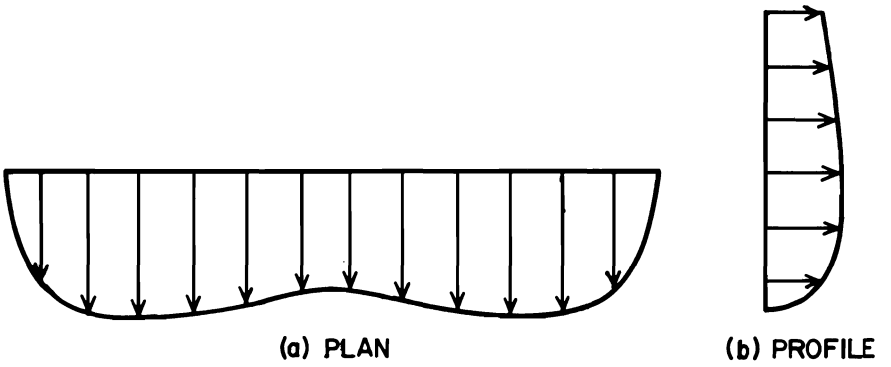

Fig. 11. Typical velocity distribution at exit of trapezoidal expansion.

Rectangular Baffled Outlets

Smith and Yu (1966) proposed a shortened outlet structure with three square baffles to rapidly spread the flow. A schematic sketch of their proposed baffled outlet structure is shown in Fig. 12.

The head loss, h_L, was calculated as the difference between the upstream specific energy, E_1, and the downstream specific energy, E_2.

$$h_L = E_1 - E_2 \quad \ldots\ldots\ldots\ldots\ldots (2)$$

where

$$E_1 = y_1 + \frac{(Q/by_1)^2}{2g} \quad \ldots\ldots\ldots (3)$$

and

$$E_2 = y_2 + \frac{(Q/By_2)^2}{2g} \quad \ldots\ldots\ldots (4)$$

in which Q is the discharge, g is the acceleration due to gravity, b is the upstream channel width, B is the downstream channel width, and y_1 and y_2 are the upstream and downstream flow depths, respectively.

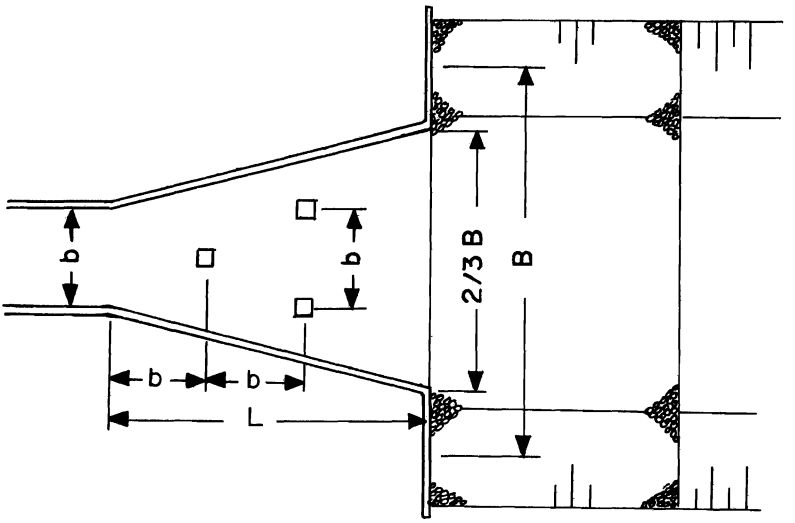

Fig. 12. Definition sketch for the baffled outlet.

A head loss coefficient, C_L , was computed from the equation

$$C_L = \frac{h_L}{(1-A_r)^2 V_1^2/2g} \quad \ldots\ldots\ldots\ldots (5)$$

in which V_1 is the approach velocity and the area ratio, A_r is computed from

$$A_r = A_1/A_2 = by_1/By_2 \quad \ldots\ldots\ldots (6)$$

Smith and Yu (1966) used Eq. 5 because it gave C_L as a constant independent of the B/b ratio. The variation in B/b is accounted for implicitly in the term $(1-A_r)^2$. The form of Eq. 5 corresponds to the Borda equation for head loss in a sudden enlargement.

The conclusions reached by Smith and Yu are listed below:

1. The natural rate of expansion of a subcritical jet is gradual, about 5(B-b).
2. To avoid flow separation from the boundary of a plain diverging transition, a long and costly outlet structure would be required.

3. A straight walled diverging transition is more efficient than a curved wall transition of the same length.
4. Flow will separate from one sidewall of a plain straight walled transition with a sidewall flare of 1 in 4, except at low values of B/b.
5. Baffles may be used advantageously to assist in spreading the flow and reducing the velocity.
6. Using a triangular baffle arrangement consisting of three square baffles extending through the full depth of flow, a subcritical jet may be decelerated in a fraction of the length required for a natural expansion. A suitable length is L = 2(0.667B-b).
7. The head loss coefficient for the outlet with three baffles may be taken as 0.8 for design purposes.

EXPERIMENTAL DESIGN

Physical Layout

The experimental expansion design and the collection of data was done in the Fluid Mechanics Laboratory (Fig. 13) located in the Engineering and Physical Science Building at Utah State University. A flume recessed in the floor having a width of 5 feet and a depth of 5 feet was employed. Water was pumped from a sump located in the basement of the laboratory into a 12-inch diameter pipeline which discharges into the flume. The depth of flow in the flume was controlled by a tailgate located near the downstream end of the flume.

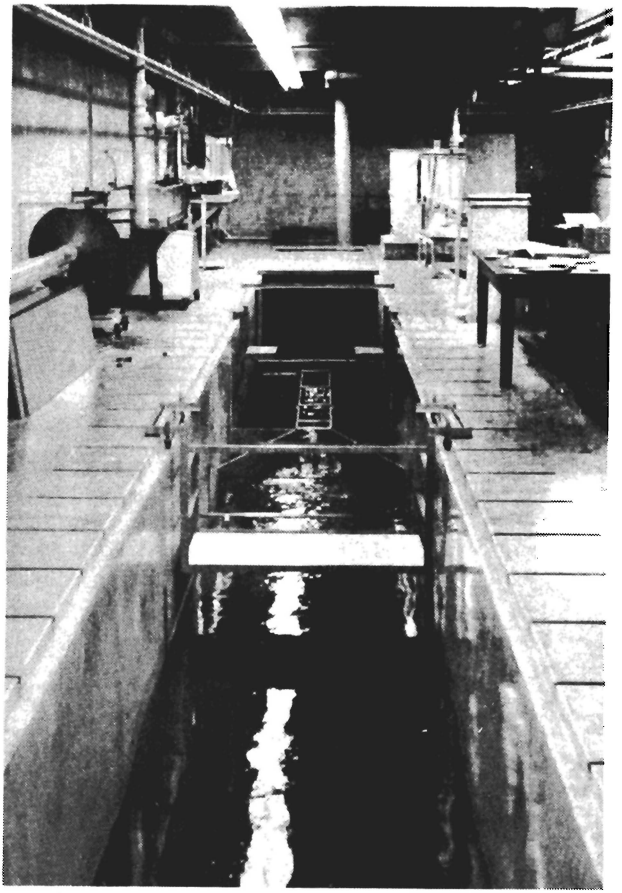

Fig. 13. Fluid Mechanics Laboratory.

The layout of the expansion in the 5-foot flume is shown in Fig. 14. The flow in the flume is first reduced to a 1-foot section by wing walls converging at a rate of 2:3 (2 transversely to 3 longitudinally). The flow stabilizes in the 1-foot section which is 12-feet long. A view of the experimental expansion design showing the inlet section and 1-foot section is shown in Fig. 15. The depth of flow (y_1) is measured 2 feet upstream from the inlet to the expansion. The experimental expansion was constructed with a plywood floor which extended 13½ feet downstream from the throat. This formed a smooth floor on which different expansion configurations could be set. A view of the experimental expansion showing the plywood floor and downstream section is shown in Fig. 16. The layout is so designed that walls can be set along the plywood floor section to form a 3-foot wide channel downstream from the expansion. The downstream section of the experimental design can also be seen in Fig. 17. The grooves in the plywood floor are cut for the 3-foot downstream section. The walls to the 3-foot section were held in place with rods fastened to nuts anchored in the plywood floor. A photo portraying the 3-foot section in place is shown in Fig. 18.

The object of the design was to allow for a wide range of expansion divergence ratios and the additional advantage of changing the width of the channel downstream from the expansion. The range of expansion divergence ratios and downstream channel widths are shown in Fig. 19. The expansions used were an abrupt, 1:1, 1:1½, 1:3, and 1:6. Each expanded from a 1-foot channel to both 3-foot and 5-foot downstream widths. For example, the 1:1 expansion is set up from the 1-foot section to the full 5-foot width of the flume (B/b = 5.0). Then, after collecting the necessary hydraulic data, the walls could be set in the plywood floor to form a 3-foot downstream channel width (B/b = 3.0) and the hydraulic data collected for the new expansion ratio. The experiment could then proceed to a new divergence ratio.

Instrumentation

The measurement of flow quantity, velocity, and depths were made by weighing tank, Ott current meter, and point gages, respectively. The depth measurement at 2 feet upstream from the expansion throat was measured with a point gage positioned over a stilling well, which was connected to the side of the 1-foot section. The location of all measurements of depth and velocity in the expansion downstream from the inlet is shown in Fig. 20. The distance downstream in each expansion to the point of depth and velocity measurements is referenced with respect to the expansion length, L.

Except for the depth at 3/4 L, all measurements in and beyond the expansion were made from a movable carriage. The carriage (Fig. 21) was designed to move along the grooves in the floor above the recessed flume. The carriage can be secured at any position along the flume by bolting into the recession in the laboratory floor along the flume. The track on which the point gage and Ott current meter are mounted is shown in Fig. 22. The point gage and meter can traverse the width of the flume, thereby allowing depth and velocity measurements to be made at any desired point.

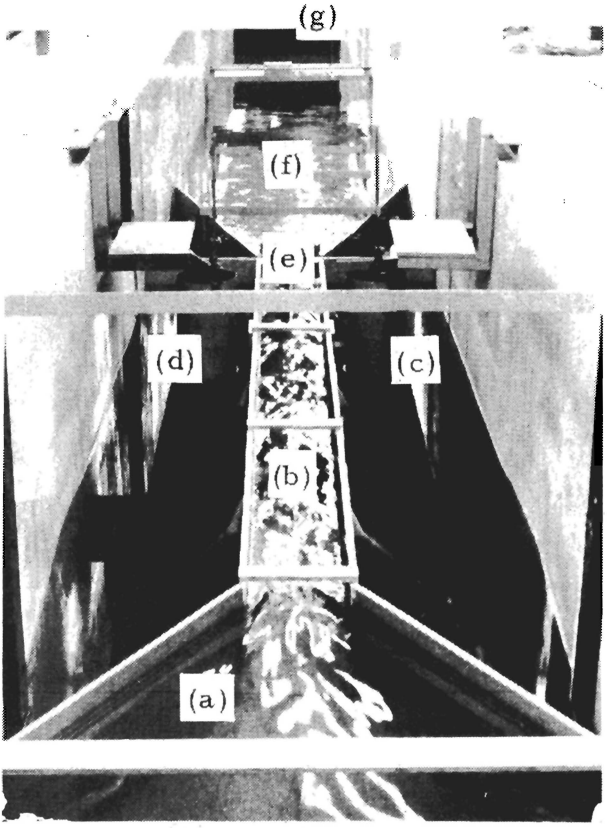

(a) inlet to 1-foot channel
(b) 1-foot channel section
(c) well for depth measurement of y_1
(d) well for depth measurement at y_2 (3/4 L)
(e) throat or inlet to expansions
(f) 13-1/2 foot long downstream section, on which expansions and channel widths of 3-foot and 5-foot are set
(g) tailgate for controlling flow depth

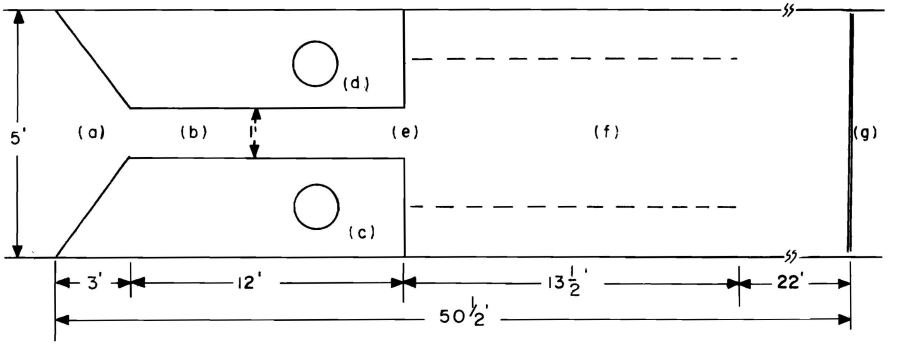

Fig. 14. Experimental expansion design layout.

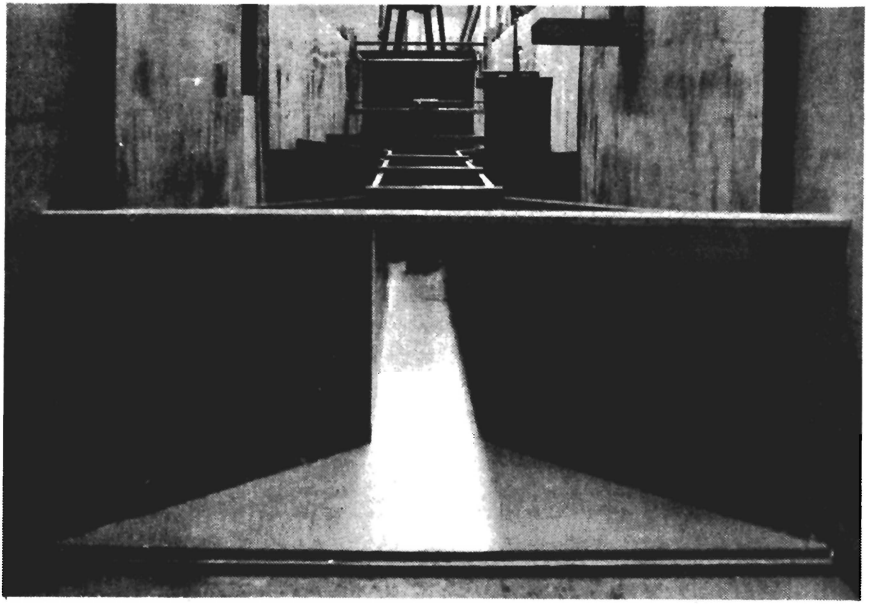

Fig. 15. View from upstream (looking downstream) of the experimental expansion design.

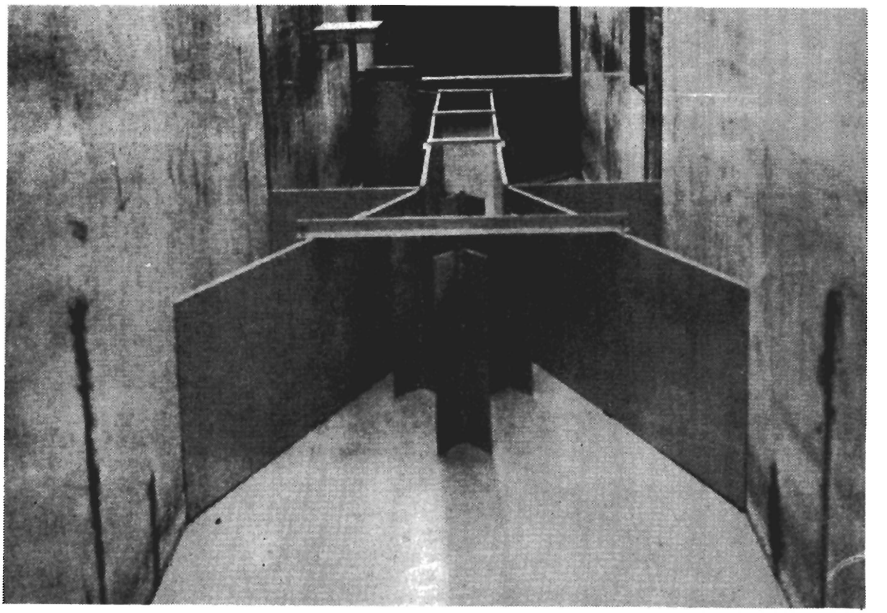

Fig. 16. View from downstream (looking upstream) of the experimental expansion design.

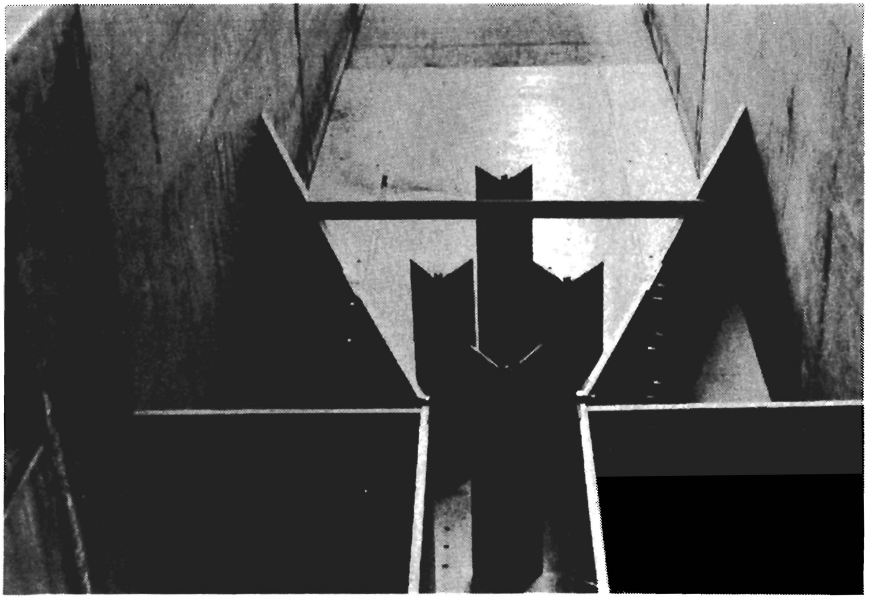

Fig. 17. View of downstream section with expansion ratio of 1:3 and B/b ratio of 5.

Fig. 18. View of downstream section with expansion ratio of 1:3 and B/b ratio of 3.

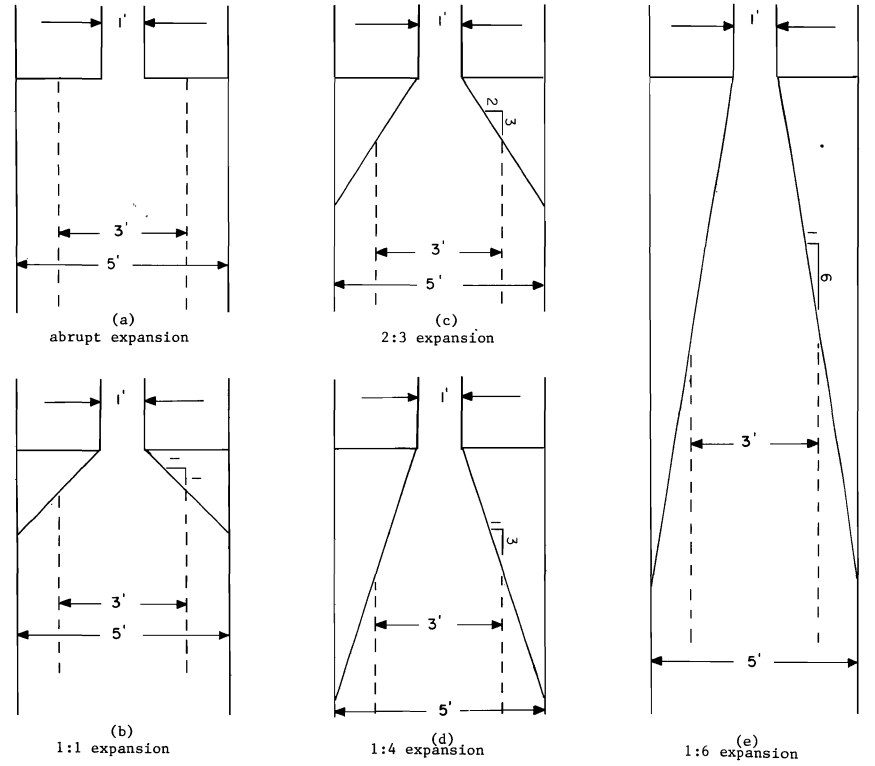

Fig. 19. Layout of flumes showing range of expansion and channel widths.

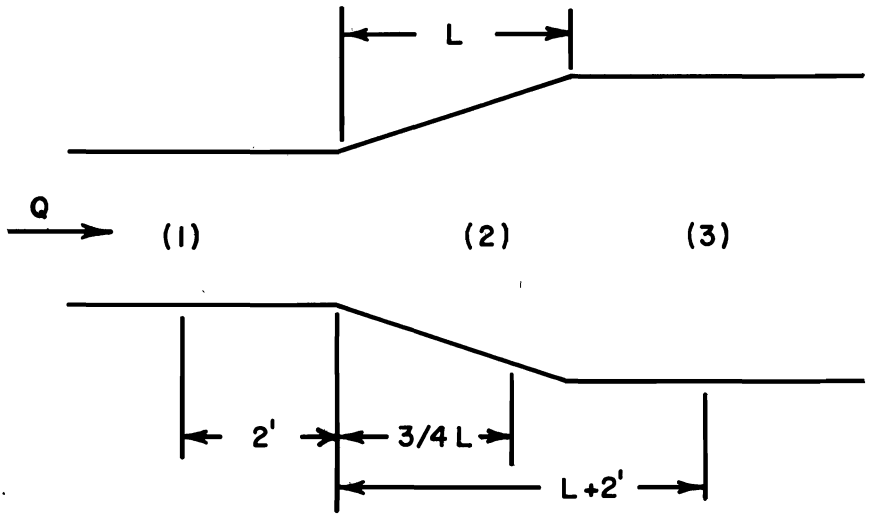

Fig. 20. Reference to points of measurement through expansion.

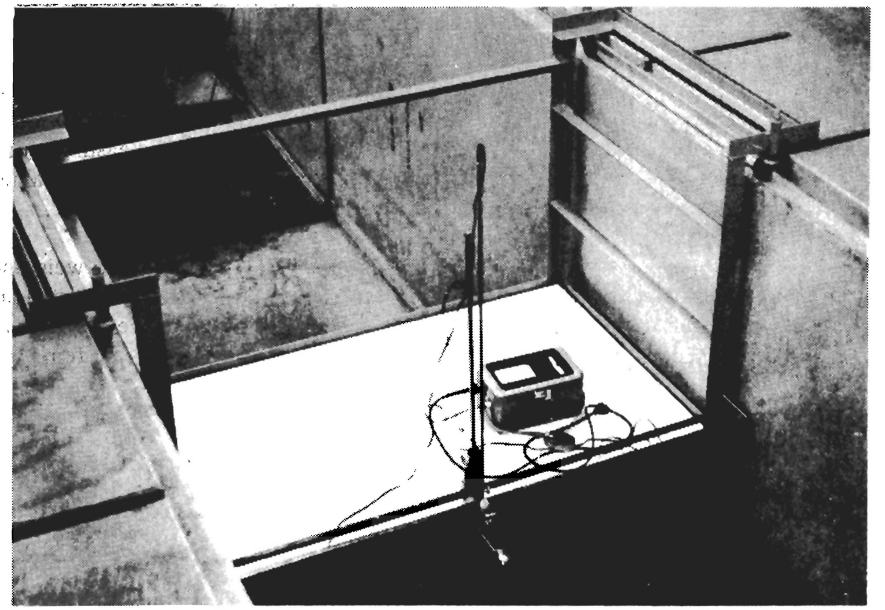

Fig. 21. Measurement carriage.

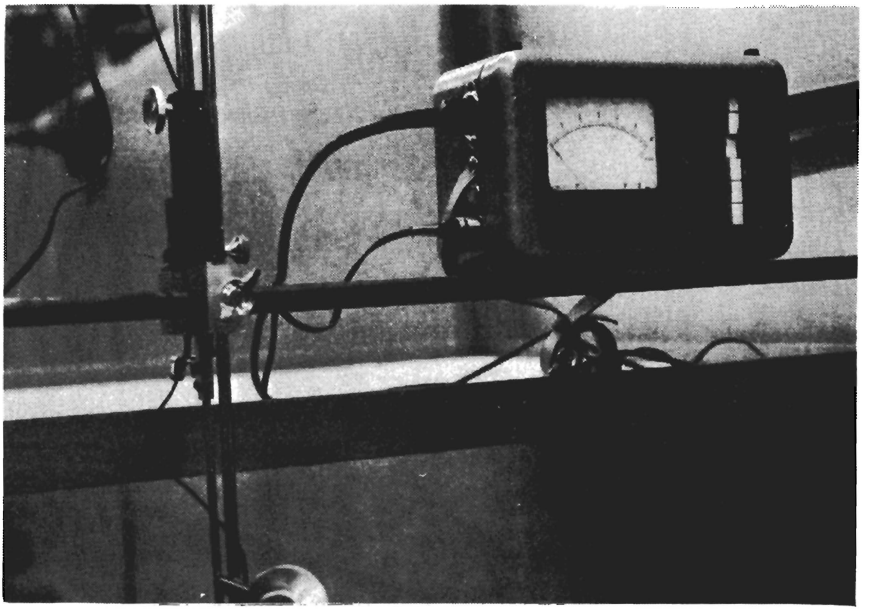

Fig. 22. Measurement carriage showing Ott current meter and point gage.

Measurements of flow depth and velocity were taken at 3/4 L, L, and L + 2, whenever possible. The depth and velocity were measured every 6 inches across the flume width at each cross section along the flume under consideration. Velocity measurements used in preparing the velocity profiles are the mean values obtained from averaging the 0.2 and 0.8 depth measurements. Velocities used in data computation of specific energy are mean values determined from the continuity equation.

The flow rate was determined by discharging the water into a weighing tank and measuring the length of time required to accumulate a particular weight of water. After obtaining a flow rate measurement, the water was discharged into the sump, where it could be recirculated through the system.

ENERGY LOSS ANALYSIS

The technique reported by Skogerboe and Hyatt (1967) for analyzing submergence in flow measuring flumes can be modified in order to analyze energy losses in open channel expansions. A typical submerged flow plot is shown in Fig. 23, where: (1) the discharge, Q, is plotted on the ordinate; (2) the change in water surface elevation, $y_u - y_d$, between a point upstream (y_u) and downstream (y_d) from the constriction is plotted along the abscissa; and (3) the submergence, y_d/y_u, is the varying parameter. By substituting E_u and E_d for y_u and y_d, where E_u and E_d are the specific energies at locations upstream and downstream from the structure being analyzed, the abscissa of a subcritical flow plot becomes the energy loss, h_L. The subscripts u and d are used to denote the general case where any depth upstream or downstream from the expansion could be used.

Data reported by Smith and Yu (1966) can be used to demonstrate the analysis of energy loss in an open channel expansion. Hydraulic data for an abrupt outlet are listed in Table 1 and plotted in Fig. 24, whereas the data for the baffled outlet are listed in Table 2 and plotted in Fig. 25. As can be seen from the plotted points in Figs. 24 and 25, the data are quite consistent. For the abrupt outlet (Fig. 24), the energy loss curves are quite different from Runs 1-11 (B/b = 3.0) than from Runs 12-22 (B/b = 1.5). Thus, the expansion ratio, B/b does have a significant effect on the head loss occurring in the structure. This same effect can be seen in the energy loss curves for the baffled outlet (Fig. 25), where Runs 7-16 (B/b = 4.0) are compatible with Runs 17-25 (shortened outlet with B/b = 4.0), but Runs 1-6 (B/b = 3.0) require a completely different family of curves to describe the head loss.

Smith and Yu (1966) arrived at an average coefficient of head loss, C_L, of 0.8 for the baffled outlet (Table 2). Yet, the energy loss curves (Fig. 25) show a definite effect due to the expansion ratio, B/b. Therefore, the coefficient of head loss should at least vary with the expansion ratio. Secondly, based upon a knowledge of subcritical flow at open channel constrictions, it would appear that the coefficient of head loss would be a function of the specific energy ratio, E_2/E_1.

Initially, the problem is to establish the validity of the Borda equation:

$$h_L = C_L (1-A_r)^2 V_1^2/2g \quad \ldots\ldots\ldots (5)$$

Since the writers have confidence in the energy loss curves (Figs. 24 and 25), a determination of the validity of the Borda equation will be attempted by relating this equation (Eq. 5) to the energy loss curves. The hypotheses for establishing the validity of Eq. 5 are listed below.

For any line of constant specific energy ratio in Fig. 24 or 25, the equation is

$$Q = Ch_L^{n_1} \quad \ldots\ldots\ldots\ldots \quad (7)$$

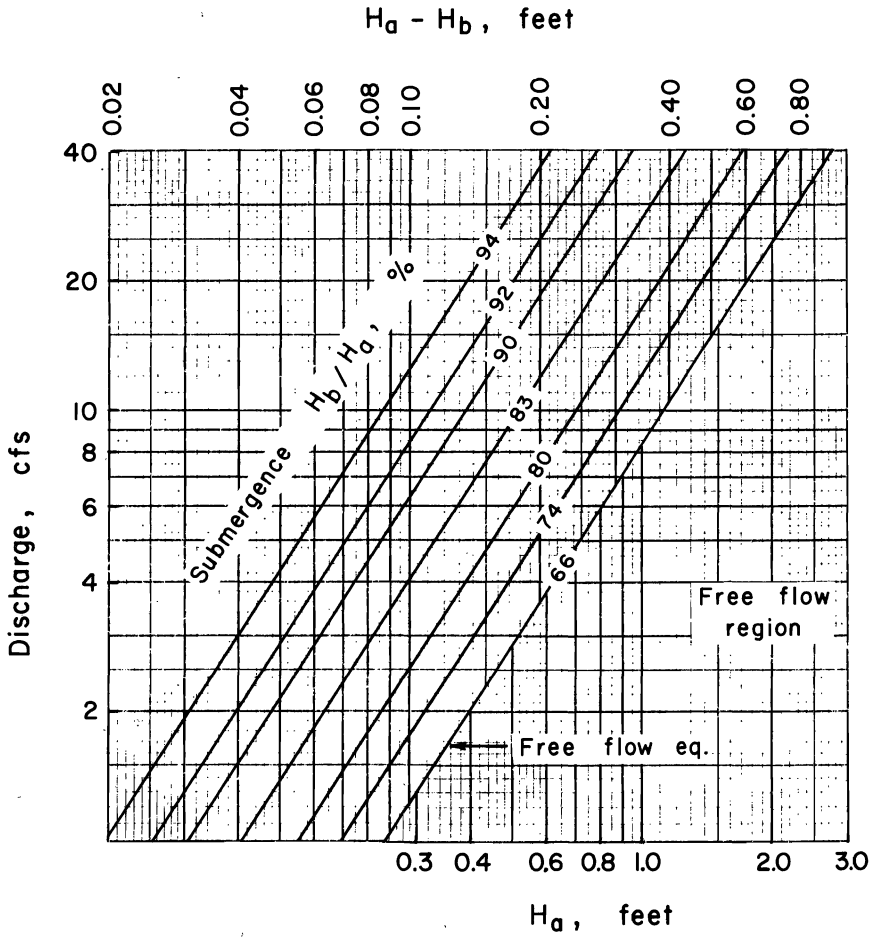

Fig. 23. Typical submerged flow calibration curves for an open channel constriction.

Table 1. Hydraulic data for abrupt outlets. (Taken from Smith and Yu, 1966.)

Run	B/b	Q	y_1	V_1	F_1	E_1	y_2	V_2	E_2	h_L	C_L	E_2/E_1
1	3.0	0.189	0.458	1.238	0.332	0.4818	0.468	0.404	0.4705	0.0113	1.042	0.9765
2	3.0	0.189	0.337	1.684	0.512	0.3811	0.352	0.537	0.3565	0.0246	1.200	0.9354
3	3.0	0.189	0.239	2.375	0.856	0.3256	0.270	0.700	0.2776	0.0480	1.101	0.8525
4	3.0	0.247	0.414	1.790	0.491	0.4637	0.433	0.570	0.4380	0.0257	1.112	0.9445
5	3.0	0.247	0.330	2.250	0.691	0.4085	0.362	0.683	0.3692	0.0393	1.040	0.9037
6	3.0	0.247	0.257	2.880	1.000	0.3859	0.302	0.818	0.3124	0.0735	1.112	0.8095
7	3.0	0.167	0.466	1.073	0.277	0.4839	0.473	0.352	0.4749	0.0090	1.113	0.9814
8	3.0	0.067	0.299	1.672	0.539	0.3424	0.315	0.529	0.3193	0.0231	1.136	0.9325
9	3.0	0.167	0.225	2.220	0.825	0.3015	0.254	0.656	0.2607	0.0408	1.077	0.8646
10	3.0	0.180	0.218	2.475	0.935	0.3132	0.253	0.711	0.2609	0.0523	1.084	0.8330
11	3.0	0.180	0.343	1.572	0.473	0.3814	0.361	0.498	0.3649	0.0165	0.922	0.9567
										AVERAGE	1.08	
12	1.5	0.264	0.2555	1.549	0.540	0.02927	0.2735	0.965	0.2879	0.0048	0.908	0.9836
13	1.5	0.264	0.217	1.842	0.681	0.2687	0.241	1.095	0.2596	0.0091	1.106	0.9661
14	1.5	0.264	0.186	2.130	0.870	0.2565	0.221	1.195	0.2432	0.0133	0.983	0.9481
15	1.5	0.285	0.368	1.160	0.337	0.3889	0.377	0.755	0.3858	0.0031	1.216	0.9920
16	1.5	0.285	0.287	1.486	0.489	0.3213	0.303	0.939	0.3167	0.0046	0.994	0.9856
17	1.5	0.285	0.246	1.735	0.615	0.2927	0.268	1.061	0.2855	0.0072	1.022	0.9754
18	1.5	0.285	0.204	2.090	0.815	0.2717	0.235	1.209	0.2577	0.0140	1.162	0.9404
19	1.5	0.224	0.393	0.855	0.241	0.4044	0.3985	0.562	0.4034	0.0010	0.744	0.9975
20	1.5	0.224	0.280	1.200	0.400	0.3024	0.291	0.770	0.3002	0.0022	0.767	0.9927
21	1.5	0.224	0.228	1.473	0.544	0.2617	0.243	0.922	0.2562	0.0055	1.158	0.9789
22	1.5	0.224	0.173	1.941	0.823	0.2314	0.200	1.120	0.2195	0.0119	1.133	0.9485
										AVERAGE	1.02	

Note: $E_1 = y_1 + V_1^2/2g$; $E_2 = y_2 + V_2^2/2g$; $h_L = E_1 - E_2$.

where C is a constant (i.e., the value of Q for $h_L = 1.0$) and n_1 is the slope of the line of constant specific energy ratio on the logarithmic plot.

Now, using any one of the sets of curves in Fig. 24 or 25 (B/b = constant), determine C and n_1 for E_2/E_1 = constant. Then, by assuming a value of discharge, Q, the head loss, h_L, can be computed. Knowing E_2/E_1 and h_L, E_1 and E_2 can be computed. By trial and error, y_1 and y_2 can be determined since E_1 and E_2 are known. Then, C_L can be computed from Eq. 5. The procedure should be repeated by assuming additional values of Q (E_2/E_1 = constant and B/b = constant) and computing C_L.

After having computed a number of values of C_L for one of the lines of constant specific energy ratio in Fig. 24 or 25, then one of the following propositions will be valid: (a) if C_L is not a constant, the Borda equation is not valid for describing the head loss in an open channel expansion under

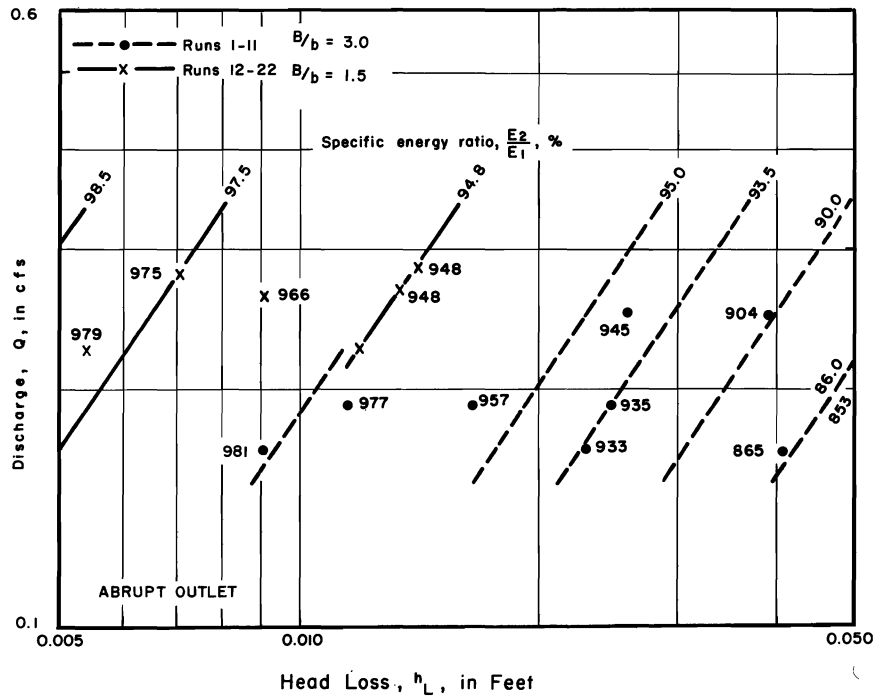

Fig. 24. Head loss for subcritical flow in abrupt outlets.

Table 2. Hydraulic data for baffled outlets. (Taken from Smith and Yu, 1966.)

un	B/b	Q	y_1	V_1	F_1	E_1	y_2	V_2	E_2	h_L	C_L	E_2/E_1
1	3.0	0.165	0.474	1.045	0.268	0.4910	0.482	0.342	0.4836	0.0072	0.938	0.9853
2	3.0	0.165	0.310	1.597	0.505	0.3496	0.331	0.499	0.3349	0.0147	0.785	0.9579
3	3.0	0.165	0.236	2.100	0.761	0.3045	0.272	0.607	0.2777	0.0268	0.774	0.9120
4	3.0	0.199	0.264	2.255	0.774	0.3431	0.306	0.649	0.3125	0.0306	0.764	0.9108
5	3.0	0.199	0.369	1.614	0.468	0.4094	0.390	0.509	0.3940	0.0154	0.813	0.9684
6	3.0	0.199	0.458	1.300	0.339	0.4843	0.470	0.422	0.4728	0.0115	0.959	0.9763
										AVERAGE	0.84	
7	4.0	0.488	0.330	1.774	0.544	0.3789	0.353	0.415	0.3557	0.0232	0.809	0.9368
8	4.0	0.267	0.316	1.013	0.318	0.3320	0.323	0.248	0.3240	0.0080	0.878	0.9759
9	4.0	0.424	0.246	2.065	0.733	0.3121	0.281	0.452	0.2842	0.0279	0.692	0.9106
10	4.0	0.326	0.374	1.044	0.301	0.3939	0.382	0.256	0.3830	0.0079	0.820	0.9798
11	4.0	0.319	0.376	1.018	0.292	0.3921	0.383	0.250	0.3840	0.0081	0.881	0.9793
12	4.0	0.421	0.394	1.282	0.360	0.4195	0.407	0.310	0.4085	0.0110	0.750	0.9738
13	4.0	0.339	0.314	1.293	0.407	0.3400	0.327	0.311	0.3285	0.0115	0.765	0.9662
14	4.0	0.434	0.329	1.581	0.486	0.3678	0.349	0.373	0.3512	0.0166	0.731	0.9547
15	4.0	0.375	0.255	1.765	0.615	0.3034	0.282	0.399	0.2854	0.0189	0.652	0.9377
16	4.0	0.403	0.259	1.867	0.646	0.3130	0.288	0.420	0.2907	0.0223	0.689	0.9288
										AVERAGE	0.77	
17	4.0	0.283	0.314	1.081	0.340	0.3322	0.323	0.294	0.3243	0.0079	0.819	0.9762
18	4.0	0.419	0.336	1.496	0.455	0.3708	0.354	0.389	0.3563	0.0145	0.760	0.9609
19	4.0	0.532	0.348	1.834	0.548	0.4001	0.375	0.460	0.3783	0.0218	0.745	0.9455
20	4.0	0.255	0.241	1.270	0.456	0.2660	0.254	0.353	0.2559	0.0101	0.777	0.9620
21	4.0	0.398	0.254	1.880	0.657	0.3089	0.283	0.485	0.2867	0.0222	0.735	0.9281
22	4.0	0.290	0.418	0.852	0.235	0.4193	0.413	0.222	0.4138	0.0055	0.890	0.9869
23	4.0	0.389	0.426	1.096	0.296	0.4446	0.434	0.280	0.4352	0.0094	0.914	0.9789
24	4.0	0.298	0.321	1.113	0.347	0.3403	0.330	0.302	0.3314	0.0089	0.870	0.9738
25	4.0	0.416	0.231	2.160	0.791	0.3034	0.268	0.541	0.2725	0.0309	0.762	0.8982
										AVERAGE	0.81	

Note: B = 1.0 foot for runs 1 to 6; b = 0.833 foot for runs 7 to 25; Runs 17 to 25 are for the shortened outlet.

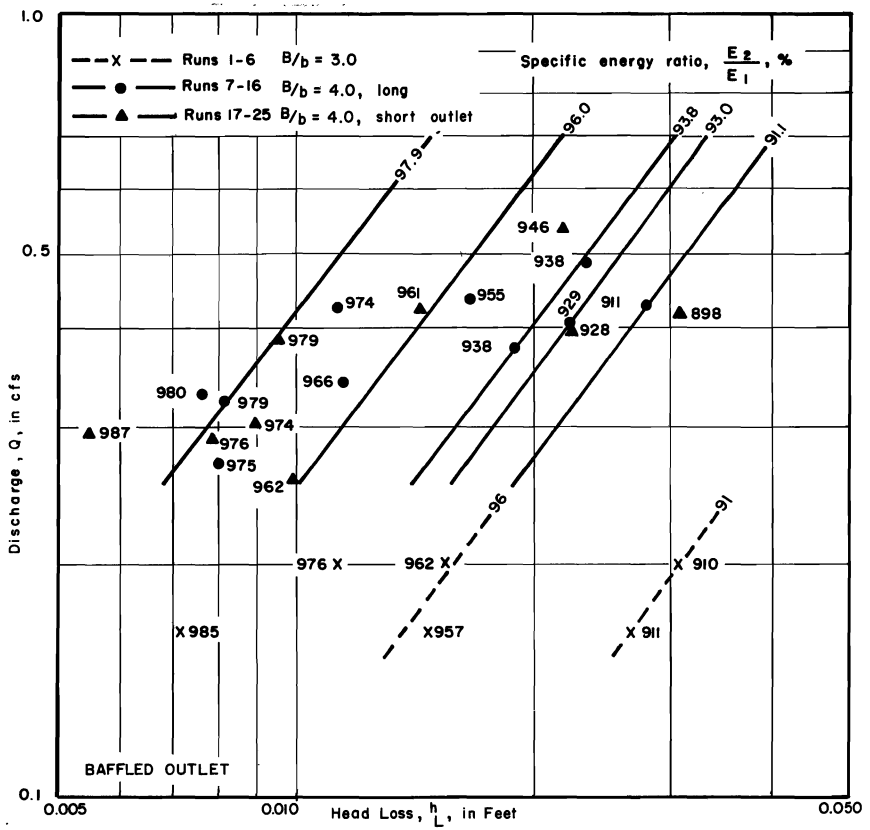

Fig. 25. Head loss for subcritical flow in baffled outlets.

subcritical flow conditions; or (b) if C_L is a constant, then the Borda equation may be valid. If (b) is true, C_L must be computed for additional lines of constant specific energy ratio. Then, one of the following propositions will be shown as valid: (c) if C_L is a constant for the different ratios, then the Borda equation is valid; or (d) if C_L is not a constant for the different specific energy ratios, then the Borda equation is not valid.

Following the above procedure, it can be shown that the coefficient of head loss, C_L, has a singular value for each line of constant specific energy ratio in Fig. 24 or 25. Thus, proposition b is true. For any family of energy loss curves in Fig. 24 or 25 (B/b = constant), C_L has a different value for each constant specific energy ratio line. Therefore, proposition d is correct. Consequently, there is a relationship between E_2/E_1 and C_L for each open channel expansion

geometry. This relationship is shown in Fig. 26 for the baffled outlet. Also, Fig. 26 shows the effect of the expansion ratio for the baffled outlet. For design purposes, it then becomes necessary to establish the C_L versus E_2/E_1 relationship for each geometry of an open channel expansion. Similar expansion geometries should yield a consistent set of relationships between the coefficient of head loss and the specific energy ratio.

For each family of specific energy ratio curves in Figs. 24 and 25, it is possible to develop a relationship between the head loss coefficient, C_L, and the Froude number in the inlet or approach channel, F_1. These relationships are shown in Fig. 27 for the baffled outlet with expansion ratios of 3 and 4. Since a unique relationship exists between the head loss coefficient and specific energy ratio for any particular geometry of open channel expansion, as well as a unique relationship between the head loss coefficient and inlet Froude number, then a unique relationship exists between the inlet Froude number and specific energy ratio for any particular open channel expansion geometry.

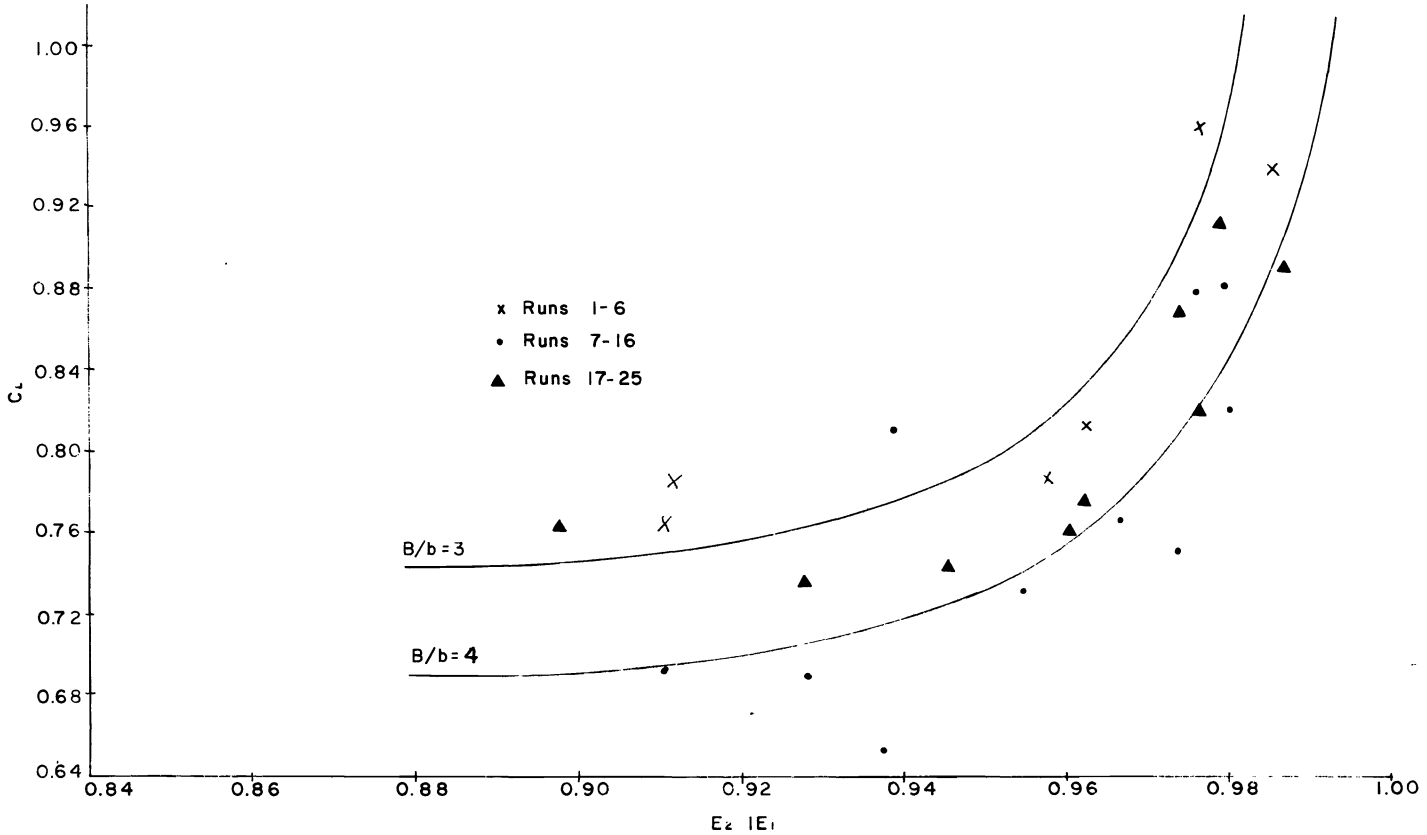

Fig. 26. Relationship between the head loss coefficient and specific energy ratio for the baffled outlet.

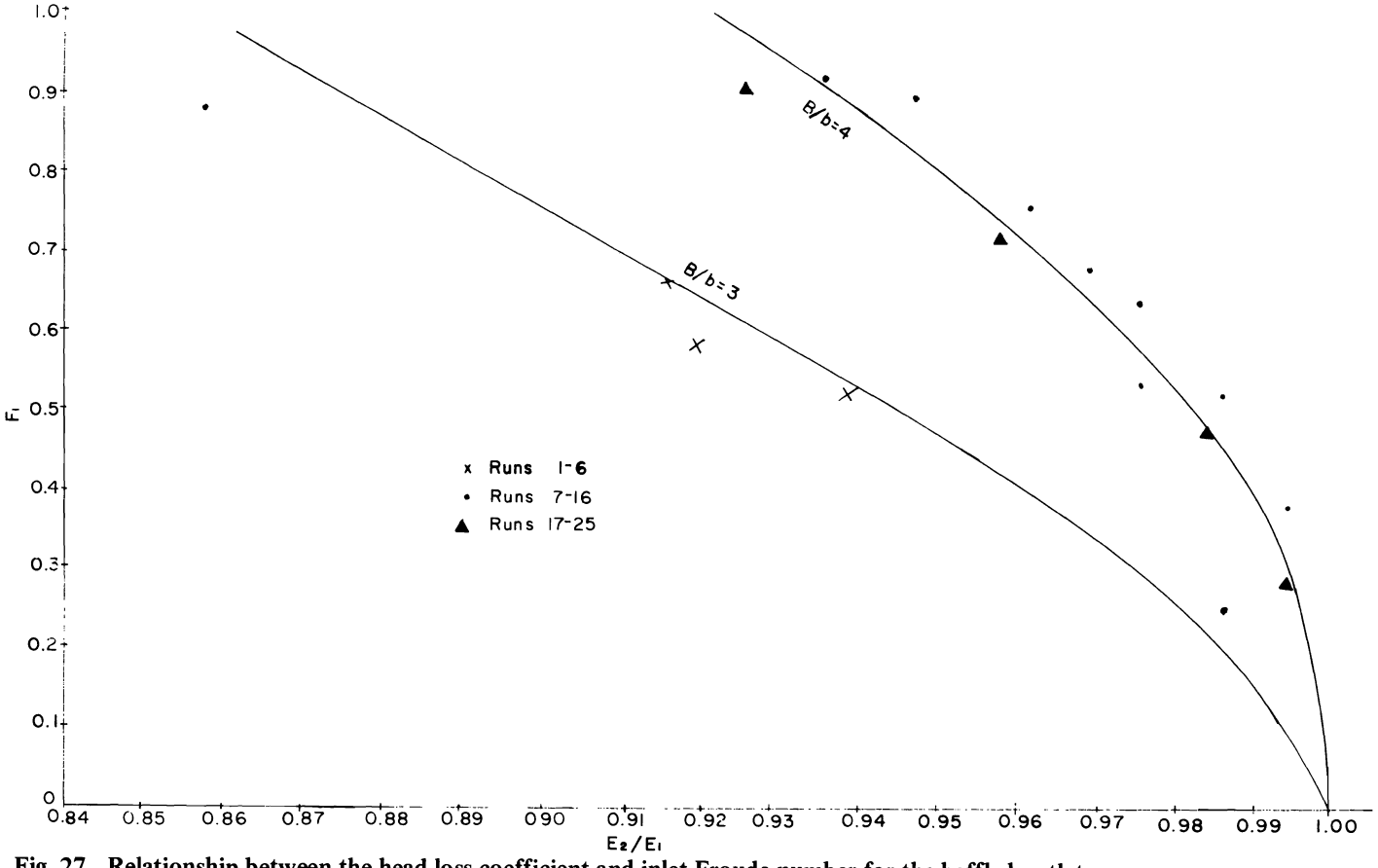

Fig. 27. Relationship between the head loss coefficient and inlet Froude number for the baffled outlet.

DEVELOPMENT OF BAFFLE DESIGN

The geometrical placement of baffles in open channel expansions was determined under the experimental program by trial and error after testing numerous baffle arrangements. Attempting to prevent flow separation was a particular problem in all of the arrangements tested. The first consideration in the design of the baffles was the use of triangular shapes (Hyatt, 1965). The second consideration was to let the divergence angle of the baffle be the same as the divergence angle of the expansion walls.

The various arrangements of baffles tested under the experimental program are shown in Fig. 28. All of the initial tests of baffle arrangements were conducted with a 1:3 divergence of the expansion walls and an expansion ratio of 5 (B/b = 5). All baffles used were set to extend through the entire depth of flow. The tests were started with the size of the baffles being 1/2 b on each side, where b is the width of the inlet section (b = 1.0 ft. in this study). As the various arrangements were tested, the size of the baffles was changed. The sizes are indicated for each arrangement shown in Fig. 28.

The placement of the baffles for the first test (Fig. 28a) was based on placements used in supercritical expansions. This arrangement will spread the baffles through the length of the expansion. For example, an expansion having a length of 3 feet would have the first baffle 1 foot downstream from the inlet section, the second at 2 feet, and the third at 3 feet. A 6-foot length would have the first baffle at 1 foot, the second at 3-1/2 feet, and the third at 4-1/2 feet. The arrangement seemed to work well for supercritical flow, but as the downstream depth was increased to cause subcritical flow, a strong central jet formed. Return eddies formed on both sides of the jet and extended along the expansion walls. When this had occurred, it was apparent that the baffles had very little effect upon the flow. The return eddies were similar to flow conditions without baffles.

The second placement of baffles (Fig. 28b) was similar to the placement used by Smith and Yu (1966). This differed from the configuration in Fig. 28a in that the second baffles were at a distance 2b from the expansion inlet and the last baffle was removed. Tests for this arrangement indicated similar results to the first placements. However, the jet shifted to one side and a large return eddy formed on the other side.

The hydraulic performance of the first two baffle arrangements indicated that a better means for laterally spreading the flow in the expansion must be developed. Even with the first baffle at a distance b downstream, the return

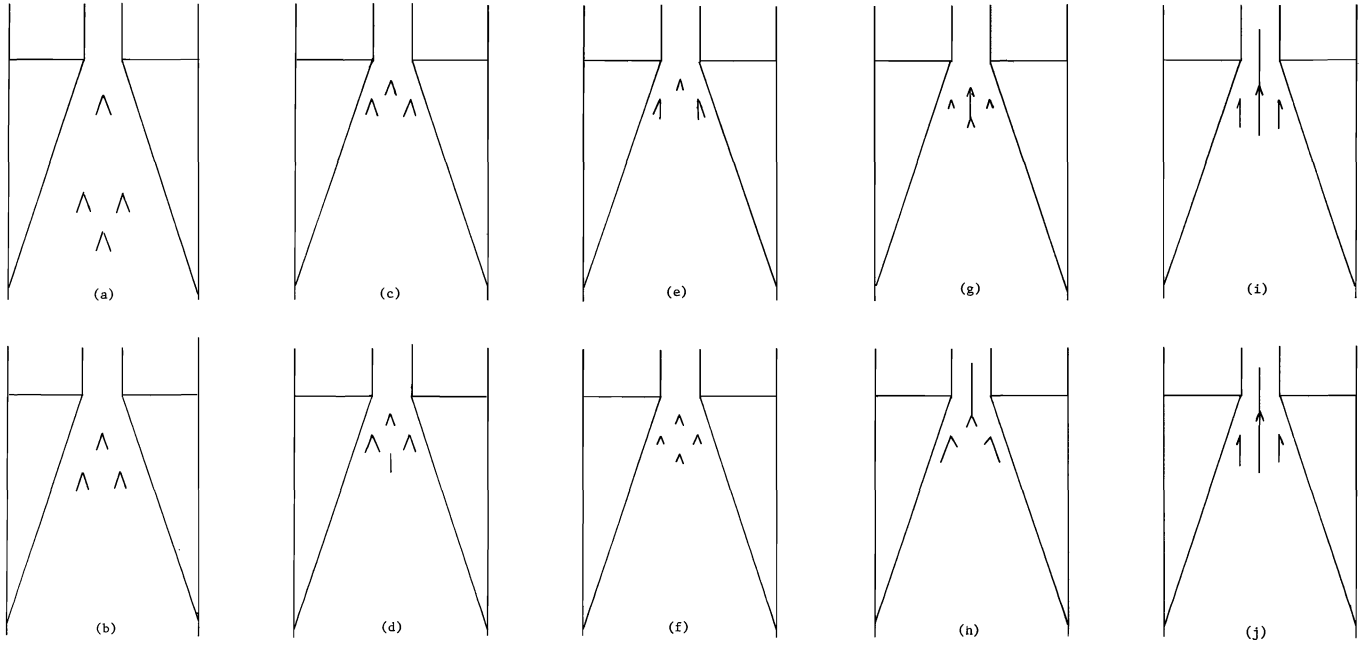

Fig. 28. Arrangement of baffles used in developing final baffle designs.

eddy follows the expansion wall upstream to a point beyond the first baffle, where the eddy currents control the direction and spreading of the flow rather than the first baffle.

For the third test of baffle arrangements (Fig. 28c), the baffles had the same configuration as in Fig. 28b, but the first baffle was at a distance b from the expansion inlet. The moving of the baffles 1/2 b nearer the expansion inlet decreased the tendency of current from the return eddy to control the flow in the expansion ahead of the first baffle. Although this baffle placement was an improvement, it still was not satisfactory. The flow separated and followed the expansion as intended, but due to the width of the lead baffle, almost all of the flow followed the expansion walls, thereby causing return eddies from both sides. The flow near the end of the expansion was quite unstable due to the mixing of these eddies. This resulted in a shifting of the downstream conditions which would form a large return eddy on one side or the other. This eddy would extend upstream to just behind the second row of baffles. The results of this test indicated that the width of the lead baffle caused nearly all the flow to follow the sides and allowed very little to pass through the center.

The next configuration tested was an attempt to allow the flow to pass through the center while at the same time directing it along the expansions walls. This baffle arrangement is shown in Fig. 28d. The first baffle was still set at 1/2 b downstream from the inlet, but the sides were cut down to 1/4 b. Reducing the width of the lead baffle allowed a significant amount of the flow to pass through the center of the expansion, while also spreading the flow along the walls. However, as the flow passes along the center, the second row of baffles directed much of the flow toward the middle. The third baffle was closed and set with the leading edge 1-1/2 b downstream from the inlet. It was expected that the third baffle would act as a fin to direct the flow, but it had little affect on changing the flow pattern established by the second row of baffles. The flow downstream still formed strong eddies on one side or the other of the channel.

The next baffle arrangement tested is shown in Fig. 28e. The baffle arrangement seemed to result in somewhat the same hydraulic problems as encountered with the baffles shown in Fig. 28d. The return eddy formed behind the center baffles depending on the separation of flow by the lead baffle. The attempt to guide the flow straight downstream by having the inside of the second baffle set parallel to the intended direction of flow showed some promise, but was unsatisfactory in this particular baffle arrangement.

The four baffles in the next test, shown in Fig. 28f, were all cut down to 1/4 b on a side. The first baffle was at 1/2 b downstream from the inlet; the next two baffles at a distance b downstream, and the fourth baffle at 1-1/2 b downstream from the inlet. The flow pattern resulting from this baffle arrangement also failed to prevent strong return eddies from forming in the downstream portion of the expansion beyond the baffles. The effect of this arrangement upon hydraulic conditions at the inlet seemed satisfactory. The next change, shown in Fig. 28g, was an attempt to better control the flow in the downstream portions of the expansion. The results indicated this to be a step in

the right direction. The problem of a return eddy forming downstream seemed mainly due to the unequal division of the flow at the lead baffle.

From this point, several arrangements (one of these is shown in Fig. 28h) were attempted to divide the flow as it entered the expansion and direct it in the downstream portion to avoid the formation of strong return eddies.

The next arrangement, shown in Fig. 28i, proved to be the best of those tested. The plate used to divide the flow extended 1-1/2 feet (3b/2) upstream from the expansion inlet. The division of the flow was very uniform at this point. The first baffle was attached directly to the plate. The sides of the baffle were attached at a point 1/2 b downstream from the inlet. The divider plate, which was 3-1/2 b long, extended to a distance of 2 b downstream from the inlet. The baffles in the second row were set as shown in Fig. 28i. As shown, one side of the baffle was lengthened to 3/4 b while the other side remained at 1/4 b. These two baffles were set so that the 1/4 b side was parallel to the expansion wall and the 3/4 b side parallel to the centerline of the outlet structure.

Although some problem of return eddies forming still persisted, the overall results from the baffle arrangement shown in Fig. 28i were quite satisfactory. The flow is first divided by the plate in the inlet section. Then, as the flow enters the expansion, the first baffle causes the initial spreading of the flow. As the flow comes in contact with the second baffles, it is approximately divided again. The edge of the baffle parallel to the expansion wall directs the flow along the expansion wall. The flow that passes between the 3/4 b edges of the second baffle and the plate in the center is stabilized to the point that it is directed downstream parallel to the intended direction of flow. The overall affect is the controlling and spreading of the flow in the downstream portion of the expansion.

When the arrangement shown in Fig. 28i was tested for expansions other than those with 1:3 divergence ratio, the approximate division of the flow by the second baffles was poor. Because of this, one more change was made from the arrangement shown in Fig. 28i; to arrive at the final design. The distance between the second two baffles, which had been b in all previous baffle arrangements tested, was made a variable distance which would depend on the width of the expansion at a distance b downstream. The final baffle design is shown in Figs. 29 and 30 operating with a divergence ratio of 2:3 and an expansion ratio of 3 and 5, respectively. The range of different expansions is illustrated in Fig. 31. The range is from an abrupt expansion (Fig. 31a), to an expansion with a 1:6 divergence ratio as shown in Fig. 31e. The lateral distance between the second baffles, except for abrupt expansions, is 0.55 W_b, where W_b is the width of the expansion at a distance b downstream from the inlet.

Although the distance W_b is a constant for any fixed values of inlet width and divergence ratio, the expansion ratio, B/b, may be varied. Analysis of data where B/b was varied while W_b remained constant will be noted later.

For the case of the abrupt expansion, the lateral distance between the second baffles is a function of the inlet width, b, and is equal to 1.5 b. For the

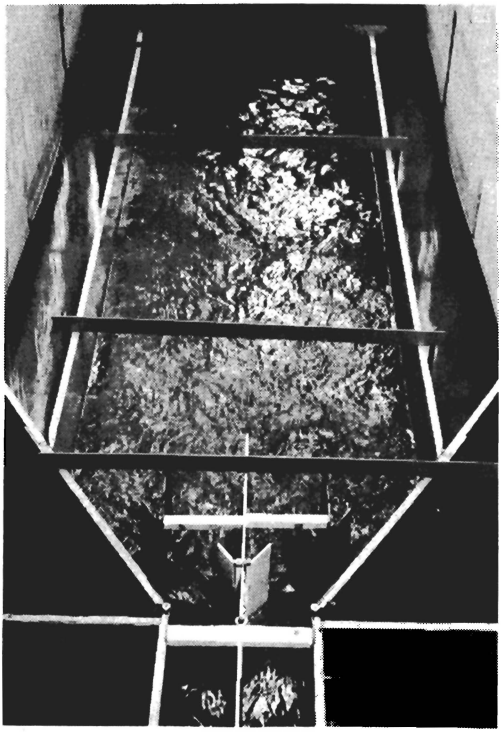

Fig. 29. Experimental flume with 2-3 expansion ratio and a B/b ratio of 3, operating with final baffle design.

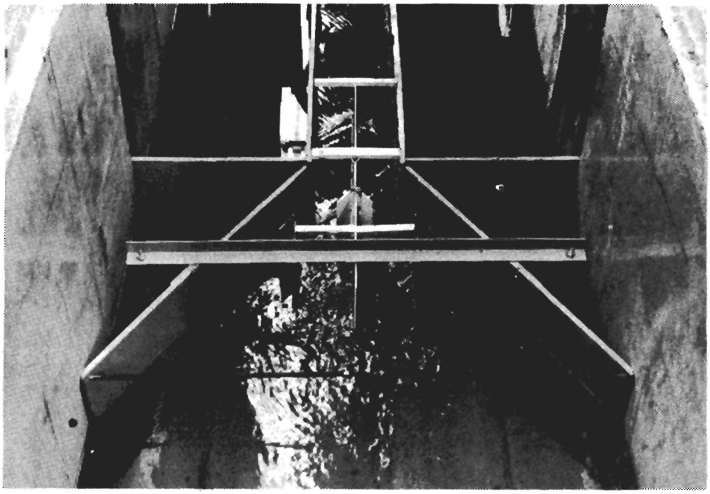

Fig. 30. Experimental flume with 2-3 expansion ratio and a B/b ratio of 5, operating with final baffle design.

abrupt expansion, the range of B/b has limits both as B/b approaches the value of b and when B/b is extremely large. Analysis of data where B/b is varied while b remains constant will be noted later. A definition sketch detailing the location of the baffles for this final design of triangular-shaped baffles for open channel expansions with vertical walls is shown in Fig. 32.

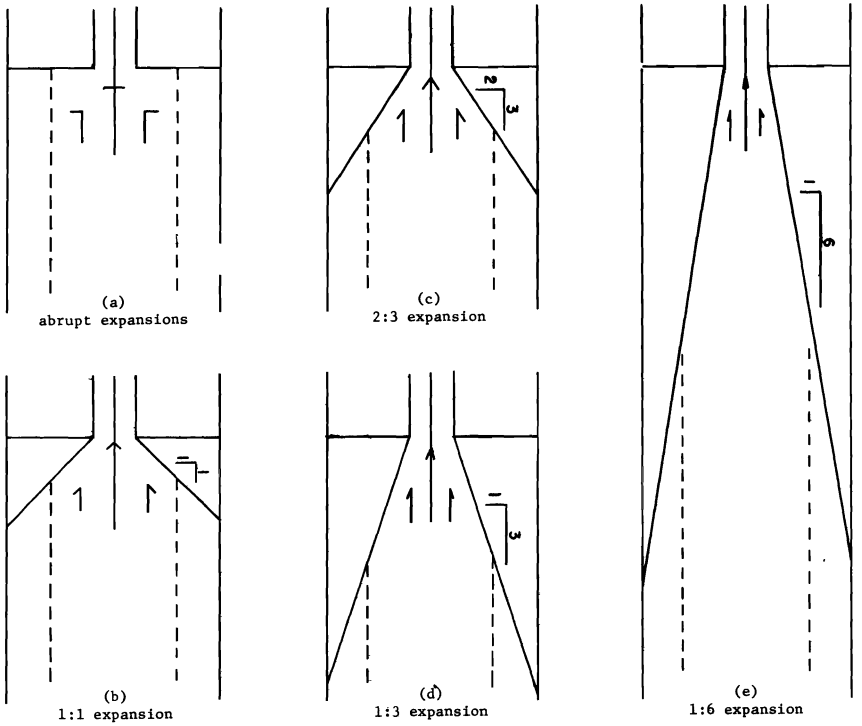

Fig. 31. Illustration of the range of divergences (abrupt to 1:6) and expansion ratios of B/b = 5 and 3 respectively.

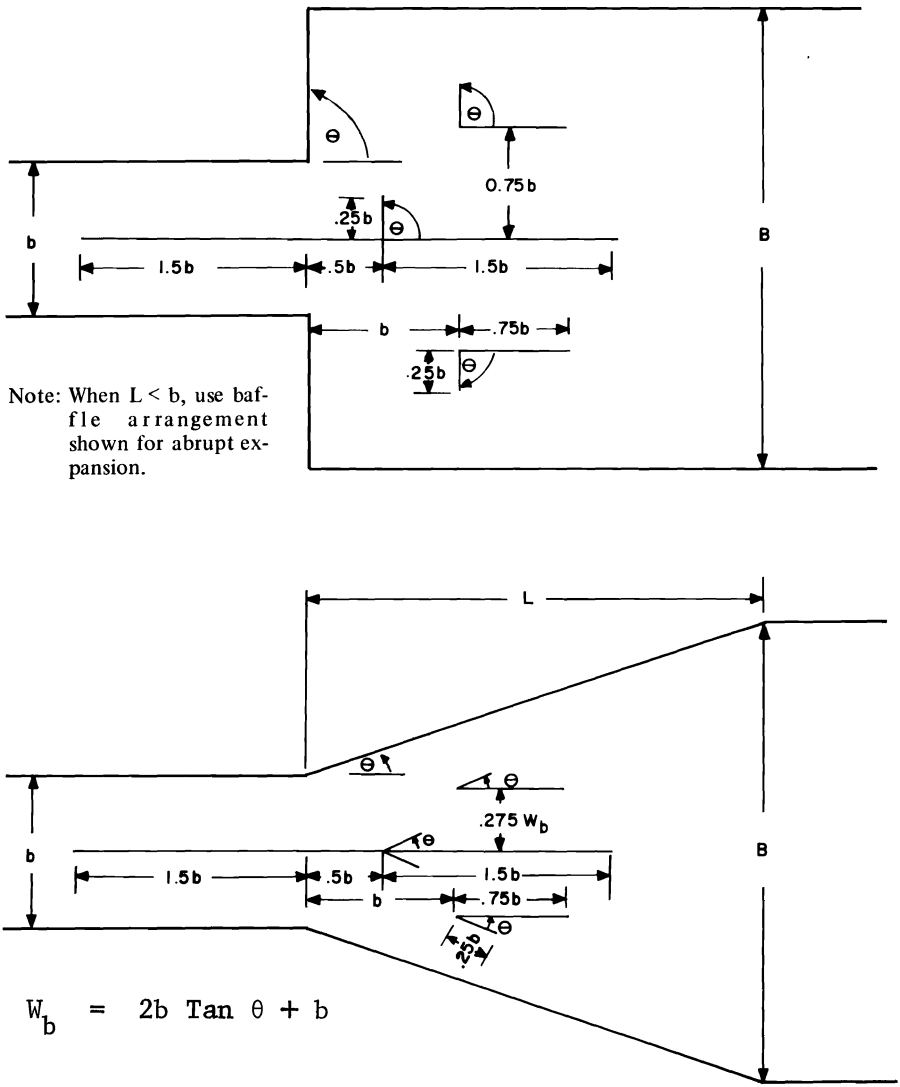

Fig. 32. A definition sketch detailing the location of the baffles for the final design of triangular-shaped baffles for open channel expansions.

HYDRAULIC CHARACTERISTICS OF FINAL BAFFLE DESIGN

In order to develop an appreciation of the flow characteristics on the outlet channel downstream from the baffles, velocity profiles were prepared for each divergence ratio and expansion ratio, B/b, studied. Velocity measurements were made for a number of discharge values. Also, the hydraulic tests were conducted using a variable tailwater control. Consequently, velocity profile data were collected for a fairly wide variation in specific energy ratio, E_3/E_1, as well as discharge.

The velocity profiles plotted in Figs. 33 and 34 are for an expansion ratio of 3, with Fig. 33 representing a discharge of approximately 1 cfs and a specific energy ratio of 90 percent, or more. The velocity profiles in Fig. 34 are for a

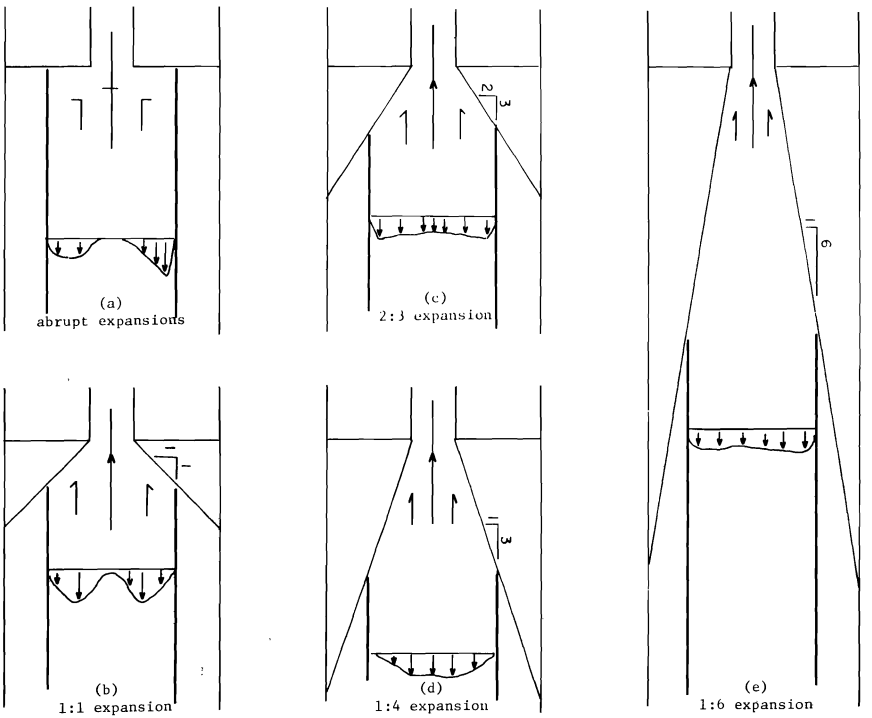

Fig. 33. Velocity distributions in downstream channel for Q = 1 cfs, B/b = 3, and $E_r > 0.9$.

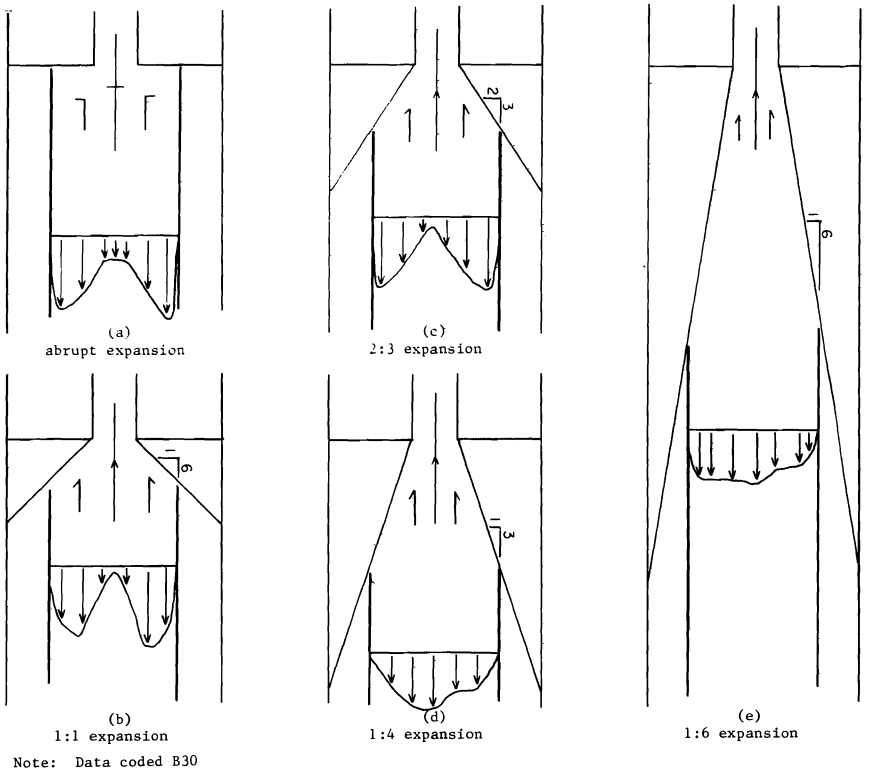

Fig. 34. Velocity distributions in downstream channel for Q = 3.5 cfs, B/b = 3, and $0.8 < E_r < 0.9$.

discharge of roughly 3.5 cfs and specific energy ratios between 80 and 90 percent, which represent extreme flow conditions of high velocities and large energy losses. The velocities plotted in Figs. 33 and 34 were measured at a cross section 2 feet downstream from the transition outlet, except for the abrupt expansion, where the velocity measurements were taken 4 feet downstream. The velocity distributions downstream from the 1:6 (Figs. 33e and 34e) and 1:4 (Figs. 33d and 34d) expansions are reasonably satisfactory. The 2:3, 1:1, and abrupt expansions resulted in velocity distributions such that more flow was moving along the sides of the outlet than in the middle of the channel.

The velocity distributions measured downstream from the transition outlets for an expansion ratio of 5 are shown in Figs. 35 and 36. The discharge was approximately 1 cfs for the velocity measurements portrayed in Fig. 35, while the specific energy ratio was greater than 90 percent. The velocities shown in Fig. 36 represent flow conditions of nearly maximum discharge used in the study (roughly 3.5 cfs) and high energy loss (specific energy ratios between 80 and 90 percent). Again, the velocities were measured 2 feet downstream from the transition outlet, except that the measurements were taken 4 feet downstream for the abrupt expansion. For the lower discharge (Fig. 35), a large

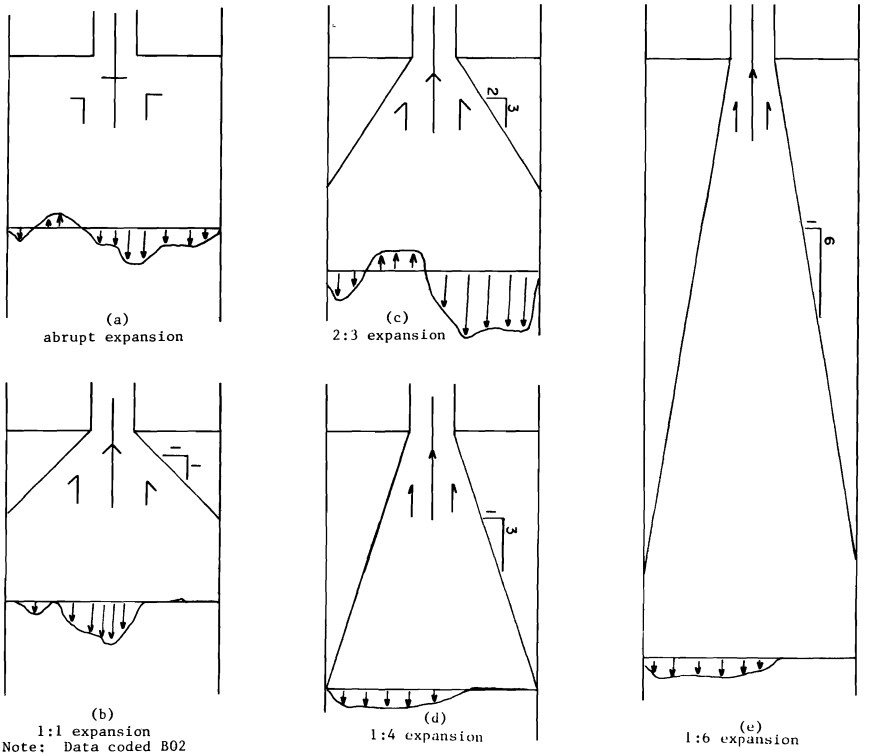

Fig. 35. Velocity distributions in downstream channel for Q = 1 cfs, B/b = 5, and E_r > 0.9.

portion of the flow moved along the right half of the 1:6 and 1:4 transitions, but the magnitude of the velocity was fairly uniform. In contrast, the rapid diverging expansions (2:3 and 1:1), as well as the abrupt expansion, showed erratic, or irregular, velocity distributions. For the high discharge and large energy loss flow conditions (Fig. 36), the 1:6 expansion showed a fairly satisfactory velocity distribution, with the 1:3 and 2:3 expansions having more flow traveling along the outsides than in the middle, and the 1:1 and abrupt expansions yielding higher velocities in the center of the outlet channel.

The effect of the expansion ratio, B/b, upon flow conditions downstream from the transition structures can be determined by comparing the velocity distributions in Fig. 33 (B/b = 3) with those in Fig. 35 (B/b = 5), which represent flow conditions at low discharges and small energy losses. As the expansion ratio is increased from 3 to 5, the flow in the 1:6 and 1:3 expansions tends to move more towards the right side (looking downstream) of the structure. For the 1:1 and abrupt expansions, the flow moves from the sides to the center of the channel as the expansion ratio is increased.

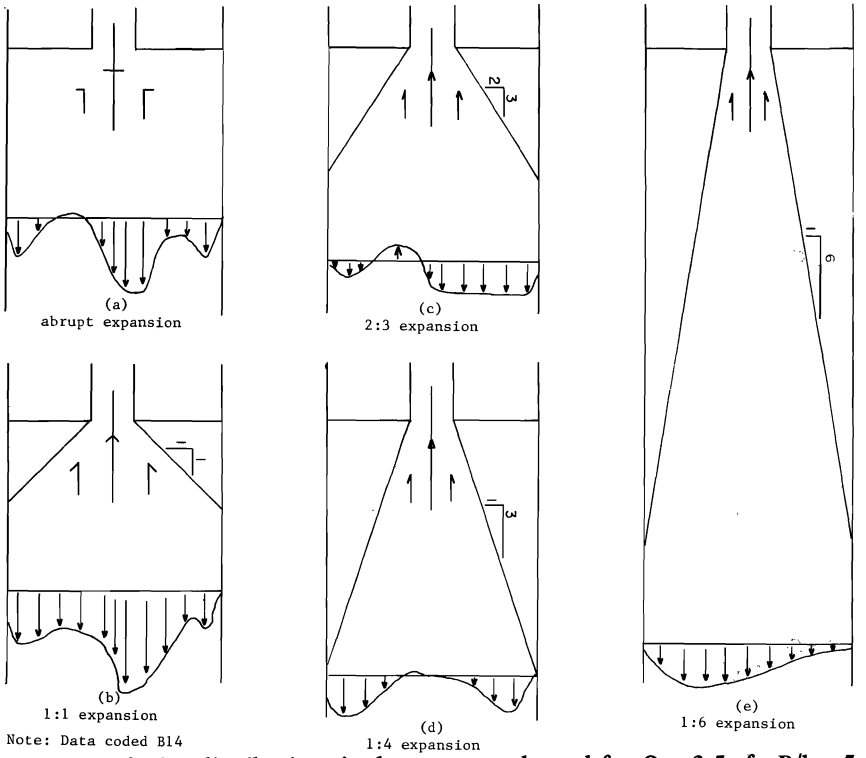

Fig. 36. Velocity distributions in downstream channel for Q = 3.5 cfs, B/b = 5, and 0.8 < E_r < 0.9.

A comparison of the velocity distributions in Fig. 34 (B/b = 3) with those shown in Fig. 36 (B/b = 5) provides an insight into the effect of the expansion ratio upon flow conditions for high discharges and large energy losses. For both expansion ratios, the flow conditions in the 1:6 expansion are fairly good, but the results are better for the lower expansion ratio (B/b = 3). In the 1:3 expansion, the flow moves from the center of the channel to the outsides as the expansion ratio is increased. For the 1:1 and abrupt expansions, the flow moves from the outsides into the center of the channel as the expansion ratio increases.

Many of the velocity distributions shown in Figs. 33, 34, 35, and 36 are quite irregular; yet, these velocity distributions are a significant improvement over the flow conditions that would be expected in these same expansions without baffles. At the same time, the velocity distributions become more uniform as the flow progresses downstream, as shown in Figs. 37 and 38.

If the geometry of an expansion structure is fixed, as well as the discharge and tailwater conditions, it is possible to develop a uniform velocity distribution in the outlet channel by the judicious placement of baffles and/or vanes. The difficulties in developing such a baffle design are twofold. First, the placement of the baffles and/or vanes must be varied as flow conditions are varied. Secondly, the number of baffles or other obstructions that must be placed in the expansion structure is likely to become cumbersome.

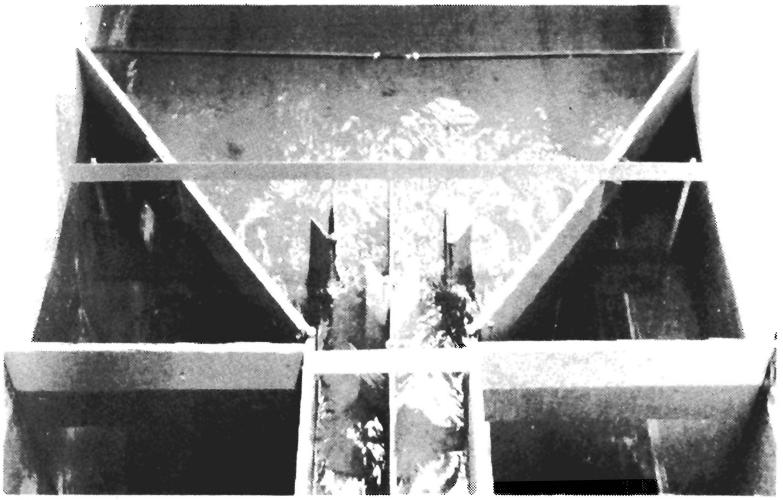

Fig. 37. Flow conditions in 2:3 expansion with B/b = 5.

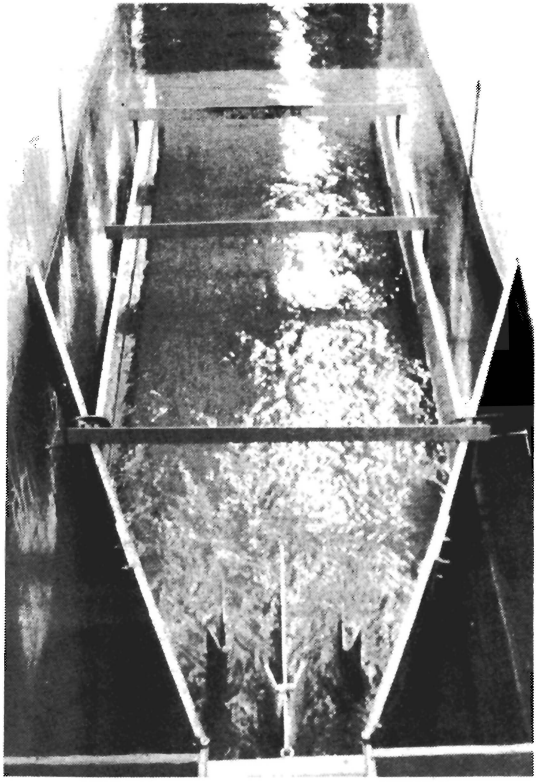

Fig. 38. Flow conditions in 1:6 expansion with B/b = 3.

HYDRAULIC DESIGN CRITERIA

As discussed earlier, the analysis of submergence in flow measuring flumes can be modified to allow the analysis of energy loss in open channel expansions. The general approximate submerged flow equation for flow measuring flumes is

$$Q = \frac{C_1(y_u - y_d)^{n_1}}{[-\log S + C_2)]^{n_2}} \quad \ldots\ldots\ldots (8)$$

where Q is the discharge, y_u is a flow depth upstream from the constriction, y_d is a flow depth downstream from the constriction, S is the submergence (y_d/y_u), C_1 is a submerged flow coefficient, n_1 is the free flow component, C_2 is a constant for the approximate submerged flow distribution (Skogerboe and Hyatt, 1967), and n_2 is a submerged flow exponent. In many cases, C_2 can be chosen as zero.

A general equation describing energy loss in an open channel constriction can be obtained by substituting E_u for y_u and E_d for y_d, where E_u and E_d are the specific energies upstream and downstream from the constriction, respectively. By defining the specific energy ratio, E_d/E_u, as E_r, and recognizing that the difference in specific energy ratios, $E_u - E_d$, is the energy loss (head loss, h_L), the general energy loss equation can be written as

$$Q = \frac{C_1 h_L^{n_1}}{[-(\log E_r + C_2)]^{n_2}} \quad \ldots\ldots\ldots (9)$$

For open channel expansions, Eq. 9 can be shown as describing the energy loss. If C_2 is assumed to be zero

$$Q = \frac{C_1 h_L^{n_1}}{(-\log E_r)^{n_1}} \quad \ldots\ldots\ldots (10)$$

A typical plot of Eq. 8 was shown in Fig. 23. The data reported by Smith and Yu (1966) were used to demonstrate the validity of Eq. 10 in describing the energy loss occurring in certain open channel expansions (Figs. 24 and 25). The data reported by Smith and Yu (1966) for an abrupt outlet are shown in Fig. 24, while Fig. 25 represents the baffled outlet with a 1:4 divergence as recommended by Smith and Yu.

Some typical discharge-energy loss curves for the triangular-shaped baffled open channel expansions studied by the writers are shown in Figs. 39 and 40. The subcritical flow curves in Fig. 39 represent data collected for the abrupt expansion with an expansion ratio, B/b, of 5. The data shown in Fig. 40 were collected for the 1:6 expansion with an expansion ratio of 5. The data shown in Figs. 39 and 40 represent some of the better data collected in the laboratory. Much of the data collected as part of this study is listed in the appendix.

The energy loss equation for the abrupt expansion (Fig. 39) or the 1:6 expansion (Fig. 40) can be developed by plotting the discharge intercept at an energy loss of 1.0 for each line of constant specific energy ratio. Defining the discharge intercept at $h_L = 1.0$ as $Q_{h_L} = 1$ and recognizing that $h_L^{n_1}$ is equal to one, when h_L is one, Eq. 10 can be reduced to

$$Q_{h_L=1} = \frac{C_1}{(-\log E_r)^{n_1}} \qquad \ldots\ldots\ldots (11)$$

By plotting $Q_{h_L} = 1$ against $-\log E_r$ on logarithmic paper, a linear relationship will result where C_1 is the value of $Q_{h_L} = 1$ at $-\log E_r = 1$ and n_2 is the slope of the straight line. This relationship for the abrupt, 1:1, 2:3, 1:3, and 1:6 expansions having an expansion ratio of 5 is shown in Fig. 41.

The limit slopes of 2/3 and 1 shown in Fig. 41 can be developed by a theoretical analysis of flow through an open channel expansion. A theoretical analysis of flow through open channel constrictions by Skogerboe, Hyatt, and Eggleston (1967) resulted in the theoretical n_2 curve shown in Fig. 42, which shows a range of n_2 between 1 and 3/2. The only theoretical difference between flow in an open channel expansion and flow in an open channel constriction is that the direction of flow is reversed. Considering this reversal of flow direction, the theoretical n_2 curve shown in Fig. 43 for open channel expansions can be developed. The theoretical range of n_2 for expansions is between 1 and 2/3.

The range between 2/3 and 1 for the subcritical flow exponent, n_2, is applicable to expansion ratios approaching infinity ($B/b = \infty$). The value of $n_2 = 2/3$ would be expected for an abrupt expansion having an expansion ratio of infinity, whereas the value of $n_2 = 1$ applies to the case of an abrupt expansion with the expansion ratio approaching one (open channel with parallel side walls and no expansion) or any other type of expansion wherein the expansion ratio is approaching one ($B/b = 1$).

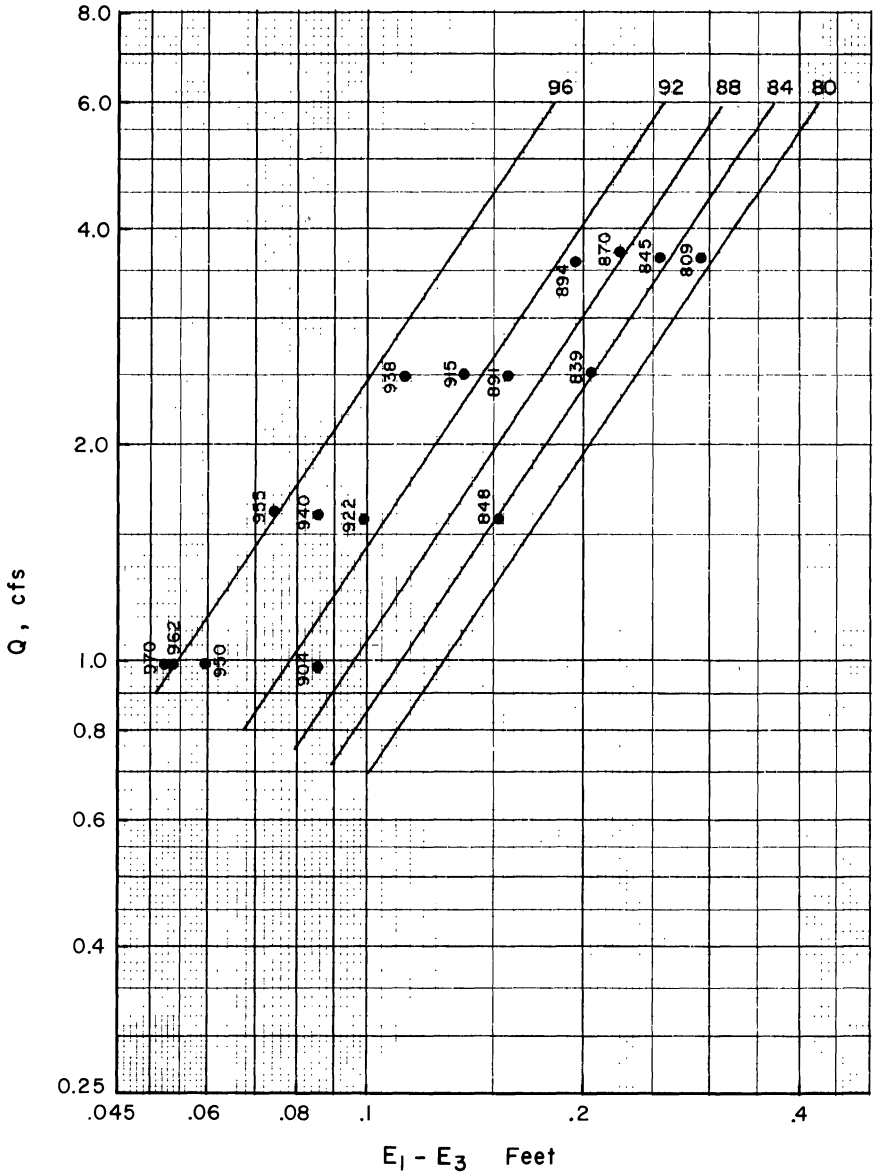

Fig. 39. Discharge-energy loss curves for abrupt expansion with B/b = 5.

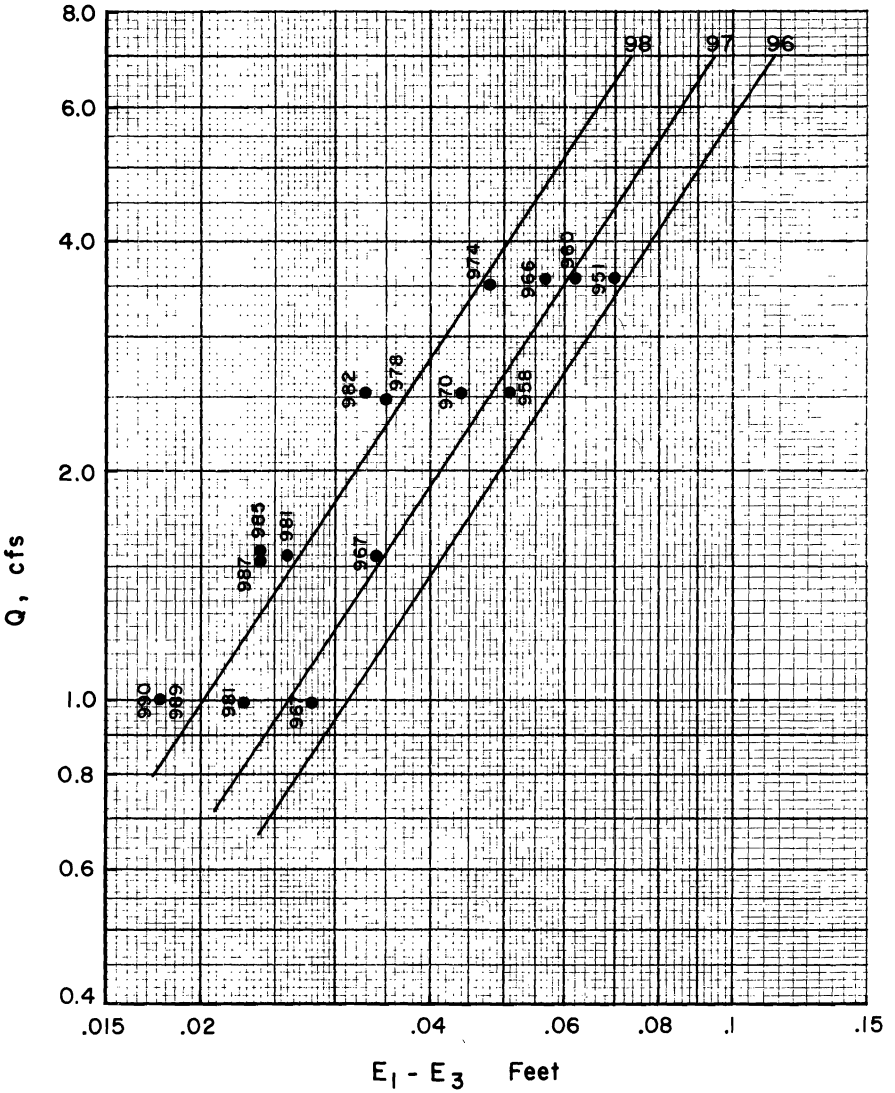

Fig. 40. Discharge-energy loss curves for 1:6 expansion with B/b = 5.

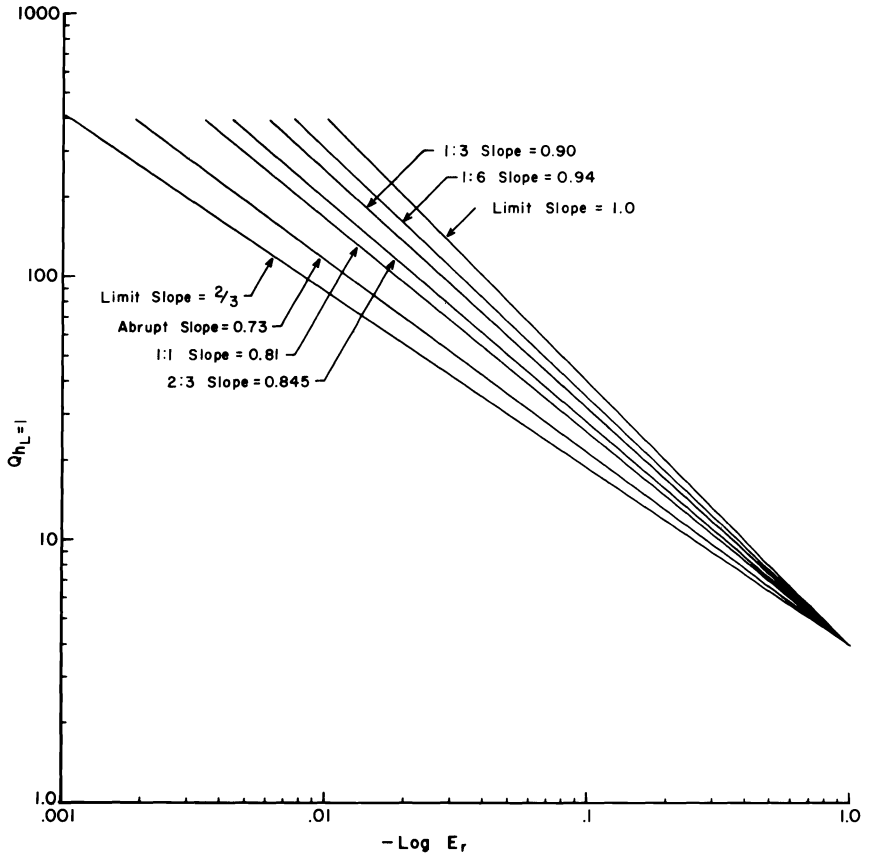

Fig. 41. Distribution of specific energy ratio for various expansions with B/b = 5.

The slope of each curve in Fig. 41 represents the value of n_2 for that expansion. Each value of n_2 determined from Fig. 41 has been plotted in Fig. 43 in order to develop the curve for the writers' data when B/b = 5. Thus, n_2 can be determined for any rate of expansion divergence. The value of C_1 determined from Fig. 41 is 4.0. Since the studies reported herein only used a single width of approach channel, namely 1 foot, the value of C_1 applies only to this single width. As a first approximation for design purposes, a value of C_1 equal to 4b could be used. Based on previous experience with open channel constrictions[5] (Skogerboe, Hyatt, and Eggleston, 1967) using Froude number models to predict prototype discharge, a more realistic estimate of the subcritical flow coefficient might be

$$C_1 = 4\, b^{0.9} \quad \ldots\ldots\ldots\ldots (12)$$

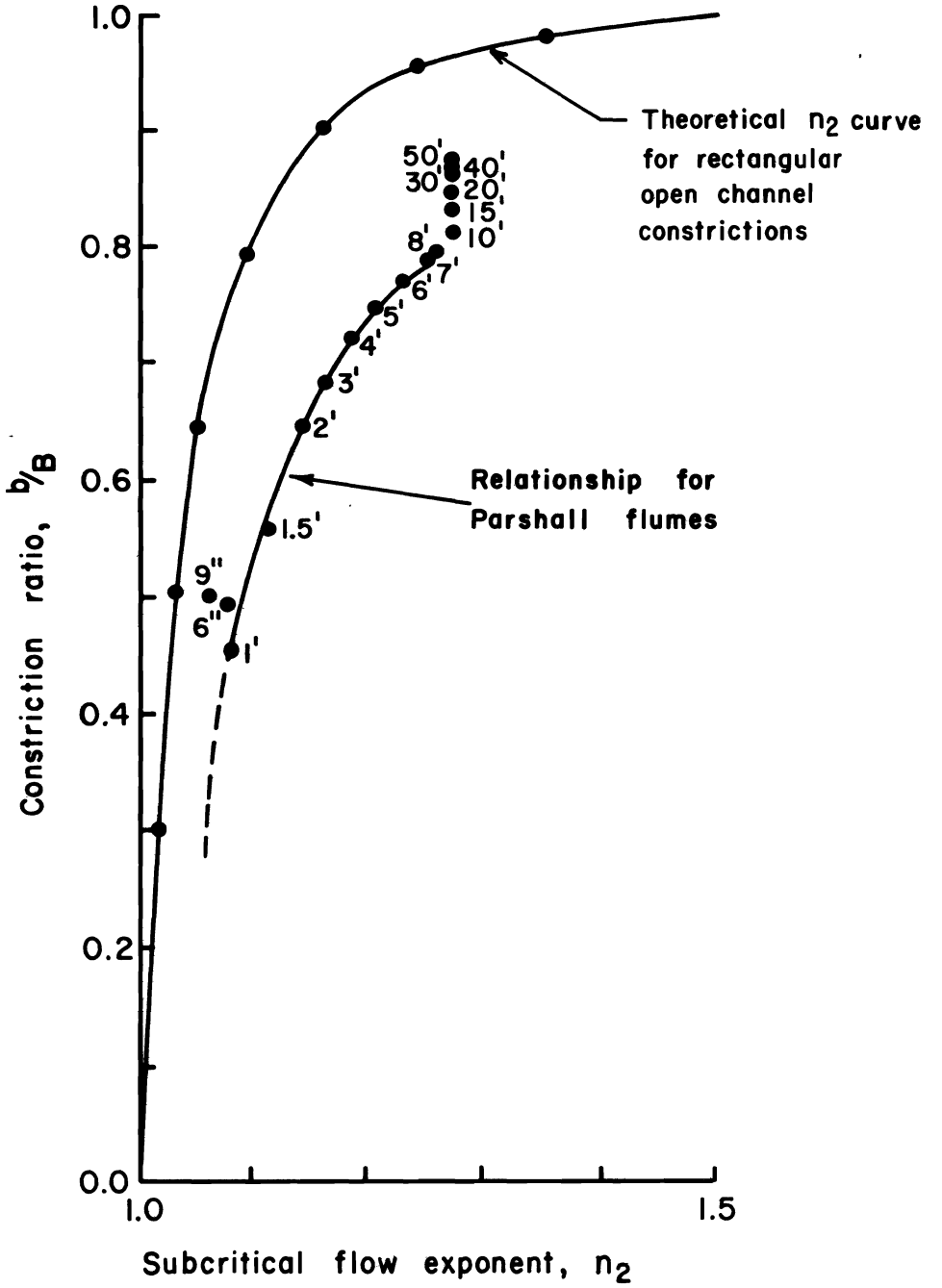

Fig. 42. Theoretical relationship between constriction ratio, b/B, and subcritical flow exponent, n_2, for open channel constrictions.

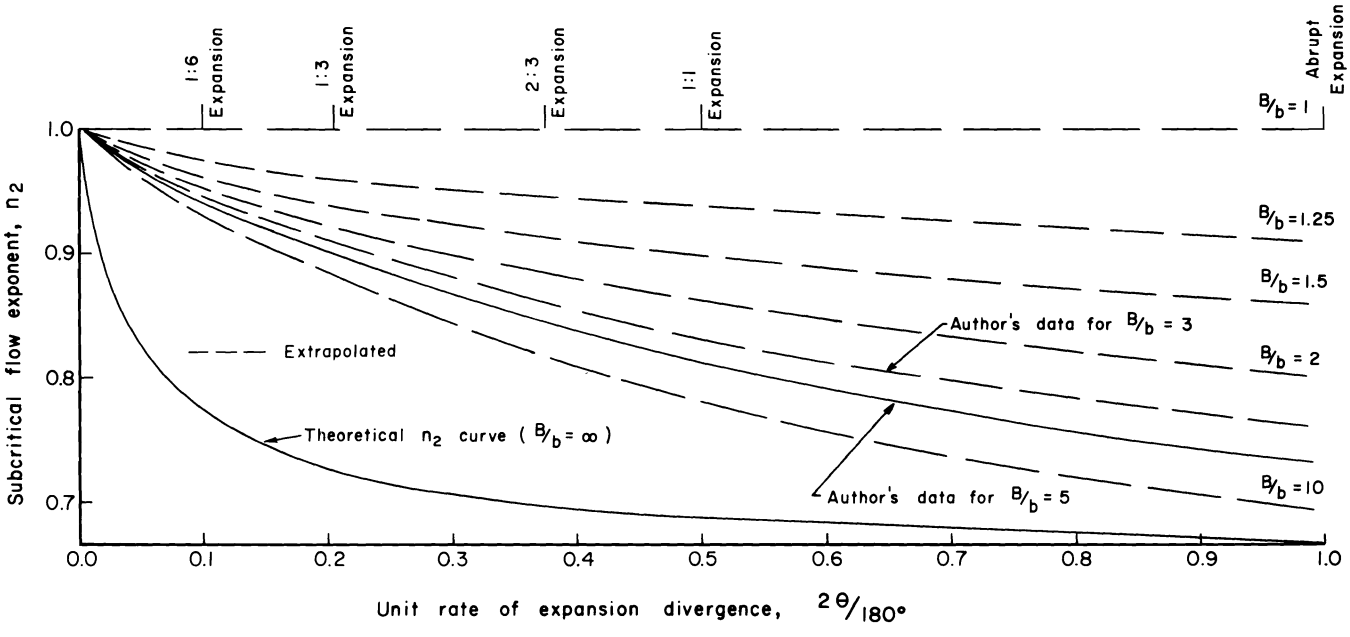

Fig. 43. Relationships between expansion ratio, B/b, and subcritical flow exponent, n_2, for open channel expansions with vertical side walls.

For the 1-foot approach channel used in this study, the subcritical flow discharge equation can be written as

$$Q = \frac{4h_L^{3/2}}{(-\log E_r)^{n_2}} \quad \ldots\ldots\ldots\ldots (13)$$

where n_2 is obtained from Fig. 43. A more general subcritical flow equation could be approximated by

$$Q = \frac{4\, b^{0.9}\, h_L^{3/2}}{(-\log E_r)^{n_2}} \quad \ldots\ldots\ldots\ldots (14)$$

where n_2 is again obtained from Fig. 43.

The relationships between the Froude number at the inlet to the open channel expansions, F_1, and the specific energy ratio, E_3/E_1, is shown in Fig. 44 for the triangular-shaped baffles used in this study. The curves in Fig. 44 are for an expansion ratio of 5. The right ordinate in Fig. 44 ($E_3/E_1 = 1.0$) is the curve for all expansions when the expansion ratio becomes unity. The area between the right ordinate and the curve for any particular expansion represents the range for expansion ratios between 1 and 5. The curves in Fig. 44 can be used for general design. Essentially, the design results will be the same if the following equation is used.

$$Q = \frac{4\, b\, h_L^{3/2}}{(-\log E_r)^{n_2}} \quad \ldots\ldots\ldots\ldots (15)$$

The subcritical flow exponent, n_2, can be obtained from Fig. 43.

The hydraulic data collected in the laboratory for the final baffled outlet designs are listed in the appendix. One of the purposes for conducting the experimental work was to establish the validity of various energy loss equations used by previous investigators in their studies of particular open channel expansion structures. The data listed in the appendix will be used to demonstrate the validity of various energy loss analyses.

A typical equation used to describe the head loss occurring in an open channel expansion is

$$h_L = K\, h_v \quad \ldots\ldots\ldots\ldots (16)$$

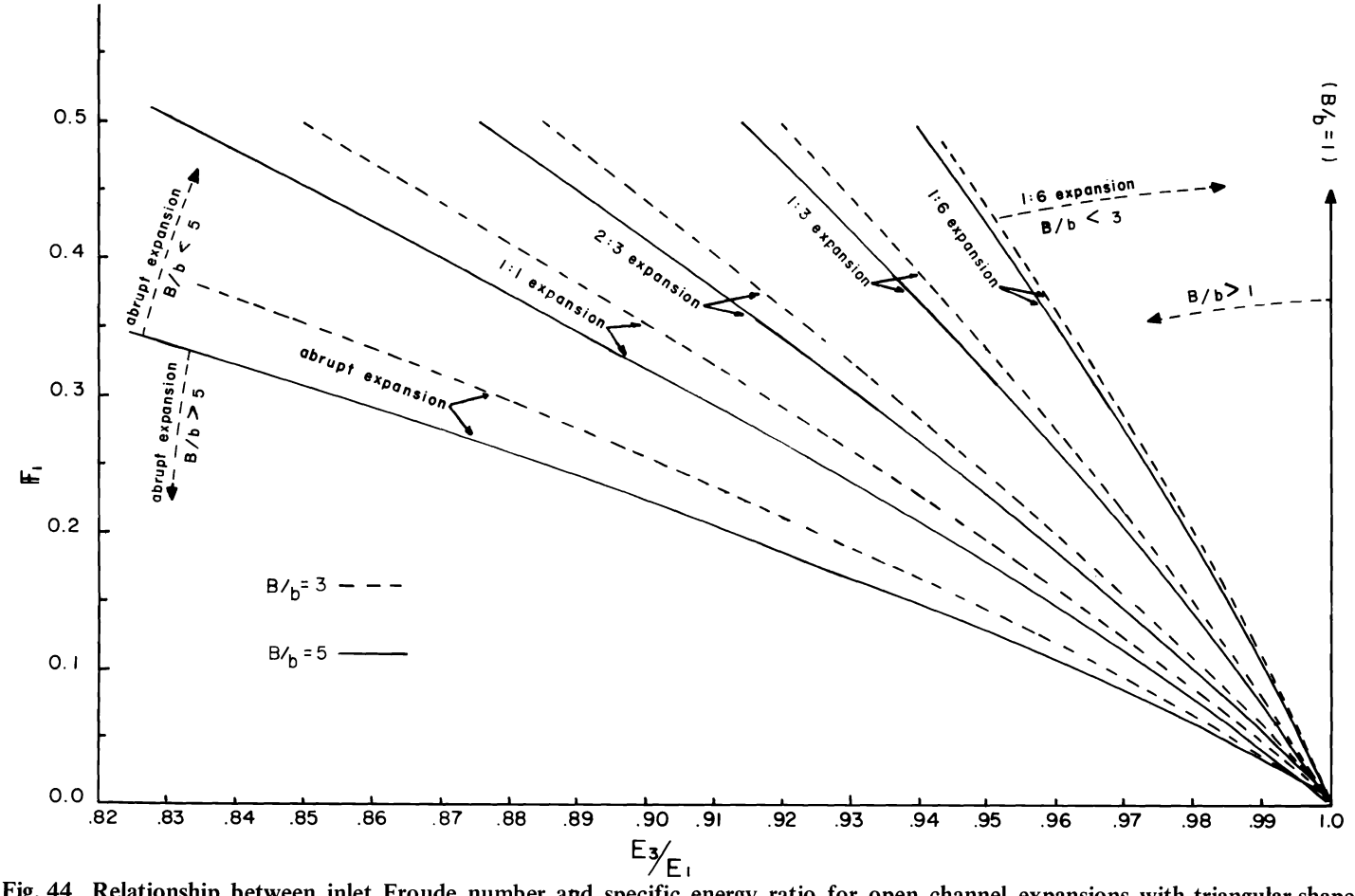

Fig. 44. Relationship between inlet Froude number and specific energy ratio for open channel expansions with triangular-shaped baffles.

where K is a constant and

$$h_v = (V_i^2 - V_o^2)/2g \quad \ldots\ldots\ldots\ldots (17)$$

with V_i being the mean velocity at the inlet and V_o is the mean outlet velocity. A plot of the head loss against the change in velocity head, h_v, is shown in Fig. 45. Obviously, K cannot be a constant for the curvilinear relationship portrayed in Fig. 45. Therefore, Eq. 16 does not adequately describe the head loss occurring in an open channel expansion. Consequently, any time that Eq. 16 is used to evaluate the head loss in an expansion, the computation could only be a rough estimate.

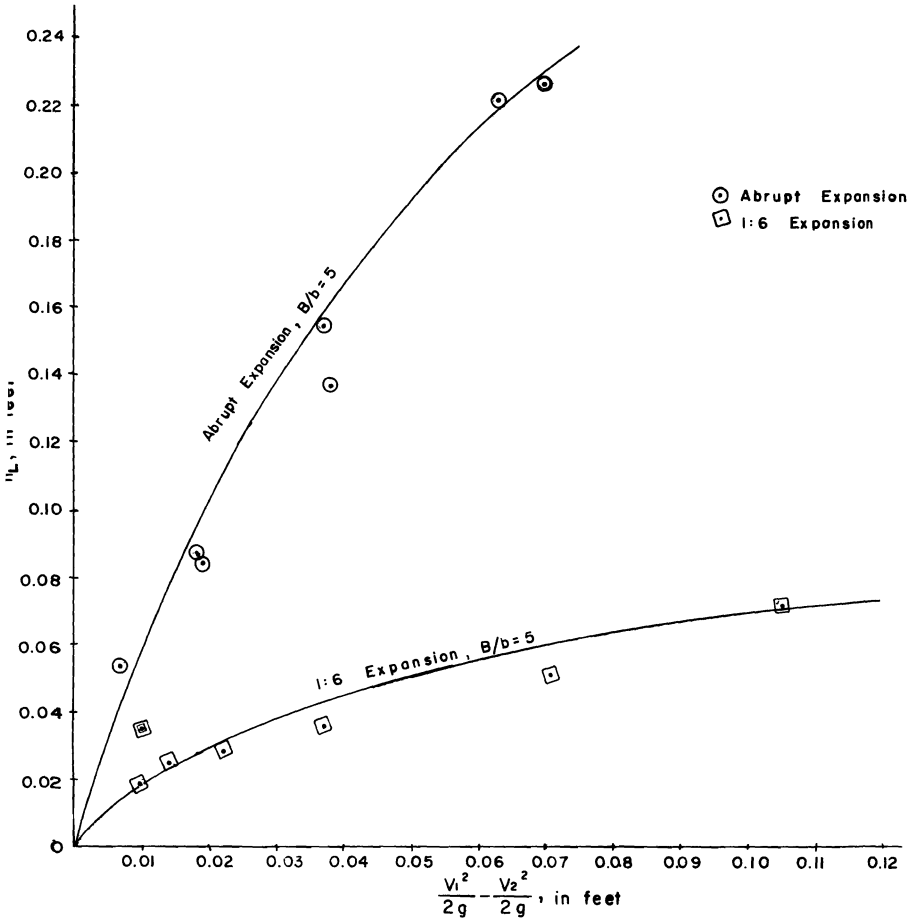

Fig. 45. Typical relationship between head loss and the change in velocity head at the inlet and outlet of an open channel expansion structure.

Ofttimes, the head loss occurring in a transition structure is described as a function of the velocity head at the inlet to the structure.

$$h_L = K_i V_1^2/2g \quad \ldots\ldots\ldots\ldots (18)$$

in which K_i is a constant and V_1 is the inlet velocity. The relationship between head loss and inlet velocity head is shown for each of the expansions (abrupt, 1:1, 2:3, 1:3, and 1:6) in Figs. 46 and 47 for expansion ratios of 5 and 3, respectively. These plots show that K_i is not a constant for any one of the open channel expansions investigated. The upper portion of each curve is represented by a linear relationship of the form

$$h_L = K_i V_1^2/2g + a_1 \quad \ldots\ldots\ldots\ldots (19)$$

in which a_1 is a constant for any particular open channel expansion geometry. If Eq. 18 had been valid, then K_i could have been used as a measure of hydraulic efficiency with lower values of K_i representing a greater degree of hydraulic efficiency. On the other hand, if the intent of the designer is to maximize the amount of energy loss, then the higher values of K_i would represent a greater efficiency for energy dissipation.

Another energy loss equation which has been proposed is

$$h_L = C_L (1-A_r)^2 V_1^2/2g \quad \ldots\ldots\ldots\ldots (5)$$

in which C_L is a head loss coefficient. Earlier in this report (Figs. 26 and 27), C_L was shown to vary with the specific energy ratio, E_2/E_1, as well as the inlet Froude number, F_1, for the baffled outlets reported by Smith and Yu (1966). Using the data listed in the appendix of this report, the variation of C_L with the inlet Froude number is shown in Figs. 48 and 49 for expansion ratios of 5 and 3, respectively.

The above analyses demonstrate that Eqs. 16, 18, and 5 are not valid for describing the energy loss occurring in open channel expansion structures. The Borda equation (Eq. 5) can be used provided the relationship between C_L and F_1 or E_2/E_1 is known, rather than using some constant for C_L.

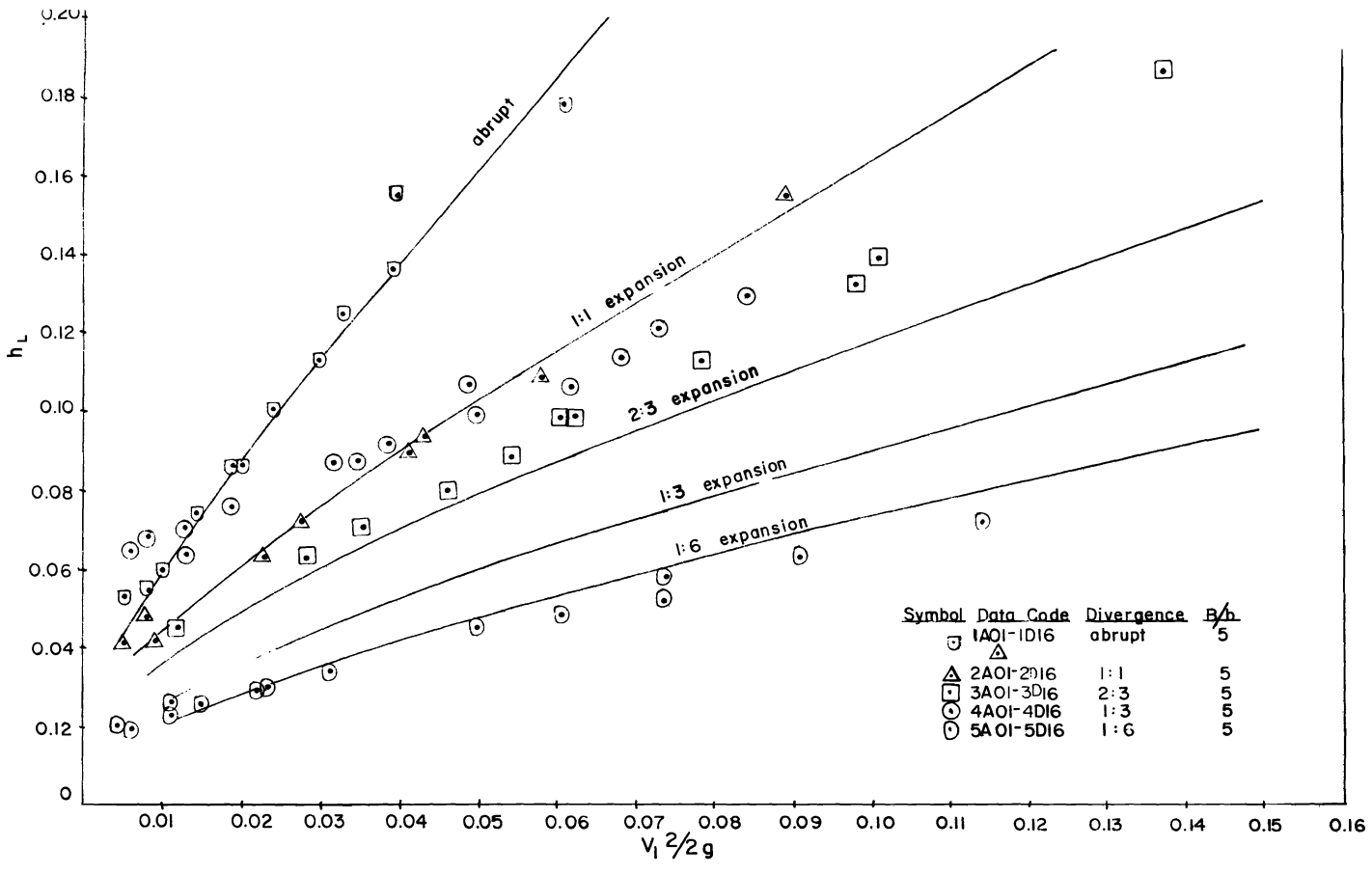

Fig. 46. Relationships between head loss and inlet velocity head for expansions having triangular-shaped baffles and vertical walls with B/b = 5.

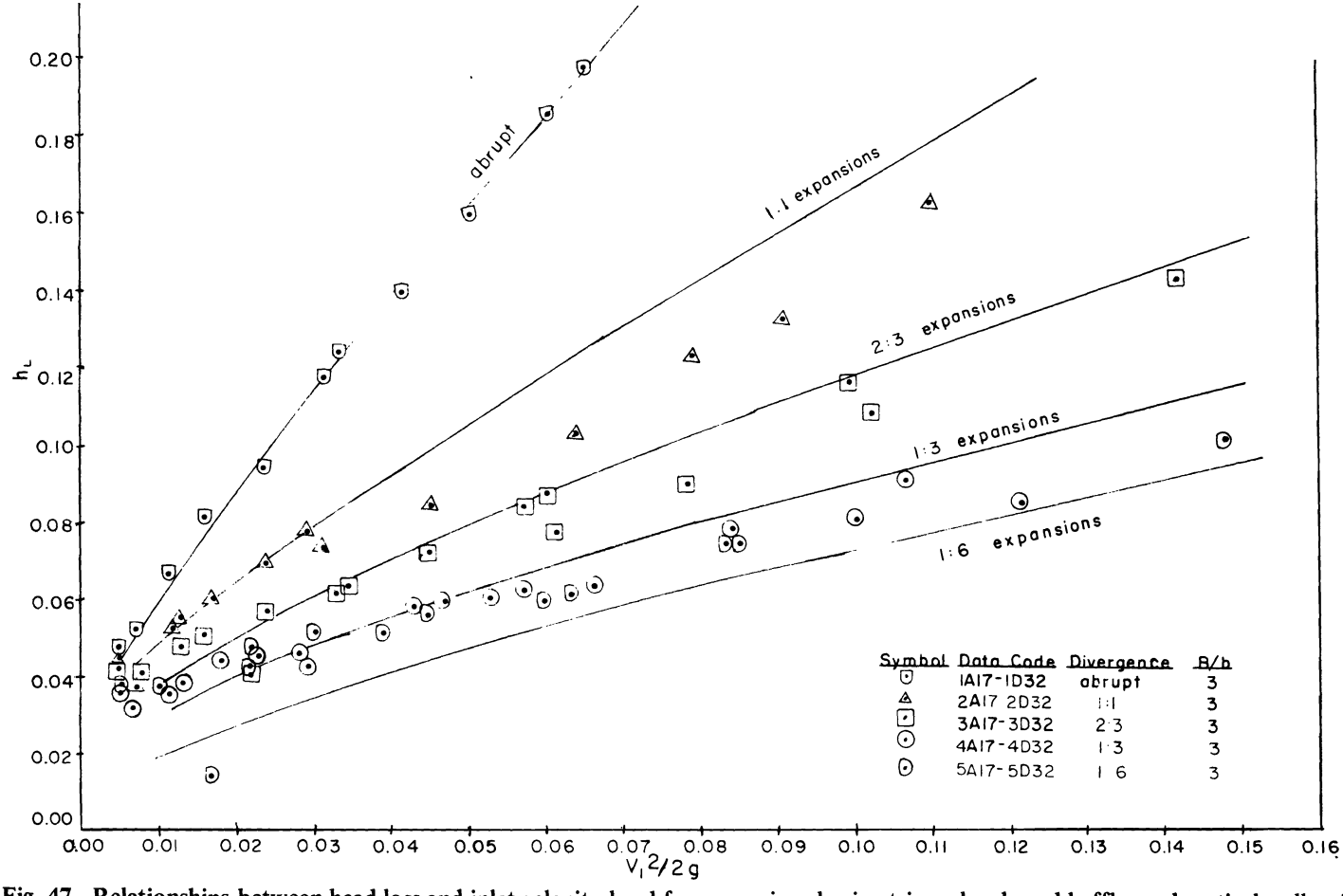

Fig. 47. Relationships between head loss and inlet velocity head for expansions having triangular-shaped baffles and vertical walls with B/b = 3.

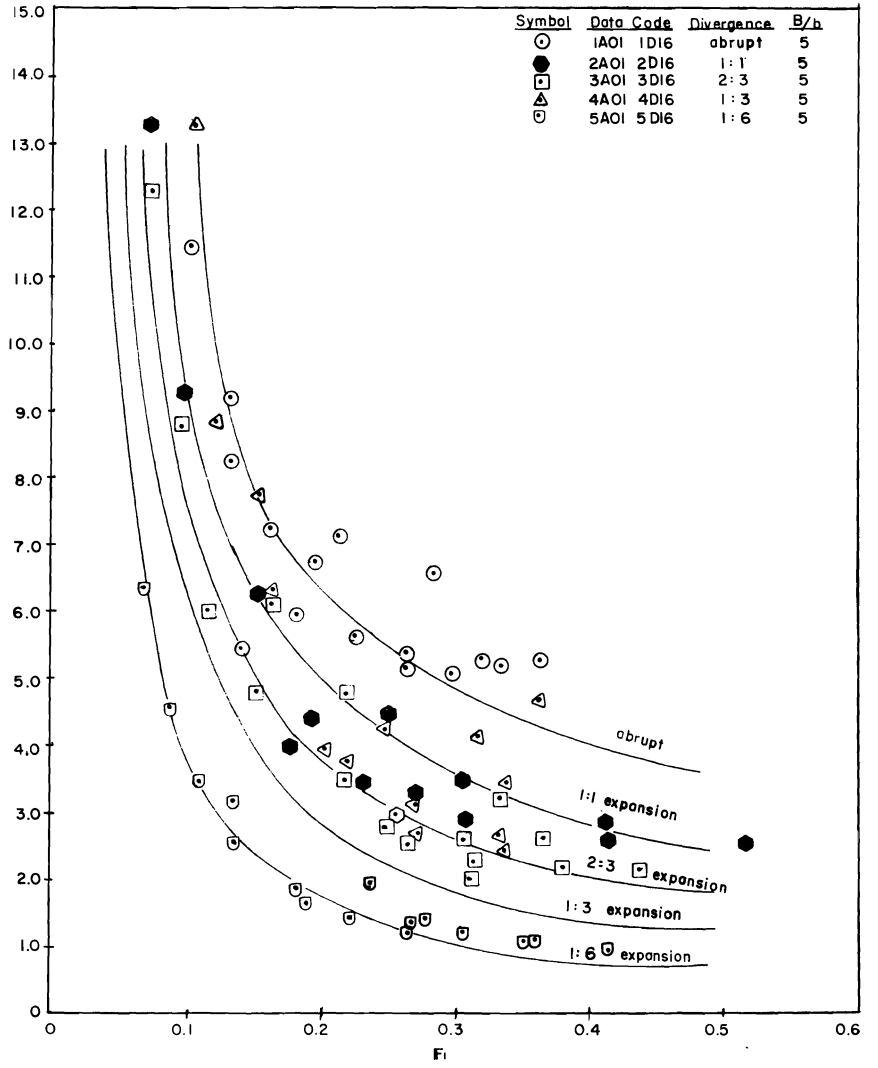

Fig. 48. Relationships between the inlet Froude number and head loss coefficient for expansions having triangular-shaped baffles and vertical walls with B/b = 5.

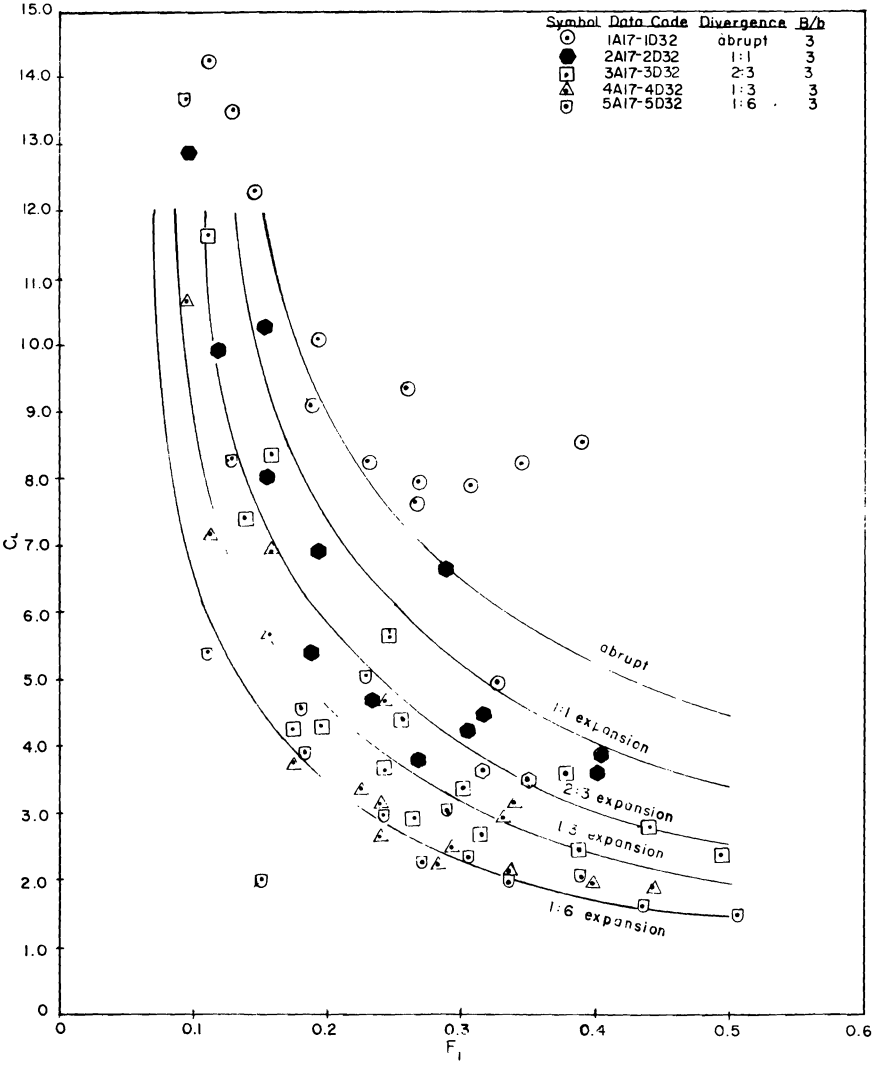

Fig. 49. Relationships between the inlet Froude number and head loss coefficient for expansions having triangular-shaped baffles and vertical walls with B/b = 3.

SUMMARY

Previous investigators have determined certain hydraulic characteristics of open channel expansions which are of importance in designing such structures. For example, Chaturvedi (1963) concluded that flow conditions in the approach channel have a significant effect upon flow conditions leaving the expansion. Any flow instability at the inlet will become more aggravated as the flow moves through the expansion. Thus, the flow at the outlet will be improved if uniform flow with uniform velocity distribution and hydrostatic pressure distribution occurs at the inlet. Although such ideal flow conditions cannot usually be expected under field conditions, they can serve as a goal for the hydraulic engineer.

The natural rate of expansion of a jet under subcritical flow conditions is reported by Smith and Yu (1966) as 1:10 ($2\theta = 11.5^{o}$). Hinds (1928) used a central angle (2θ) of expansion of 12.5^{o}. On the other hand, Nikuradse's (Goldstein, 1965) experiments on expansions with vertical walls show that flow separation does not occur for central angles less than 8^{o} ($2\theta = 8^{o}$ or 1:14 divergence), but flow separation does occur with the jet traveling along one of the walls when the central angle of divergence (2θ) is between 8^{o} and 10^{o}. Although a relationship has not been developed between the maximum central divergence angle at which separation does not occur and the expansion ratio, B/b, it would be expected that as B/b is increased, 2θ must be decreased.

The expansion ratio, B/b, has a significant influence upon the hydraulic characteristics of open channel expansions. As the expansion ratio is increased, the degree of nonuniformity of velocity distributions in the expansion structure will increase with consequent increases in energy loss. For example, if B/b = 1.01, then it is not difficult to visualize that there is little practical difference between a divergence of 1:10 and an abrupt outlet, whereas for large expansion ratios, there is considerable difference.

The warped transition (Hinds, 1928), which can be used as either an inlet or outlet structure, has been investigated by Haszpra (1961, 1962) and Smith and Yu (1966). In each case, the warped transition has been rejected because of poor hydraulic performance, as well as high construction costs when compared with either the broken plane transition or the simple expansions having vertical walls with, or without, baffles.

A comparison of various methods reported by previous investigators in accounting for the energy (head) loss occurring in open channel expansions has been made. For the equation

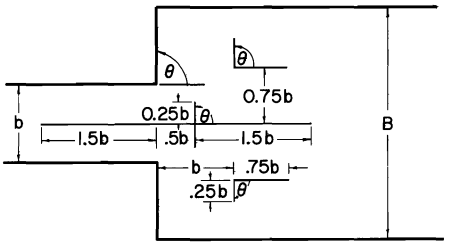

Note: When L < b, Use Baffle Arrangement Shown For Abrupt Expansion.

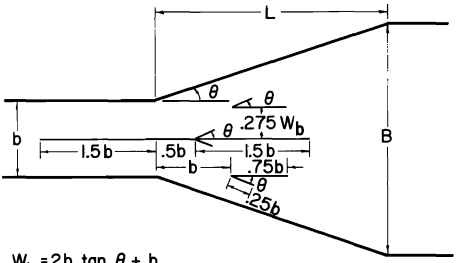

$W_b = 2b \tan \theta + b$

(a) Definition Sketch of Triangular Shaped Baffle Arrangements For Open Channel Expansions With Vertical Walls.

General Solution

$$Q = \frac{4b^{0.9} h_L^{3/2}}{(-\log E_r)^{n_2}}$$, Obtain n_2 From (b)

The Exponent 0.9 Is Used As An Approximation To Correct For Scale Effects When b > 1'.

y_1 = Flow Depth At Section 1 In Inlet Channel

y_3 = Flow Depth At Section 3 In Oulet Channel

V_1 = Mean Velocity At Section 1

V_3 = Mean Velocity At Section 3

Q = Discharge

$F_1 = V_1/\sqrt{g y_1}$

$h_L = E_1 - E_3$

$E_r = E_3/E_1$

$E_1 = y_1 + V_1^2/2g$

$E_3 = y_3 + V_3^2/2g$

Er	-log Er
0.67	0.1739
0.68	0.1675
0.69	0.1612
0.70	0.1549
0.71	0.1487
0.72	0.1427
0.73	0.1367
0.74	0.1308
0.75	0.1249
0.76	0.1192
0.77	0.1132
0.78	0.1079
0.79	0.1024
0.80	0.0969
0.81	0.0915
0.82	0.0862
0.83	0.0809
0.84	0.0757
0.85	0.0706
0.86	0.0655
0.87	0.0605
0.88	0.0555
0.89	0.0506
0.90	0.0458
0.91	0.0410
0.92	0.0362
0.93	0.0315
0.94	0.0269
0.95	0.0223
0.96	0.0177
0.97	0.0132
0.98	0.0088
0.99	0.0044

Fig. 50. Design procedure for open channel expansions with vertical walls and triangular-shaped baffles.

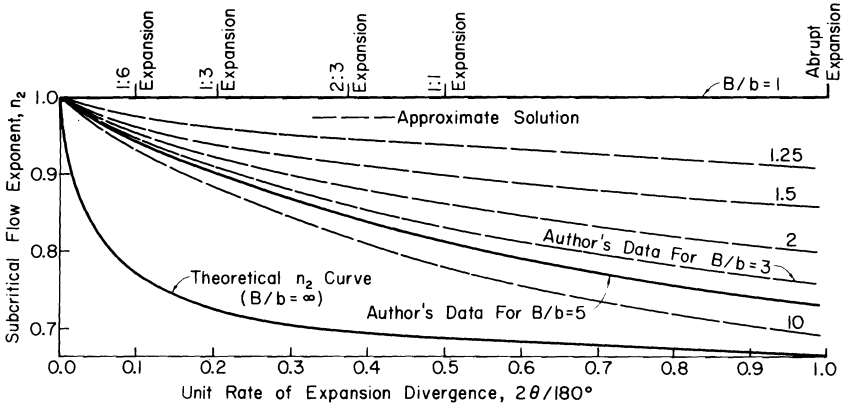

(b) Relationships Between Expansion Ratio, B/b, and Subcritical Flow Exponent, n_2, For Open Channel Expansions With Vertical Side Walls.

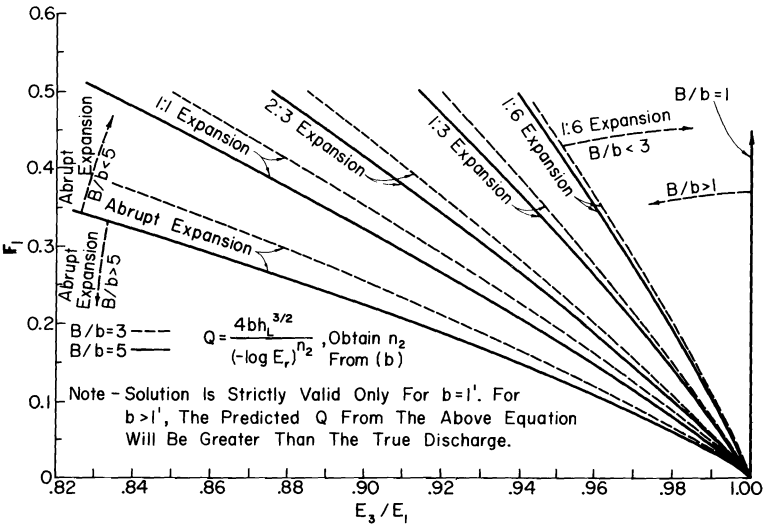

(c) Relationship Between Inlet Fronde Number and Specific Energy Ratio For Open Channel Expansions With Triangular-Shaped Baffles.

Fig. 50. Continued.

$$h_L = K\, h_v \quad \ldots\ldots\ldots\ldots\ldots\ldots (16)$$

t can be shown that K is not a constant.

If the head loss, h_L, is listed in terms of the inlet velocity head

$$h_L = K_i\, V_1^2/2g \quad \ldots\ldots\ldots\ldots\ldots\ldots (18)$$

in approximate straight-line relationship can be developed, but there is a small ıead loss correction which will vary for each expansion. Thus, the head loss :quation could be written as

$$h_L = K_i\, V_1^2/2g + a_1 \quad \ldots\ldots\ldots\ldots\ldots\ldots (19)$$

in which a_1 is a constant for any particular open channel expansion geometry.

Another energy loss equation which has been proposed is

$$h_L = C_L\, (1-A_r)^2\, V_1^2/2g \quad \ldots\ldots\ldots\ldots\ldots\ldots (5)$$

in which C_L is a head loss coefficient. The head loss coefficient, C_L, is not a constant, but is a function of the inlet Froude number, F_1, and the expansion ratio, B/b. Also, data collected by other investigators as well as data reported herein, has been analyzed using subcritical flow techniques as previously reported to show that the head loss coefficient is a function of the specific energy ratio, E_r. At the same time, it was shown that the inlet Froude number is a function of the specific energy ratio for any constant expansion ratio, thereby proving again that the head loss coefficient is a function of the specific energy ratio.

The subcritical flow techniques previously employed by the writers for analyzing the flow in open channel constrictions have been modified to allow the analysis of energy loss in open channel expansions. The modified technique has been applied to the hydraulic data collected in the laboratory on open channel expansions with vertical walls and triangular-shaped baffles. The design procedure for the baffled outlet structures developed as part of this study is described in Fig. 50.

SELECTED REFERENCES

Chaturvedi, R. S. 1963. Expansive sub-critical flow in open channel transitions. Journal of the Institution of Engineers, Civil Engineering Division, India, Vol. 43, May, pp. 447-487.

Chow, Ven Te. 1959. Open-channel hydraulics. McGraw-Hill, New York. 680 p.

Goldstein, S. 1965. Modern developments in fluid dynamics. Vol. II. Dover Publications, Inc., New York.

Haszpra, O. 1961. A törtlapú átmenet: sikeres kísérletek a torzfeluletnel olcsóbb és hidraulikailay kedvezőbb átmeneti felülettel. (Broken plane transition: successful experiments with a cheaper and hydraulically more favorably shaped transition surface, superior to warped surfaces.) Hidrológiai Közlöny, 6. pp. 494-504.

Haszpra, O. 1962. A törtlapú átmenet vizsgálata. (Investigations of broken plane transitions.) Hidrológiai Közlöny, 2, pp. 153-157.

Henderson, F. M. 1966. Open channel flow. The Macmillan Company, New York. 522 p.

Hinds, J. 1928. The hydraulic design of flume and siphon transitions. Transactions, ASCE, 91:1423-1459. Paper 1690.

Hyatt, M. L. 1965. Design, calibration, and evaluation of a trapezoidal measuring flume by model study. M.S. Thesis, Utah State University, Logan, Utah.

Kalinske, A. A. 1946. Conversion of kinetic energy to potential energy in flow expansions. Transactions, ASCE, Vol. III, pp. 355-390.

Simmons, W. P., Jr. 1964. Hydraulic design of transitions for small canals. A Water Resources Technical Publication, Engineering Monograph No. 33, U.S. Dept. of Interior, Bureau of Reclamation.

Skogerboe, G. V., M. L. Hyatt, J. D. England, and J. R. Johnson. 1965. Submergence in a two-foot Parshall flume. PRWR6-2, Utah Water Research Laboratory, College of Engineering, Utah State University, Logan, Utah.

Skogerboe, G. V., W. R. Walker, and L. R. Robinson. 1965. Design, operation, and calibration of the Canal A submerged rectangular measuring flume. PRWG24-3, Utah Water Research Laboratory, College of Engineering, Utah State University, Logan, Utah.

Skogerboe, G. V., and M. L. Hyatt. 1966. Use of baffles in open channel expansions. Discussion of Proc. Paper 4703 by Smith and Yu. ASCE, Journal of the Hydraulics Division, 92(HY5):255-259. Proc. Paper 4891. September.

kogerboe, G. V., M. L. Hyatt, and L. H. Austin. 1966. Stagefall-discharge relations for flood flows over highway embankments. PRWG6-7, Utah Water Research Laboratory, College of Engineering, Utah State University, Logan, Utah.

kogerboe, G. V., and M. L. Hyatt. 1967. Analysis of submergence in flow measuring flumes. Proceedings, ASCE, J. Hyd. Div., 93(HY4):183-200. Proc. Paper 5348. July.

kogerboe, G. V., M. L. Hyatt, and K. O. Eggleston. 1967. Design and calibration of submerged open channel flow measurement structures. Part 1–Submerged flow. PRWG31-2, Utah Water Research Laboratory, College of Engineering, Utah State University, Logan, Utah.

kogerboe, G. V., M. L. Hyatt, J. D. England, and J. R. Johnson. 1967. Design and calibration of submerged open channel flow measurement structures. Part 2–Parshall flumes. PRWG31-3, Utah Water Research Laboratory, College of Engineering, Utah State University, Logan, Utah.

kogerboe, G. V., M. L. Hyatt, R. K. Anderson, and K. O. Eggleston. 1967. Design and calibration of submerged open channel flow measurement structures. Part 3–Cutthroat flumes. PRWG31-4, Utah Water Research Laboratory, College of Engineering, Utah State University, Logan, Utah.

kogerboe, G. V., M. L. Hyatt, and L. H. Austin. 1967. Design and calibration of submerged open channel flow measurement structures. Part 4–Weirs. PRWG31-5, Utah Water Research Laboratory, College of Engineering, Utah State University, Logan, Utah.

kogerboe, G. V., W. R. Walker, B. B. Hacking, and L. H. Austin. 1968. Unpublished material on transitions collected as background material to "Analysis of Small Water Management Structures in Irrigation Distribution Systems." PRWG55-1, Utah Water Research Laboratory, College of Engineering, Utah State University, Logan, Utah.

mith, C. D., and J. N. G. Yu. 1966. Use of baffles in open channel expansions Proceedings, ASCE, J. Hyd. Div., 92(HY2):1-17. Paper 4703. March.

mith, C. D. 1967. Simplified design for flume inlets. Proc., ASCE, J. Hyd. Div., 93(HY6):25-34. Paper 5550. November.

homas, A. R. 1940. Flow in expansions in open channels. Proc. Punjab Engr. Congress, Lahore. Paper 236. 23 p.

u, J. N. G. 1965. The hydraulics of outlets for open channel flow. Unpublished M.S. Thesis, University of Saskatchewan, Saskatoon, Saskatchewan, Canada.

APPENDIX

HYDRAULIC DATA

LOCATION SKETCH AND HYDRAULIC DEFINITIONS

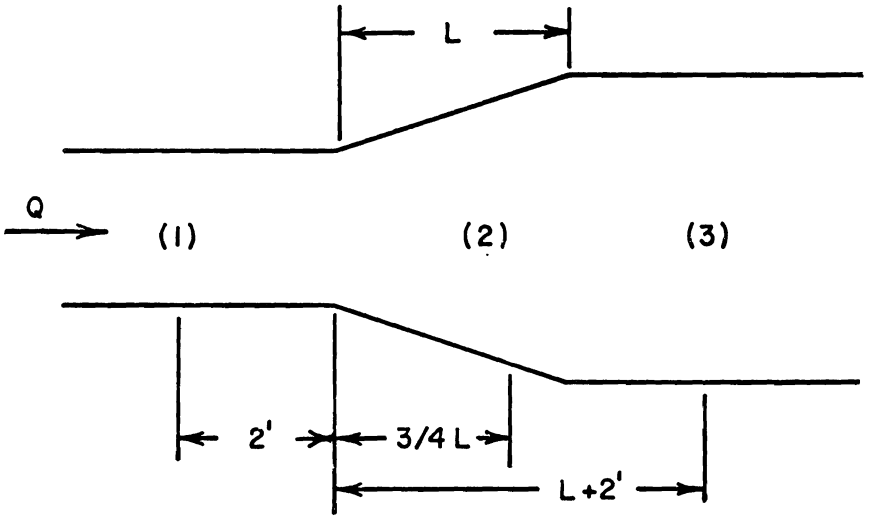

Fig. 51. Reference to location of point measurements.

1. Point of measurement 2' upstream from expansion in one foot section.

2. Point of measurement 3/4 through the expansion.

3. Point of measurement 2' beyond the expansion (L+2') except for the abrupt expansion which was 4' beyond the expansion (L+4').

L = the length of expansion
b = the width (=1') at section 1
W_b = the width at section 2

B = the width of the downstream channel of section 3
Q = the flow rate or discharge
y_1 = the flow depth at section 1
y_2 = the flow depth at section 2
y_3 = the flow depth at section 3
V_1 = the mean velocity at section 1
V_2 = the mean velocity at section 2
V_3 = the mean velocity at section 3
A_1 = the area at section 1
A_2 = the area at section 2
A_3 = the area at section 3
A_r = the area ratio of A_1/A_2 or A_1/A_3

pecific energy at sections 1, 2, and 3, $E_{(\,)}$

$$E_{(\,)} = \frac{(Q/y_{(\,)}b)^2}{2g}$$

lead loss between sections 1 and 2 or 1 and 3, $H_{L(\,,\,)}$.

$$H_{L(\,,\,)} = \left[y_{(\,)} + \frac{(Q/by_{(\,)})^2}{2g} \right] - \left[y_{(\,)} + \frac{(Q/W_b y_{(\,)})^2}{2g} \right]$$

Head loss coefficient between sections 1 and 2 or 1 and 3, $C_{L(,)}$.

$$C_{L(\,,\,)} = \frac{H_{L(\,,\,)}}{(1-A_{r(\,,\,)})^2 \times V_1^2/2g}$$

Froude number $$F_1 = \frac{V_1}{\sqrt{gy_1}}$$

DEFINITIONS OF TABLE HEADING

FOR HYDRAULIC DATA

Run 1st digit refers to the expansion ratio where:

1 refers to an abrupt expansion
2 refers to a 1:1 expansion ratio
3 refers to a 2:3 expansion ratio
4 refers to a 1:3 expansion ratio
5 refers to a 1:6 expansion ratio

2nd digit refers to relative degrees of submergence where A, B, C, and D are used; A having the least and D the greatest submergence for a given rate.

3rd and 4th digits refer to the run number where runs 1-16, for each expansion ratio, have B/b values of 5 and runs 17-32, for each expansion ratio, have B/b values of 3.

Q flowrate or discharge
EL12 head loss between sections 1 and 2, E_1-E_2
E1E2 energy ratio E_2/E_1
EL13 head loss between sections 1 and 3, E_1-E_3
E1E3 energy ratio E_3/E_1
Y1 flow depth at section 1
Y2 flow depth at section 2
Y3 flow depth at section 3
VM1 mean velocity at section 1
VM2 mean velocity at section 2
VM3 mean velocity at section 3
E1 specific energy at section 1, E_1
E2 specific energy at section 2, E_2
E3 specific energy at section 3, E_3
F1 Froude number at section 1, F_1
CL head loss coefficient, C_L

Table 3. Hydraulic data for abrupt expansions for B/b = 5 (Runs 1-16) and B/b = 3. (Runs 17-32)

RUN	Q	EL12	E1E2	EL13	E1E3	Y1	Y2	Y3	VM1	VM2	VM3	E1	E2	E3	F1	CL
1A01	.976	.069	.923	.086	.904	.870	.820	.803	1.122	.238	.243	.890	.821	.804	.212	7.141
1B02	.981	.062	.949	.060	.950	1.197	1.145	1.147	.820	.171	.171	1.207	1.145	1.147	.132	9.184
1C03	.981	.028	.980	.054	.962	1.410	1.389	1.363	.696	.141	.144	1.418	1.389	1.363	.10311	.463
1D04	.986	.027	.985	.053	.970	1.773	1.751	1.725	.556	.113	.114	1.778	1.751	1.725	.07417	.355
1A05	1.560	.129	.874	.154	.848	.978	.887	.861	1.595	.352	.362	1.018	.889	.863	.284	6.546
1B06	1.560	.078	.939	.100	.922	1.254	1.199	1.177	1.244	.260	.265	1.278	1.200	1.178	.196	6.716
1C07	1.590	.064	.956	.086	.940	1.431	1.385	1.363	1.111	.230	.233	1.450	1.386	1.364	.164	7.215
1D08	1.600	.051	.970	.075	.955	1.656	1.619	1.595	.966	.198	.201	1.670	1.620	1.596	.132	8.227
1A09	2.500	.192	.850	.206	.839	1.211	1.082	1.068	2.064	.462	.468	1.277	1.085	1.071	.331	5.201
1B10	2.490	.129	.911	.158	.891	1.408	1.325	1.296	1.768	.376	.384	1.457	1.327	1.298	.263	5.320
1C11	2.490	.119	.926	.137	.915	1.564	1.483	1.465	1.592	.336	.340	1.603	1.485	1.467	.224	5.609
1D12	2.490	.087	.952	.113	.938	1.783	1.725	1.699	1.397	.289	.293	1.813	1.726	1.700	.184	5.974
1A13	3.600	.278	.820	.295	.809	1.452	1.264	1.247	2.479	.570	.577	1.547	1.269	1.252	.363	5.257
1B14	3.610	.237	.857	.257	.845	1.581	1.421	1.401	2.283	.508	.515	1.662	1.425	1.405	.320	5.291
1C15	3.640	.206	.881	.226	.870	1.668	1.532	1.512	2.182	.475	.481	1.742	1.536	1.516	.298	5.039
1D16	3.590	.179	.903	.197	.894	1.795	1.675	1.657	2.000	.429	.433	1.857	1.678	1.660	.263	5.174
1A17	.976	.065	.924	-.907	2.068	.828	.782	1.756	1.179	.416	.185	.850	.785	1.757	.228	******
1B18	.970	.035	.970	.060	.949	1.177	1.151	1.126	.824	.281	.287	1.188	1.152	1.127	.13413	.460
1C19	.972	.027	.982	.052	.966	1.498	1.477	1.452	.649	.219	.223	1.505	1.478	1.453	.09318	.393
1D20	.975	.025	.986	.048	.972	1.696	1.676	1.653	.575	.194	.197	1.701	1.677	1.654	.07821	.393
1A21	1.470	.096	.907	.125	.879	1.001	.934	.905	1.469	.525	.541	1.034	.938	.910	.259	9.361
1B22	1.470	.069	.945	.095	.924	1.219	1.170	1.144	1.206	.419	.428	1.242	1.173	1.147	.19210	.090
1C23	1.470	.055	.963	.081	.946	1.471	1.430	1.404	.999	.343	.349	1.487	1.432	1.406	.14512	.276
1D24	1.480	.041	.977	.067	.963	1.767	1.736	1.710	.838	.284	.288	1.778	1.737	1.711	.11114	.226
1A25	2.500	.157	.882	.187	.860	1.271	1.166	1.136	1.967	.715	.734	1.331	1.174	1.144	.307	7.905
1B26	2.500	.134	.907	.160	.889	1.392	1.302	1.275	1.796	.640	.654	1.442	1.308	1.282	.268	7.918
1C27	2.500	.164	.896	.140	.911	1.536	1.498	1.432	1.628	.592	.582	1.577	1.413	1.437	.231	8.238
1D28	2.480	.085	.952	.118	.934	1.758	1.700	1.667	1.411	.486	.496	1.789	1.704	1.671	.187	9.087
1A29	3.600	.140	.906	.322	.784	1.384	1.337	1.150	2.601	.898	1.043	1.489	1.350	1.167	.390	8.551
1B30	3.610	.246	.846	.278	.826	1.505	1.336	1.303	2.399	.901	.924	1.594	1.349	1.316	.345	8.230
1C31	3.580	.106	.935	.139	.915	1.550	1.517	1.484	2.310	.787	.804	1.633	1.527	1.494	.327	3.943
1D32	3.610	.161	.913	.198	.893	1.784	1.679	1.641	2.024	.717	.733	1.848	1.687	1.649	.267	7.669

Table 4. Hydraulic data for 1:1 expansion for B/b = 5 (Runs 1-16) and B/b = 3. (Runs 17-32)

RUN	Q	EL12	E1E2	EL13	E1E3	Y1	Y2	Y3	VM1	VM2	VM3	E1	E2	E3	F1	CL
2A01	.987	.044	.946	.067	.917	.787	.766	.743	1.254	.336	.266	.811	.768	.744	.249	4.438
2B02	.985	.025	.978	.049	.956	1.098	1.085	1.061	.897	.236	.186	1.110	1.086	1.062	.151	6.230
2C03	.979	.017	.988	.041	.972	1.468	1.457	1.434	.667	.175	.137	1.475	1.457	1.434	.097	9.299
2D04	.978	.015	.992	.041	.977	1.753	1.743	1.717	.558	.146	.114	1.758	1.743	1.717	.07413.275	
2A05	1.545	.071	.927	.093	.904	.927	.896	.875	1.667	.449	.353	.970	.899	.877	.305	3.479
2B06	1.550	.037	.972	.063	.951	1.270	1.255	1.229	1.220	.322	.252	1.293	1.257	1.230	.191	4.338
2C07	1.562	.026	.983	.053	.967	1.569	1.557	1.531	.996	.261	.204	1.584	1.558	1.532	.140	5.422
2D08	1.552	.198	.900	.222	.888	1.978	1.789	1.765	.785	.226	.176	1.988	1.790	1.765	.09838.592	
2A09	2.507	.146	.872	.155	.864	1.048	.984	.978	2.392	.663	.513	1.137	.991	.982	.412	2.822
2B10	2.505	.085	.941	.103	.928	1.391	1.353	1.336	1.801	.482	.375	1.441	1.357	1.338	.269	3.268
2C11	2.500	.072	.955	.089	.944	1.541	1.507	1.491	1.622	.432	.335	1.582	1.510	1.493	.230	3.465
2D12	2.490	.048	.974	.071	.962	1.846	1.824	1.802	1.349	.356	.276	1.874	1.826	1.803	.175	3.979
2A13	3.500	.250	.804	.233	.817	1.124	1.012	1.034	3.114	.901	.677	1.275	1.025	1.041	.518	2.532
2B14	3.490	.181	.872	.179	.873	1.301	1.223	1.229	2.683	.743	.568	1.413	1.232	1.234	.414	2.574
2C15	3.470	.124	.925	.135	.918	1.582	1.527	1.518	2.193	.592	.457	1.657	1.532	1.521	.307	2.894
2D16	3.470	.093	.950	.109	.941	1.791	1.752	1.738	1.937	.516	.399	1.849	1.756	1.740	.255	2.962
2A17	.987	.057	.924	.080	.894	.718	.684	.664	1.375	.636	.495	.747	.690	.668	.286	6.626
2B18	.986	.030	.972	.056	.949	1.083	1.063	1.038	.910	.409	.317	1.096	1.066	1.040	.15410.285	
2C19	.989	.011	.992	.038	.975	1.495	1.489	1.463	.662	.293	.225	1.502	1.490	1.464	.09512.864	
2D20	.991	.016	.991	.046	.974	1.717	1.705	1.676	.577	.256	.197	1.722	1.706	1.677	.07820.315	
2A21	1.530	.071	.925	.086	.909	.897	.862	.851	1.706	.782	.599	.942	.871	.857	.317	4.503
2B22	1.560	.048	.963	.070	.946	1.263	1.234	1.214	1.235	.557	.428	1.287	1.239	1.217	.194	6.909
2C23	1.560	.034	.977	.060	.959	1.471	1.451	1.426	1.061	.474	.365	1.488	1.454	1.428	.154	8.033
2D24	1.560	.027	.985	.053	.970	1.753	1.736	1.711	.890	.396	.304	1.765	1.738	1.712	.118	9.914
2A25	2.560	.131	.887	.141	.879	1.074	1.012	1.010	2.384	1.114	.845	1.162	1.031	1.021	.405	3.839
2B26	2.550	.096	.929	.108	.920	1.295	1.247	1.240	1.969	.901	.685	1.355	1.260	1.247	.305	4.218
2C27	2.550	.073	.954	.085	.946	1.543	1.504	1.495	1.653	.747	.569	1.585	1.513	1.500	.234	4.679
2D28	2.500	.057	.968	.074	.959	1.756	1.724	1.710	1.424	.639	.487	1.787	1.730	1.714	.189	5.420
2A29	3.590	.157	.893	.166	.887	1.353	1.282	1.283	2.653	1.234	.933	1.462	1.306	1.297	.402	3.607
2B30	3.580	.128	.918	.136	.914	1.483	1.426	1.427	2.414	1.106	.836	1.573	1.445	1.438	.349	3.509
2C31	3.590	.113	.932	.124	.926	1.590	1.540	1.536	2.258	1.027	.779	1.669	1.556	1.545	.316	3.644
2D32	3.580	.096	.948	.104	.943	1.768	1.723	1.720	2.025	.915	.694	1.832	1.736	1.727	.268	3.787

Table 5. Hydraulic data for 2:5 expansion for B/b = 5 (Runs 1-16) and B/b = 3. (Runs 17-32)

RUN	Q	EL12	E1E2	EL13	E1E3	Y1	Y2	Y3	VM1	VM2	VM3	E1	E2	E3	F1	CL
4A01	1.030	.031	.958	.087	.880	.691	.692	.637	1.491	.422	.323	.726	.695	.639	.316	4.107
4B02	1.030	.017	.985	.064	.944	1.118	1.113	1.067	.921	.262	.193	1.131	1.114	1.068	.154	7.724
4C03	1.020	.014	.990	.067	.953	1.419	1.412	1.360	.719	.205	.150	1.427	1.413	1.360	.10613	.271
4D04	1.050	.010	.994	.064	.963	1.705	1.700	1.647	.616	.175	.128	1.711	1.700	1.647	.08317	.186
4A05	1.530	.065	.928	.106	.884	.860	.840	.801	1.779	.516	.382	.909	.844	.803	.338	3.494
4B06	1.530	.030	.973	.086	.921	1.058	1.058	1.003	1.446	.410	.305	1.090	1.061	1.004	.248	4.255
4C07	1.530	.020	.985	.075	.947	1.386	1.383	1.329	1.104	.313	.230	1.405	1.385	1.330	.165	6.336
4D08	1.530	.018	.990	.070	.959	1.701	1.695	1.643	.899	.256	.186	1.714	1.696	1.644	.122	8.865
4A09	2.550	.056	.956	.113	.913	1.223	1.229	1.175	2.085	.588	.434	1.291	1.234	1.178	.332	2.660
4B10	2.550	.039	.973	.098	.933	1.418	1.425	1.368	1.798	.507	.373	1.468	1.429	1.370	.266	3.108
4C11	2.540	.031	.981	.091	.945	1.610	1.615	1.556	1.578	.446	.326	1.649	1.618	1.558	.219	3.743
4D12	2.550	.031	.982	.087	.950	1.698	1.699	1.645	1.502	.425	.310	1.733	1.702	1.646	.203	3.924
4A13	3.420	.078	.948	.256	.829	1.408	1.414	1.239	2.429	.685	.552	1.500	1.421	1.244	.361	4.678
4B14	3.430	.071	.954	.128	.918	1.477	1.483	1.429	2.322	.655	.480	1.561	1.490	1.433	.337	2.432
4C15	3.420	.063	.962	.120	.927	1.573	1.578	1.523	2.174	.614	.449	1.646	1.584	1.526	.305	2.603
4D16	3.400	.051	.971	.106	.940	1.699	1.705	1.653	2.001	.565	.411	1.761	1.710	1.656	.271	2.690
4A17	.980	.025	.970	.047	.943	.800	.795	.774	1.225	.493	.422	.823	.799	.777	.241	4.648
4B18	.978	.018	.983	.040	.963	1.061	1.054	1.033	.922	.371	.316	1.074	1.056	1.035	.158	6.948
4C19	.972	.015	.990	.031	.979	1.490	1.481	1.465	.652	.263	.221	1.497	1.482	1.466	.09410	.585
4D20	.980	.011	.994	.036	.980	1.809	1.802	1.777	.542	.218	.184	1.814	1.803	1.778	.07118	.115
4A21	1.520	.043	.953	.060	.935	.870	.867	.852	1.747	.701	.595	.917	.875	.857	.330	2.905
4B22	1.520	.028	.976	.042	.963	1.119	1.115	1.102	1.358	.545	.460	1.148	1.120	1.105	.226	3.379
4C23	1.550	.022	.985	.044	.970	1.448	1.441	1.420	1.070	.430	.364	1.466	1.444	1.422	.157	5.642
4D24	1.532	.018	.990	.036	.980	1.782	1.774	1.756	.860	.345	.291	1.793	1.776	1.757	.113	7.196
4A25	2.520	.079	.928	.083	.924	.995	1.000	1.001	2.533	1.008	.839	1.095	1.016	1.012	.447	1.856
4A26	2.520	.048	.965	.062	.955	1.319	1.319	1.307	1.911	.764	.643	1.376	1.328	1.313	.293	2.495
4C27	2.510	.040	.974	.059	.962	1.505	1.501	1.484	1.668	.669	.564	1.548	1.508	1.489	.240	3.131
4D28	2.490	.027	.986	.046	.975	1.846	1.843	1.825	1.349	.540	.455	1.874	1.848	1.828	.175	3.709
4A29	3.450	.085	.941	.092	.936	1.323	1.327	1.325	2.608	1.040	.868	1.429	1.344	1.337	.400	1.955
4B30	3.450	.069	.956	.078	.950	1.486	1.487	1.482	2.322	.928	.776	1.570	1.500	1.491	.336	2.112
4C31	3.440	.057	.967	.065	.963	1.666	1.665	1.660	2.065	.826	.691	1.732	1.676	1.667	.282	2.210
4D32	3.430	.047	.975	.061	.968	1.863	1.860	1.849	1.841	.738	.618	1.916	1.868	1.855	.238	2.614

Table 6. Hydraulic data for 1:3 expansion for B/b = 5 (Runs 1-16) and B/b = 3. (Runs 17-32)

RUN	Q	EL12	E1E2	EL13	E1E3	Y1	Y2	Y3	VM1	VM2	VM3	E1	E2	E3	F1	CL
3A01	.978	.046	.933	.071	.896	.647	.634	.610	1.512	.411	.321	.682	.637	.612	.331	3.218
3B02	.971	.022	.979	.053	.949	1.029	1.020	.989	.944	.254	.196	1.043	1.021	.990	.164	6.139
3C03	.967	.016	.989	.037	.975	1.469	1.459	1.438	.658	.177	.134	1.476	1.459	1.438	.096	8.791
3D04	.969	.012	.993	.038	.978	1.738	1.730	1.705	.558	.149	.114	1.743	1.730	1.705	.07512	.299
3A05	1.500	.065	.925	.087	.898	.806	.791	.770	1.861	.506	.390	.860	.795	.772	.365	2.600
3B06	1.530	.040	.966	.062	.948	1.145	1.131	1.110	1.336	.361	.276	1.173	1.133	1.111	.220	3.524
3C07	1.590	.031	.979	.053	.965	1.501	1.486	1.465	1.059	.285	.217	1.518	1.487	1.466	.152	4.784
3D08	1.510	.020	.989	.044	.975	1.746	1.737	1.713	.865	.232	.176	1.758	1.738	1.713	.115	5.995
3A09	2.560	.112	.900	.131	.883	1.021	.999	.983	2.507	.683	.521	1.119	1.006	.987	.437	2.145
3B10	2.540	.076	.944	.099	.927	1.291	1.271	1.250	1.967	.533	.406	1.351	1.275	1.253	.305	2.604
3C11	2.540	.056	.963	.080	.947	1.477	1.464	1.441	1.720	.463	.353	1.523	1.467	1.443	.249	2.756
3D12	2.530	.048	.972	.068	.961	1.697	1.681	1.662	1.491	.401	.304	1.732	1.684	1.663	.202	3.115
3A13	3.580	.164	.878	.186	.861	1.205	1.168	1.150	2.971	.817	.623	1.342	1.178	1.156	.477	2.173
3A14	3.560	.114	.924	.139	.907	1.396	1.376	1.354	2.550	.690	.526	1.497	1.383	1.358	.380	2.180
3A15	3.560	.084	.949	.112	.933	1.589	1.577	1.552	2.240	.602	.459	1.667	1.583	1.555	.313	2.266
3A16	3.550	.070	.962	.099	.946	1.774	1.762	1.735	2.001	.537	.409	1.836	1.766	1.738	.265	2.505
3A17	.982	.035	.957	.057	.930	.790	.774	.754	1.243	.574	.434	.814	.779	.757	.246	5.617
3B18	.979	.026	.975	.048	.956	1.059	1.043	1.023	.924	.425	.319	1.072	1.046	1.025	.158	8.378
3C19	.978	.020	.985	.041	.970	1.348	1.334	1.314	.726	.332	.248	1.356	1.336	1.315	.11011	.646
3D20	.975	.020	.989	.043	.975	1.728	1.712	1.689	.564	.258	.192	1.733	1.713	1.690	.07620	.203
3A21	1.540	.074	.913	.085	.901	.803	.773	.768	1.918	.901	.668	.860	.786	.775	.377	3.514
3B22	1.530	.057	.947	.064	.940	1.035	1.005	1.001	1.478	.689	.509	1.069	1.012	1.005	.256	4.385
3C23	1.670	.034	.976	.040	.972	1.413	1.396	1.392	1.182	.541	.400	1.435	1.401	1.394	.175	4.234
3D24	1.680	.024	.986	.051	.970	1.659	1.648	1.622	1.013	.461	.345	1.675	1.651	1.624	.139	7.384
3A25	2.570	.105	.906	.118	.894	1.019	.991	.988	2.522	1.173	.867	1.118	1.012	1.000	.440	2.777
3B26	2.590	.068	.950	.088	.936	1.317	1.296	1.282	1.967	.904	.673	1.377	1.309	1.289	.302	3.389
3C27	2.580	.053	.966	.071	.954	1.521	1.503	1.489	1.696	.780	.578	1.566	1.512	1.494	.242	3.679
3D28	2.580	.040	.977	.062	.965	1.761	1.747	1.728	1.465	.668	.498	1.794	1.754	1.732	.195	4.300
3A29	3.490	.167	.871	.145	.889	1.158	1.100	1.138	3.014	1.436	1.022	1.299	1.132	1.154	.494	2.351
3B30	3.490	.118	.920	.110	.925	1.364	1.326	1.344	2.559	1.191	.866	1.466	1.348	1.356	.386	2.472
3C31	3.470	.093	.943	.091	.944	1.553	1.521	1.531	2.234	1.032	.755	1.631	1.538	1.540	.316	2.670
3D32	3.460	.074	.959	.078	.957	1.748	1.722	1.724	1.979	.909	.669	1.809	1.735	1.731	.264	2.921

Table 7. Hydraulic data for 1:6 expansion for B/b = 5 (Runs 1-16) and B/b = 3. (Runs 17-32)

RUN	Q	EL12	E1E2	EL13	E1E3	Y1	Y2	Y3	VM1	VM2	VM3	E1	E2	E3	F1	CL
5A01	.991	.018	.978	.028	.967	.819	.822	.813	1.210	.294	.244	.842	.823	.814	.236	1.919
5B02	.994	.014	.988	.023	.981	1.165	1.162	1.153	.853	.209	.172	1.176	1.163	1.153	.139	3.174
5C03	.998	.010	.994	.018	.989	1.577	1.573	1.565	.633	.155	.128	1.583	1.573	1.565	.089	4.531
5D04	.997	.008	.996	.018	.990	1.840	1.836	1.826	.542	.132	.109	1.845	1.836	1.826	.070	6.321
5A05	1.540	.024	.976	.034	.967	.989	1.000	.991	1.557	.376	.311	1.027	1.002	.992	.276	1.416
5B06	1.560	.015	.989	.026	.981	1.316	1.322	1.311	1.185	.288	.238	1.338	1.323	1.312	.182	1.861
5C07	1.560	.013	.992	.024	.985	1.603	1.604	1.593	.973	.237	.196	1.618	1.605	1.594	.135	2.570
5D08	1.520	.014	.992	.024	.987	1.815	1.811	1.801	.837	.205	.169	1.826	1.812	1.801	.110	3.521
5A09	2.510	.043	.965	.051	.958	1.147	1.174	1.167	2.188	.521	.430	1.221	1.178	1.170	.360	1.073
5B10	2.510	.045	.969	.044	.970	1.402	1.404	1.406	1.790	.436	.357	1.452	1.407	1.408	.266	1.373
5C11	2.470	.030	.981	.035	.978	1.573	1.579	1.575	1.570	.382	.314	1.611	1.581	1.577	.221	1.418
5D12	2.520	.013	.993	.033	.982	1.772	1.789	1.769	1.422	.344	.285	1.803	1.791	1.770	.188	1.650
5A13	3.580	.071	.950	.070	.951	1.323	1.359	1.362	2.706	.643	.526	1.437	1.365	1.366	.415	.954
5B14	3.550	.051	.967	.062	.960	1.470	1.504	1.495	2.415	.576	.475	1.561	1.509	1.499	.351	1.062
5C15	3.550	.051	.970	.057	.966	1.623	1.642	1.637	2.187	.527	.434	1.697	1.646	1.640	.303	1.201
5D16	3.500	.041	.978	.048	.974	1.759	1.776	1.770	1.990	.481	.395	1.820	1.780	1.772	.264	1.217
5A17	.994	.019	.978	.047	.945	.837	.836	.809	1.188	.487	.410	.859	.840	.812	.229	5.032
5B18	.997	.011	.991	.037	.970	1.223	1.221	1.195	.815	.335	.278	1.233	1.223	1.196	.130	8.286
5C19	.999	.011	.993	.039	.975	1.521	1.516	1.488	.657	.270	.224	1.528	1.517	1.489	.09413.368	
5D20	.996	.004	.998	.037	.979	1.773	1.773	1.740	.562	.230	.191	1.778	1.774	1.741	.07417.473	
5A21	1.505	.027	.973	.053	.947	.947	.953	.929	1.589	.647	.540	.986	.960	.934	.288	3.082
5B22	1.570	.019	.986	.043	.968	1.327	1.326	1.303	1.183	.485	.402	1.349	1.330	1.306	.181	4.559
5C23	1.520-	.0161	.011	.015	.990	1.463	1.493	1.463	1.039	.417	.346	1.480	1.496	1.465	.151	2.000
5D24	1.560	.012	.994	.027	.985	1.817	1.815	1.800	.859	.352	.289	1.828	1.817	1.801	.112	5.388
5A25	2.510	.053	.955	.075	.936	1.083	1.100	1.082	2.318	.935	.773	1.166	1.114	1.091	.392	2.028
5B26	2.510	.038	.972	.061	.954	1.278	1.290	1.270	1.964	.797	.659	1.338	1.300	1.277	.306	2.312
5C27	2.500	.039	.974	.057	.963	1.491	1.488	1.473	1.677	.689	.566	1.535	1.495	1.478	.242	2.958
5D28	2.490	.023	.987	.051	.972	1.796	1.798	1.771	1.386	.568	.469	1.826	1.803	1.774	.182	3.933
5A29	3.540	.093	.928	.103	.920	1.147	1.178	1.176	3.086	1.232	1.003	1.295	1.202	1.192	.508	1.533
5B30	3.540	.073	.948	.087	.937	1.267	1.296	1.288	2.794	1.119	.916	1.388	1.315	1.301	.437	1.592
5C31	3.520	.052	.967	.075	.953	1.504	1.523	1.505	2.340	.947	.780	1.589	1.537	1.514	.336	1.973
5D32	3.520	.039	.979	.063	.965	1.744	1.758	1.737	2.018	.821	.675	1.807	1.768	1.744	.269	2.256